

<https://doi.org/10.15388/vu.thesis.497>

<https://orcid.org/0000-0002-5679-0705>

VILNIUS UNIVERSITY

CENTER FOR PHYSICAL SCIENCES AND TECHNOLOGY

Vitaliy Romanenko

The Study of Anthropogenic Radionuclide Transport with Suspended Matter in the System Neman River – Baltic Sea

DOCTORAL DISSERTATION

Natural Sciences,
Physics (N 002)

VILNIUS 2023

The dissertation was prepared between 2019 and 2023 at Center for Physical Sciences and Technology.

Academic supervisor – Dr. Galina Lujanienė (Center for Physical Sciences and Technology, Natural sciences, Physics, N 002).

This doctoral dissertation will be defended in a public meeting of the Dissertation Defence Panel:

Chairman – Dr. Evaldas Maceika (Center for Physical Sciences and Technology, Natural Sciences, Physics, N 002)

Members:

Prof. Dr. Arturas Katelnikovas (Vilnius university, Natural sciences, Chemistry, N 003).

Prof. Dr. Şule Aytaş (EGE University Institute of Nuclear Sciences, Natural sciences, Chemistry, N 003).

Dr. Danguolė Montvydienė (Nature research centre, Natural sciences, Ecology and environmental science, N 012).

Dr. Arūnas Gudelis (Center for Physical Sciences and Technology, Natural sciences, Physics, N 002).

The dissertation shall be defended at a public meeting of the Dissertation Defence Panel at 10 a.m. on 29th September 2023 in the meeting room D401 of the Center for Physical Sciences and Technology.

Address: Saulėtekio av. 3, LT-10257 Vilnius, Lithuania.

Tel. +37052649211; e-mail: office@ftmc.lt

The text of this dissertation can be accessed at the libraries of Vilnius University and Center for Physical Sciences and Technology, as well as on the website of Vilnius University: www.vu.lt/lt/naujienos/ivykiu-kalendorius

<https://doi.org/10.15388/vu.thesis.497>

<https://orcid.org/0000-0002-5679-0705>

VILNIAUS UNIVERSITETAS
FIZINIŲ IR TECHNOLOGIJOS MOKSLŲ CENTRAS

Vitaliy Romanenko

Antropogeninių radionuklidų pernašos
su pakibusiomis dalelėmis sistemoje
Nemunas upė – Baltijos jūra tyrimas

DAKTARO DISERTACIJA

Gamtos mokslai,
Fizika (N 002)

VILNIUS 2023

Disertacija rengta 2019-2023 metais Fizinių ir technologijos mokslų centre.

Mokslinė vadovė – dr. Galina Lujanienė (Fizinių ir technologijos mokslų centras, gamtos mokslai, fizika, N 002).

Gynimo taryba:

Pirmininkas – dr. Evaldas Maceika (Fizinių ir technologijos mokslų centras, gamtos mokslai, fizika, N 002).

Nariai:

Prof. dr. Arturas Katelnikovas (Vilniaus universitetas, gamtos mokslai, chemija, N 003).

Prof. dr. Šulė Aytas (EGE universiteto branduolinių mokslų institutas, gamtos mokslai, chemija, N 003).

dr. Danguolė Montvydienė (Gamtos tyrimų centras, gamtos mokslai, ekologija ir aplinkotyra, N 012).

dr. Arūnas Gudelis (Fizinių ir technologijos mokslų centras, gamtos mokslai, fizika, N 002).

Disertacija ginama viešame Gynimo tarybos posėdyje 2023 m. rugsėjo mėn. 29 d. 10:00 val. Fizinių ir technologijos mokslų centro D401 auditorijoje.

Adresas: Savanorių pr. 231, LT-02300 Vilnius, Lietuva.

Tel. +37052649211; el. paštas office@ftmc.lt

Disertaciją galima peržiūrėti Fizinių ir technologijos mokslų centro bei Vilniaus universiteto bibliotekose ir VU interneto svetainėje adresu:

<https://www.vu.lt/naujienos/ivykiu-kalendorius>

CONTENTS

1. LITERATURE REVIEW	14
1.1. Application of particle-reactive radionuclides in recent sediment transport studies	14
1.2. Radionuclide's origin and behaviour in the water systems	16
1.3. Radionuclide applications for studies of sediment sources	20
1.4. Sediment transport studies.....	27
1.4.1 Sediment transport in catchments	27
1.4.2 Studies of mixing zones of fresh and seawater	29
1.4.3 Sediment transport in marine waters.....	33
1.5. Applications of radionuclides for study sediments accumulation	36
1.6. The summary of chapter	39
2. MATERIALS AND METHODS	41
2.1 Study area.....	41
2.2 Sampling	44
2.3. Samples preparation	46
2.4. Samples analysis	48
3. RESULTS AND DISCUSSION.....	50
3.1 The studies of the radionuclide export to the Curonian lagoon with the Neman River	50
3.1.1. Activity levels.....	50
3.1.2. Radionuclide flux	53
3.1.3. Chapter conclusions.....	56
3.2. The study of factors influencing the distribution of radionuclides in the Baltic Sea.....	57
3.2.1. Curonian Lagoon.....	57
3.2.2. Coastal region of the south-eastern part of the Baltic Sea.....	59
3.2.2.1. Activity levels of $^{239,240}\text{Pu}$, ^{137}Cs , ^{241}Am	59
3.2.2.2. Estimation of the share of Chernobyl-derived radionuclides	64
3.2.2.3. Chapter conclusions.....	70

3.2.3. Southern Baltic Sea area and Skagerrak Bay area	72
3.2.3.1 Grain size distributions	72
3.2.3.1 Radionuclides activities	73
3.2.3.3. General trends.....	78
3.2.3.4. Chapter conclusions.....	82
CONCLUSIONS.....	84
4. SANTRAUKA	85
ĮVADAS	85
4.1. MEDŽIAGOS IR METODAI	91
4.1.1 Tyrimo erdvė.....	91
4.1.2 Mėginių ėmimas bei tyrimas	91
4.2. REZULTATAI IR APTARIMAS	93
4.2.1 Radionuklidų patekimo iš Nemuno upės į Kuršių marias tyrimas	93
4.2.1.1. Aktyvumo lygis	93
4.2.1.2. Radionuklidų srautas	94
4.2.2. Faktorių, paveikiančių radionuklidų pasiskirstymą Baltijos jūroje, tyrimas.....	96
4.2.2.1. Pietrytinės Baltijos jūros dalies pakrančių regionas.....	96
4.2.2.1.1. $^{239,240}\text{Pu}$, ^{137}Cs ir ^{241}Am aktyvumo lygis	96
4.2.2.1.2. Černobylio kilmės radionuklidų dalies nustatymas.....	96
4.2.2.2. Pietinė Baltijos jūros teritorija ir Skagerako įlankos teritorija	98
4.2.2.2.1. Grūdelių dydžio pasiskirstymas	98
4.2.2.2.2. Radionuklidų aktyvumas	98
4.2.2.2.3. Bendrosios tendencijos	98
4.3 IŠVADOS	100
REFERENCES.....	101
ACKNOWLEDGEMENTS	128

INTRODUCTION

The transport of suspended matter and sediments influences the dispersion of various pollutants and radioactive substances, and at the same time affects the ecological status of water bodies. In recent decades, the pollution of European seas, including the Baltic Sea, with radionuclides has become a significant problem. Pollution by radionuclides in this area results from direct fallout from atmospheric nuclear weapons testing and the Chernobyl accident, as well as from the delayed transport of radionuclides from these sources via rivers from contaminated basins (Povinec et al., 2003). These sources have contributed to the total amount of harmful substances in the marine ecosystem, posing a potential threat to both human health and the environment (Winkler, P. and Roider, 1997, Livingston and Povinec, 2002). The radioecological situation of the Baltic Sea is significantly influenced by the input of nutrients from the rivers. The sea has an extensive catchment area of $1.6 \times 10^5 \text{ km}^2$ (Matthäus and Schinke, 1999), with the rivers being the largest contributors of water and sediment. More than 250 rivers flow into the Baltic Sea, providing an average of $446 \text{ km}^3/\text{year}$ of freshwater (Graham and Bergstrom, 2001), along with significant amounts of suspended matter and pollutants that can have negative impacts on the environment and human health. Knowledge of potential ecological risks associated with pollutants transported by suspended matter and bottom sediments is essential for a comprehensive understanding of changes in the ecological status of the Baltic Sea.

Suspended particulate matter (SPM) is a critical component in the movement, dispersal and redistribution of pollutants in aquatic ecosystems. In fact, fluxes are responsible for about 90% of the trace elements found in association with suspended particles in the marine environment. The shallow water depth of the Baltic Sea contributes to wave-induced resuspension, which redistributes pollutants over a large part of the sea (Almroth-Rosell et al., 2011).

The main sources of suspended sediment in the south-eastern Baltic Sea are the Vistula and the Neman Rivers, which have catchment areas of $1.9 \times 10^5 \text{ km}^2$ and $0.98 \times 10^5 \text{ km}^2$ respectively. In this area, plutonium, americium and radiocaesium are the most important long-lived radionuclides that pose a threat to the environment. In the Baltic region, the typical deposition of $^{239,240}\text{Pu}$ is estimated to be about $40\text{-}50 \text{ Bq/m}^2$ (Holm, 1995).

In comparison to plutonium, caesium exhibits higher solubility and mobility in water systems (Michel et al., 2002). This property governs the transportation of caesium over greater distances and its penetration into living

organisms. A study by Monte et al. (2002) reported the deposition of ^{137}Cs in the Neman catchment at levels up to 100 kBq/m^2 . Smith et al. (1987) estimated that $^{239,240}\text{Pu}$ and ^{137}Cs could remain in the catchment for 3000 and 1000 years, respectively. Considering these long residence times of radionuclides in the catchment area and the contamination of the Neman catchment by fallout radionuclides, it can be deduced that this catchment could serve as a long-term source of radionuclides for the Curonian Lagoon and the Baltic Sea. A similar situation exists in the neighbouring catchment area - the Vistula. According to Skwarzec and Bojanowski, R. (1992) the Vistula River contributes an average of 192 MBq/year of $^{239,240}\text{Pu}$ on suspended particles (> 0.45 microns) to the Gdansk Basin, with an average activity of $6.5 \pm 2.8 \text{ mBq/m}^3$ in the inflow. Skwarzec et al. (2011) reported that 2 to 52% of the plutonium released during the Chernobyl accident was found in the Vistula, with an average annual concentration of about 3 mBq/m^3 . Skwarzec et al. (2003) estimated that 78% of the $^{239,240}\text{Pu}$ deposited in the Gdansk Basin originated from rivers, with a bottom sediment inventory of 3.8 TBq .

Previous estimations of the annual flux of $^{239,240}\text{Pu}$ from the Neman catchment supposedly derived from the studies on the Vistula River; at the same time, no consistent studies on the inflow of $^{239,240}\text{Pu}$ seem to have been carried out to substantiate the actual figures for the Neman. Current data do not appear to include comprehensive information on the content and occurrence of $^{239,240}\text{Pu}$ and ^{137}Cs in suspended sediments for the Neman River catchment, and data on the Curonian Lagoon are also reported only sporadically. There are limited number publications on the transport of radionuclides with suspended solids in the Neman River (such as Lujanás et al. (2002), Lujanienė et al. (2014)). Further researches are needed to fill the gap in understanding the specifics of radionuclide transport from the Neman River catchment, radionuclide activity levels and fluxes.

The Neman River is the main source of suspended sediment in the Curonian Lagoon. The hydrological conditions of the lagoon are influenced by a variety of factors, including water depth, precipitation, river flow, evaporation, wind-driven movement and water exchange through the strait of Klaipėda. The permeability of the strait can be affected by dredging and differences in water levels between the lagoon and the Baltic Sea (Jakimavičius and Kovalenkoviėnė, 2010).

The dynamic environmental conditions of the lagoon are reflected in the fluctuations of various parameters, such as suspended sediment concentrations, salinity, and the distribution of radionuclides. For example, Lujanienė et al. (2013) found that the concentration of suspended particles in the Curonian Lagoon varies widely, from 2 to 304 mg/L , with an average

value three times higher than in the south-eastern coastal area of the Baltic Sea. Reported activities of ^{137}Cs in suspended solids and bottom sediments also show a wide range from 20 to 250 Bq/L and from 0.4 to 208 Bq/kg, respectively. Notably, approximately 62% of sediment material settles within the lagoon's territory (Mėžinė et al. (2019)). Thus, the lagoon serves as both a supplier and an accumulator of sediment material along with the pollutants associated with it (Davulienė et al., 2006; Stakėnienė et al., 2019; Jokšas et al., 2016; Lujanienė et al., 2014).

Due to the significant difference in the size of the catchment area between the Neman River and the Curonian Lagoon (more than 30 times), the transport of radionuclides from the catchment to the lagoon results in a proportional increase in activity corresponding to their respective areas. It is important to note that the accumulation of long-lived radionuclides such as $^{239,240}\text{Pu}$ and ^{241}Am in certain regions of the lagoon could lead to potential environmental hazards in the future. Knowledge of the fate of radionuclides during their transport through the lagoon enables a comprehensive understanding of sediment dynamics and the impact of pollutants on this sensitive ecosystem.

Several studies of plutonium and caesium in water, bottom sediments and suspended particles were carried out in the Curonian Lagoon and the coastal areas of the south-eastern Baltic Sea. These studies served as a basis for understanding the possible use of these radionuclides as sediment and pollutant tracers in this area. According to the findings of Lujanienė et al. (2004) and Lujanienė et al. (2010), who studied the behaviour of ^{137}Cs in suspended sediments and bottom sediments (0.2-50 μm), variations in caesium activities are associated with seasonal variations in the chemical composition of suspended sediments. Lujanienė et al., (2014) found a clear gradient in the activity of soluble ^{137}Cs between the coastal areas of the Baltic Sea and the Curonian Lagoon, while the ^{137}Cs concentrations in bottom sediments were similar in both regions. To determine the origin of plutonium in the suspended matter and bottom sediments, the authors used the atomic ratios $^{238}\text{Pu}/^{239,240}\text{Pu}$ and $^{240}\text{Pu}/^{239}\text{Pu}$. Their analysis showed a higher contribution of the Chernobyl accident signal in the particles in the range of 0.2-1 μm in the Klaipėda Strait in 2011-2012. The plutonium ratios also provided evidence that the Chernobyl-derived fallout is transported by the river into the lagoon after being washed out of the catchment. Lujanienė et al. (2013) reported strong correlation between the massic activities of ^{137}Cs and total organic carbon (TOC) in the Baltic Sea ($r=0.75$) and with clay minerals ($r=0.95$). The $^{239,240}\text{Pu}$ massic activities varied from 0.03 to 7.5 Bq/kg, and a high correlation with TOC was found for both $^{239,240}\text{Pu}$ ($r=0.98$) and ^{241}Am

($r=0.96$). Lujaniene et al., (2017) reported that the plutonium origin of the global fallout is prevalent in the deeper areas of the south-eastern Baltic Sea, while other sources such as Chernobyl fallout may play a greater role in coastal areas.

The high cost of sample collection and the complexity of conducting analysis for americium and plutonium significantly restrict the opportunities for researchers in south-eastern Baltic Sea region. Information regarding the influence of seabed topography, ocean currents, salinity gradients, wave processes, and other factors on the behaviour of these radionuclides in the Baltic Sea environment remains insufficient. Further research offers a chance to discover novel patterns and acquire fresh insights into the transfer and redistribution of radionuclides and exploring their potential applications in tracer studies.

THE MAIN AIM AND TASKS

Study of the transport and distribution of particle-reactive radionuclides in the suspended and bottom sediments of the Neman River, the Curonian Lagoon and the Baltic Sea in order to use them as environmental tracers. To achieve the aims of the study, the following tasks were formulated:

1. Determining the distribution of radionuclides among different particle size ranges of suspended sediment of the Neman River (Neris tributary) and Curonian Lagoon.

2. Assessment of technogenic radionuclide release (^{137}Cs and $^{239,240}\text{Pu}$) by the Neman River Catchment to the Curonian lagoon.

3. Estimation of the spatial distribution of $^{239,240}\text{Pu}$, ^{241}Am and ^{137}Cs in the bottom sediments of the Curonian Lagoon and the coastal area of the south-eastern Baltic Sea.

4. Assessment of the origin of $^{239,240}\text{Pu}$ and ^{241}Am in the bottom sediments of the Curonian Lagoon and the coastal area of the south-eastern Baltic Sea.

5. Evaluation the influence of factors (grain size, sampling depth, activities of other nuclides such as ^{210}Pb , ^{214}Pb , ^{40}K , proximity to the coastline) on the distribution of $^{239,240}\text{Pu}$, ^{241}Am , ^{137}Cs in the bottom sediments of the Baltic Sea.

NOVELTY

This study presents the results of the most comprehensive investigation of ^{241}Am and Pu isotopes in suspended matter and bottom sediments in the south-eastern part of the Baltic Sea. As far as known at present, ^{241}Pu values have been estimated for the first time in bottom sediments of the Curonian Lagoon and the Baltic Sea of the Lithuanian Economic Zone. The ratio $^{241}\text{Am}/^{239,240}\text{Pu}$ was used to assess the impact of natural and anthropogenic sediment transport in the coastal area adjacent to the Curonian Lagoon. In addition, the sedimentation rate in the coastal zone adjacent to the Curonian Lagoon was estimated. The input of plutonium isotopes from the Neman catchment was estimated to be 62 MBq/year, and the amount of plutonium accumulating in the Curonian Lagoon each year was estimated to be 39 MBq/year.

STATEMENTS TO DEFENCE

1. The 25 – 63 μm fraction of suspended sediments is the main carrier of ^{137}Cs and natural radionuclides (^7Be , ^{40}K , ^{210}Pb , ^{214}Pb) activity to the Curonian Lagoon with the Neman River.

2. The transport of $^{239,240}\text{Pu}$ and ^{137}Cs on particles from the catchment area of the Neman River into the Curonian Lagoon is about 62 MBq and 3.6 GBq, respectively. These radionuclides accumulate in certain areas of particle deposition, and over time the amounts of $^{239,240}\text{Pu}$ potentially can reach ecologically significant levels.

3. The spatial distribution of radionuclides ($^{239,240}\text{Pu}$ and ^{241}Am) in the coastal area of the Baltic Sea and accumulation zone of the Curonian Lagoon show a characteristic pattern that supports the use of these radionuclides as environmental tracers.

The particles of 30 μm size play an important role in the transport of ^{137}Cs (and also ^{40}K , ^{214}Pb), while suspended particles of $< 20 \mu\text{m}$ size influence on transport of ^{210}Pb in the Baltic Sea.

SCIENTIFIC AND PRACTICAL SIGNIFICANCE OF THE RESULTS

Currently, due to climate change, there is an increase in natural disasters, floods and rising water levels. This in turn increases soil erosion and resuspension, which ultimately increases the amount and rate of redistribution of various pollutants. The results of these studies will contribute to knowledge about tools for assessing environmental pollution and climate change impacts.

The obtained data on the activity levels of ^{137}Cs and $^{239,240}\text{Pu}$ in suspended solids and bottom sediments have expanded the knowledge about the transport and distribution of pollutants with river runoff. The results can be incorporated into models to estimate pollutant transport from watersheds.

In addition, the details of the distribution of $^{239,240}\text{Pu}$ and ^{241}Am , as well as the information on their origin from the coastal zone, will serve as a basis for further research on the dispersion of river sediments and contaminants in runoff areas, as well as for predictive models.

The details of radionuclide distribution over different size ranges of particles can be useful in modelling the transport of pollutants in river and marine systems.

The results of the study can be used to assess the potential impact of future environmental changes on pollutants distribution and transport.

LIST OF PUBLICATIONS

1. **Romanenko, V.**, Lujanienė, G., 2023. Short review of plutonium applications for the sediment transport studies. *Journal of Environmental Radioactivity*. <https://doi.org/10.1016/j.jenvrad.2022.107066>.

2. Lujanienė, G., Šilobritienė, B., Tracevičienė, D., Šemčuk, S., **Romanenko, V.**, Garnaga-Budrė, G., Kaizer, J., Povinec, P.P., 2022. Distribution of ^{241}Am and Pu isotopes in the Curonian Lagoon and the south-eastern Baltic Sea seawater, suspended particles, sediments and biota. *Journal of Environmental Radioactivity*. <https://doi.org/10.1016/j.jenvrad.2022.106892>.

3. **Romanenko V.**, Lujanienė G., Šemčuk S., Mažeika J., Jefanova O., 2023. Assessment of the input of particulate $^{239,240}\text{Pu}$ and ^{137}Cs from the Neman River into the Curonian Lagoon. *Lithuanian Journal of Physics*, 64(2). <https://doi.org/10.3952/physics.2023.63.2.6>.

LIST OF CONFERENCES

1. **Vitaliy Romanenko**, Galina Lujanienė, $^{239,240}\text{Pu}$ balanso vertinimas Kuršių Mariosė. estimation of $^{239,240}\text{Pu}$ balance in the Curonian Lagoon, 44th National Lithuanian physics conference (LNFK), 6-8th of October, 2021, Vilnius, Lithuania, poster presentation.

2. **Vitaliy Romanenko**, Galina Lujanienė, Sergej Šemčuk, Raman Novikau, Jonas Mažeika, Olga Jefanova, The study of radionuclides levels in the suspended particulate matter of the Neris River, 64th International Conference for Students of Physics and Natural Sciences „Open Readings 2021“, 16-19th of March, 2021, Vilnius, Lithuania, poster presentation.

3. **Vitaliy Romanenko**, Galina Lujanienė, Sergej Šemčuk, Jonas Mažeika, Olga Jefanova, The estimation of anthropogenic radionuclides levels in the Curonian Lagoon due to the increasing environmental risk, Conference of Doctoral Students and Young Researchers FizTech (FizTech2021), 20 – 21th October 2021, Vilnius, Lithuania, oral presentation.

4. **Vitaliy Romanenko**, Galina Lujanienė, Sergej Šemčuk, Raman Novikau, Jonas Mažeika, Olga Jefanova, Assessment of radionuclide input into the Curonian Lagoon by suspended matter, international conference on radiation in various fields of research (RAD2020), 25-29th July, 2022, Herceg Novi, Montenegro. Poster.

5. **Vitaliy Romanenko**, Galina Lujanienė, Sergej Šemčuk, Jonas Mažeika, Olga Jefanova, Investigation of the transport of $^{239,240}\text{Pu}$ and ^{137}Cs in the water system Curonian Lagoon – Neman River, Conference of Doctoral Students and Young Researchers FizTech (FizTech2022), 19-20th October 2022, Vilnius, Lithuania, oral presentation.

AUTHOR'S CONTRIBUTION

The author's contribution to the present study can be described as follows: Preparation and publication of a comprehensive literature review on the subject, organization and implementation of sampling in the Neris River and the Curonian Lagoon, preparation of samples for laboratory analysis, radiochemical laboratory separation of $^{239,240}\text{Pu}$ and ^{241}Am . Measuring the activity values of the radionuclides, processing the data, performing calculations, preparing maps, visualizing the results, interpreting the results and preparing the study for publication.

1. LITERATURE REVIEW

1.1. Application of particle-reactive radionuclides in recent sediment transport studies

The transport of sediments through surface waters is of great ecological importance. Fine particles in fluvial, coastal and marine ecosystems are involved in various physical, chemical and biological processes (Sternecker et al, 2013). Sediments fill reservoirs, change the morphology of rivers, coastal areas, shelves and sea beds. The transfer of nutrients and carbon occurs through particle flux (Worrall et al., 2014; Owens et al., 2015).

Since 1950, the amount of sediment has increased by more than 460% as a result of anthropogenic activities. More than 94% of the global net sediment transport from land to sea is due to anthropogenic activities (Syvitski et al., 2022). The disturbed natural balance of sediments in water bodies leads to various environmental problems.

Excessive sedimentation degrades water quality, river morphology and living organisms (Gleason et al., 2003; Kitheka et al., 2021), disrupts structures and increases the area of floodplains. The decrease in sediments caused by human activities leads to beach degradation and increased coastal erosion, which is accompanied by degradation of lowland areas (Peychev and Stancheva, 2009). Various particle-reactive substances such as toxic metals (Asowata and Akinwumiju, 2020) and organic compounds, plastic particles (Andersen et al., 2021; Juez et al., 2018) and radionuclides are transported in particles with river runoff. Therefore, sediment transport is an important indicator of the "health" of water bodies and is used to assess the ecological status of surface waters (Håkanson, 2006).

Numerous studies have been conducted in recent decades to improve the understanding of sediment transport mechanisms and factors affecting the spatial and temporal distribution of particles and associated pollutants (Vercruyssen et al., 2017; Owens et al., 2016). Sediment transport studies use various properties to identify sediments. These include physical parameters (e.g., particle size, colour, shape) (Pulley and Collins, 2021), stable isotopes ($^{12,13}\text{C}$, $^{14,15}\text{N}$) (Rose et al., 2018), trace metals and microelements (Nosrati et al., 2018; Chen et al, 2019; Habibi et al, 2019) and radionuclides (e.g., $^{239,240}\text{Pu}$, ^{137}Cs , ^7Be , ^{234}Th , ^{14}C , ^{40}K , ^{232}Th , ^{226}Ra) (Lujanienė et al, 2013; Lujanienė et al, 2017; Benoit et al, 2020; Wang et al, 2020).

Natural and anthropogenic radionuclides are an important component of sediment transport studies. They have different origins and mechanisms of interaction with particles and have been a useful tool in sediment transport

studies for several decades. Particle reactive radionuclides (PRRs) have proven to be a good tool for studying the different parameters from entry into the water stream to permanent deposition (Figure 1).

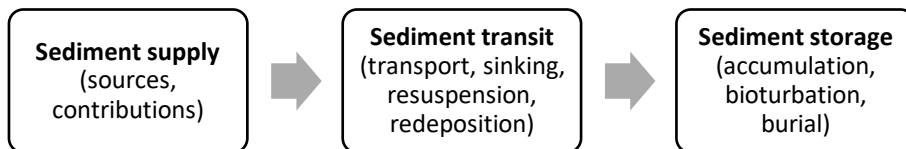


Figure 1. *Simplified scheme of sediment transport processes studied with particle-reactive radionuclides*

Sediment input to water bodies via various sources depends on natural and anthropogenic factors. The sediment sources and their contributions are studied using the fingerprint method (Tang et al., 2019). This approach includes different models of varying complexity, from single tracers to complex composite fingerprints (Haddadchi et al., 2013). A wide range of radionuclides can be used (e.g., $^{239,240}\text{Pu}$, ^{137}Cs , ^7Be , ^{234}Th , ^{232}Th , ^{226}Ra), depending on localisation (surface, subsurface), source mechanism (fallout, geological derivation), origin (natural, anthropogenic). These radionuclides are used to distinguish sources of sediments based on isotope ratios and other characteristics. Information on the contribution of target areas to sedimentation is important for the development of conservation measures to reduce soil erosion, as well as for the evaluation of their effectiveness.

The transfer of sediments from sources to sites of their deposition can take from a few days to millennia (Gellis, et al., 2019). In watersheds, sediment transit time describes the time it takes for sediment to travel from the adsorption of the tracer at the source to its destination in the river. ^7Be , ^{210}Po , and $^{210}\text{Pb}_{\text{ex}}$ are used in the models to calculate sediment transport time. The transport of sediment at different scales from the river to the ocean is studied with plutonium isotopes (^{239}Pu , ^{240}Pu) (Lindahl et al., 2010; Zhuang et al., 2019).

In deeper waters, the vertical transport of particles has a strong influence on the distribution of particulate organic carbon and particle-reactive substances. Elements vital to marine organisms are transported to the depths by the flow of sinking particles. These particles also trap radionuclides from the water column that make it possible to study transport processes (scavenging, sinking flux etc.). Radionuclide disequilibrium (^{238}U : ^{234}Th , ^{210}Pb : ^{210}Po , ^{228}Ra : ^{228}Th , ^{234}U : ^{230}Th) is a common method to study vertical particle flux and input to the ocean (Hayes et al., 2018). Resuspension, sediment residence time in the water column, sediment and radionuclide

transport and other parameters are estimated using mass balance models (Zang et al., 2019; Baskaran et al., 2020).

Sediments accumulating on the bottom "write" the history of the accumulation of radionuclides and contaminants that can be deciphered with dating models (^{14}C , ^{210}Pb , ^{137}Cs) as long as they remain undisturbed. The sediment and radionuclide sources in the sediment profiles are investigated by a combination of dating and fingerprinting approaches. The inventories of radionuclides in the sediments and the source contributions of both radionuclides and sediments are estimated using mass balance models (Hong et al., 2021). Sediment mixing due to bioturbation in sediment profiles is investigated with $^{234}\text{Th}_{\text{xs}}$, ^{137}Cs , ^7Be , ^{14}C , $^{210}\text{Pb}_{\text{ex}}$ in estuaries, coastal areas and deep-sea sediments on different time scales (Li et al., 2021).

The radionuclides mentioned above have great potential to be used in the investigation of the fate of sediments and associated nutrients and pollutants in the Neman River- Baltic Sea system. The aim of the literature review is to examine the approaches currently used to utilise particle-reactive radionuclides in order to select those potentially useful in achieving the aim of the study.

1.2. Radionuclide's origin and behaviour in the water systems

The naturally occurring isotopes ^7Be , ^{210}Pb are commonly used for sediment transport in riverine and coastal areas. The major advantage of these fallout radionuclides is their independence of soil type and lithology (Griffins et al., 1977; Walling and Woodward 1992). ^7Be and ^{210}Pb constantly enter the soil and water surface in discrete pulses during rainfall and storms. Once at the surface, ^7Be comes into contact with vegetation, the water surface and soil particles. It quickly combines with soil particles or suspended matter in the water (Mabit et al., 2008; Olsen et al., 1986). Since the half-life of ^7Be is relatively short compared to its vertical migration in the soil, it is found in the uppermost layer. The factors influencing the stability of beryllium binding to the sediment during transport were investigated by Taylor et al. (2013).

Naturally, there are two types of ^{210}Pb typically found in soil. The lead supplied by dry and wet atmospheric deposition is unsupported ($^{210}\text{Pb}_{\text{ex}}$), while the second, termed supported, is formed by locally decayed ^{222}Rn . After burial in the soil layer, the unsupported $^{210}\text{Pb}_{\text{ex}}$ are no longer supplied by the atmosphere and their amount decreases (Baskaran, 2011). The highest activities of $^{210}\text{Pb}_{\text{ex}}$ are observed in the top 10 cm and of ^7Be in the top 3 cm of the soil (Bonniwell et al., 1999).

Man-made fallout radionuclides (^{137}Cs , Pu and ^{241}Am and others) have been brought to the Earth's surface by nuclear testing and various accidents over certain periods of time. The main major sources of $^{239,240}\text{Pu}$, ^{137}Cs and ^{241}Am in the environment are atmospheric nuclear tests (1945-1963), nuclear reactor accidents at Chernobyl (1986) and Fukushima (2011), and emissions from nuclear fuel reprocessing plants (Sellafield since 1950 and La Hague since 1966) (HELCOM, 2003).

Table 1. Estimated radioactivity release by different sources

Source	$^{239,240}\text{Pu}$, PBq	^{137}Cs , PBq	^{241}Pu , PBq	^{241}Am , PBq	Source
Atmospheric nuclear explosions	12 [i]	960 [ii]	170-190 [iii]	3.1 [ii]	[i] Hardy et al., 1973 [ii] UNSCEAR, 1982 [iii] Izrael et al., 1990
Sellafield	0.61 [iv]	39 [v];	22 [vi];	0.95 [vi] 0.54 [vii]	[iv] Cook, et al., 1997 [v] Boelens et al., 2016 [vi] Thakur and Ward, 2018
La Hague	0.0034[vi]	0.96 [v]	0.12 [vi]	-	[vi] Vintro et al., 2000
Chernobyl accident	0.072 [iix]	85 [ix]	1.5-4.0 [iix]	~(1.5-4.0)	[iix] Geckeis et al., 2019
Fukushima accidents	<0.000003 [iix]	8.8 [x]	<0.0003 [iix]	~(<0.0003)	[ix] UNSCEAR, 2000 [x] Imanaka et al., 2015

Atmospheric nuclear tests caused the widest and highest depositions of radionuclides (Table 1). The highest deposition of radionuclides was observed in the Northern Hemisphere (1963), as this is a major area of testing. Two years later, the peak deposition was observed in the Southern Hemisphere (1965) (Evrard et al., 2020). Contamination of the marine environment with plutonium isotopes occurred from discharges from spent fuel reprocessing plants and the Fukushima nuclear power plant accident, while the land area was contaminated to a greater extent by fallout from Chernobyl accident. The peak of caesium emissions (> 5 PBq/year) with liquid waste at the Sellafield plant was observed in 1975 (Gray et al., 1995), at the La Hague plant the maximum emissions (> 0.1 PBq/year) were recorded in 1972 (Guegueniat et al., 1997).

Huge amounts of produced ^{241}Pu ($T_{1/2} = 14.35$ years, more than 200 PBq) decay to the more dangerous ^{241}Am ($T_{1/2} = 432.2$ years), leading to its accumulation due to substantial disparities in their respective half-lives. By 2023, the total activity of ^{137}Cs has decreased more than three times due to radioactive decay. Thus, the widespread use of ^{137}Cs as a tracer in the environment is gradually decreasing, with spatial availability limited to areas of high initial concentrations (Foucher et al., 2021). Among the tracers under

consideration, the plutonium isotopes ($^{239,240}\text{Pu}$) and ^{241}Am will be more available for the sediment transport studies in the near future.

In freshwaters, ^{137}Cs , Pu and ^{241}Am are considered strongly bound to particulate matter and are used for suspended matter and sediment transport studies.

Caesium. Caesium-137 is one of the best known and most widely used radioactive tracers for the study of soil erosion, sediment transport, dynamics and sources, dating of sediments and other applications (Loba et al., 2022; Evrard et al., 2020; Li et al., 2021). It is an alkali metal that occurs in the natural environment mainly as Cs(I), and in general caesium exists in the environment as the easily soluble ion Cs^+ (Holleman et al., 2001).

In soil, it is mainly associated with clay minerals (especially illite, montmorillonite and zeolites), and its mobility is influenced by the content of organic compounds, the presence of nitrogen and potassium, and pH (Livens & Loveland, 1988). Giannakopoulou et al. (2007) observed the highest caesium sorption in soils at pH8. Korobova and Chizhikova (2007) demonstrated that labile and amorphous forms of iron influence the fate of ^{137}Cs in alluvial soils.

In freshwater, ^{137}Cs is characterised by a high particular reactivity with a coefficient of distribution between solid and liquid phase (K_d) of up to $5 \cdot 10^5$ L/kg water, and this value decreases significantly with increasing water salinity and can be observed in the areas of transition from freshwater to seawater (Hong et al., 2012).

When sorption occurs on soil and sediment particles, caesium is deposited on the clay minerals at specific locations. In this case, part of the process occurs rapidly, while the slow binding at less accessible sites can take up to 100 days. The results of Smith and Comans, 1996 suggest that there are several phases of remobilisation of caesium from lake sediments. The proportion of ^{137}Cs inventory remobilised from lake sediments each year was 3% and 0.04% after 2 and 30 years after fallout, respectively. Tomczak et al. 2021 found that the caesium K_d in a river system depends on several factors, including the physicochemical properties of the suspended particles and the hydrodynamics.

In brackish and salt water, ^{137}Cs acts as a conservative tracer similar to other alkali elements (Brewer et al., 1972). The distribution of ^{137}Cs between seawater and sediment depends on the geochemistry of the water, the mineralogical composition of the sediment and other contaminants (Lujanienė et al., 2004; Olsen et al., 1980; Hong et al., 2011).

Plutonium. Plutonium forms a wide range of compounds with oxides and organic substances and has the most complex chemistry among the

radioactive elements used for environmental research. Pu isotopes have a high ionic potential, are strongly bound to iron/manganese oxides and humic substances and are retained in the upper soil layer (Portes et al., 2018). The isotopes ^{239}Pu ($T_{1/2} = 24\ 100$ years) and ^{240}Pu ($T_{1/2} = 6560$ years) have low mobility in the environment.

In natural waters, sorption behaviour, solubility, complexation and redox reactions depend on pH, oxidation reduction potential (Eh) and CO_2 content. These factors lead to a variability of the partition coefficient of plutonium in freshwater, ranging from 11000 to 5200000 mL/g and in soils from 32 to 9600 mL/g. In the absence of clay particles and organic colloids, plutonium can be mobilised by macromolecular humic or fulvic acids (HAs/FAs) in the liquid phase; in contrast, plutonium is immobilised by HAs/FAs that are in a solid phase (Geckeis et al., 2019). Sorption of plutonium (V) in the presence of humic substances or Fe (II) is accompanied by reduction to Pu (IV) and Pu (III) (Lujaniene et al., 2012). Lin et al. (2019) investigated the long-term fate of plutonium (Pu) in sediment cores of Nagasaki sediments and concluded that the factor of natural organic matter content may play a major role in the sequestration of plutonium in sediment profiles than the other factors such as sorption to mineral surfaces and limits of solubility. Sorption process of plutonium in sediments include ion exchange reactions, the formation of surface complexes and the slow incorporation into the crystal structure of iron minerals can be observed. Plutonium from nuclear weapons tests and reactor particles is found in a form that is difficult to dissolve or in a form that associates rapidly with particles and tends to become immobilised. Emissions from reprocessing plants or nuclear waste may show greater mobility (Choppin and Morgenstern, 2001).

Americium. Under the given environmental conditions, the stable state of ^{241}Am ($T_{1/2} = 432$ years) is Am(III). Americium and plutonium behave similarly in the environment and the partition coefficient for americium was found to be more than 10 times that of plutonium (Kinoshita et al., 2021; IAEA, 2004). The mobility of americium as a member of the actinide group in nature is influenced by several competing mechanisms such as pH, temperature, Eh, colloid formation and the availability of complex ligands. At neutral pH, americium has good thermodynamic stability over a wide range of oxidative-reducing potential (Morris and Raiswell, 2002). In natural waters, americium can form stable complexes with humic substances (Takahashi et al., 1994). Kuwabara et al. (1999) reported similar behaviour of americium and plutonium in deposition and transport processes in the Irish Sea.

The presence of organic matter, minerals and oxides in soils, has a greater influence on the mobility of plutonium than americium and it is found

in the soluble and exchangeable fraction. The distribution of americium among the different fractions of soil particles is more uniform than that of plutonium, which is more closely related to the fraction of smaller particles (Fukai and Yokoyama, 1982).

1.3. Radionuclide applications for studies of sediment sources

The development of measures to reduce water and soil pollution requires the investigation of the sources of sediments and pollutants in watersheds, and one of the effective approaches to identify the sources is the fingerprinting approach (Gellis and Noe, 2013). Among the other approaches, this method shows satisfactory results and has been positively received by many scientists (Evrard et al., 2020). Oldfield et al. (1979) formulated the sediment fingerprint method as a way to quickly assess sediment sources by examining the properties of the sediment themselves.

Particle-reactive radionuclides have been shown to retain their characteristics during sediment transport (Walling and Woodward 1992). In river systems, they are used as sediment properties to distinguish sources based on the characteristics of radionuclide occurrence and distribution. The tracers ^{137}Cs , ^7Be , ^{210}Pb , $^{239,240}\text{Pu}$ are commonly used in various approaches to study the origin of sediments. The radionuclides can be used alone (Wang et al., 2021a; Zhuang et al., 2019; Gellis et al., 2019) or can be included to composite fingerprints (Lizaga et al., 2020; Navas et al., 2020; Zeng et al., 2022).

Activities of particle-reactive radionuclides (also known as fingerprints) can be used to distinguish between sediments of different origins in the soil layer (surface, subsurface), different soil disturbances (natural, cultivated), the type of anthropogenic impact (mining, nuclear accidents), areas affected by forest fires, between fluvial sources, to determine the relative age of sediments and others (Table 2).

Table 2. Particle-reactive radionuclides application in the studies of sediment sources

#	Sediment source	Tracers	Indicator	Example
1	Topsoil, subsoil	$^{210}\text{Pb}_{\text{ex}}$, ^{137}Cs , ^7Be	Surface sediments enriched with ^{137}Cs ; Subsurface sediments depleted with ^{137}Cs	Chen et al., 2021 Gellis et al., 2019 Lamba et al., 2019
2	Recent, old sediment	^7Be , $^{210}\text{Pb}_{\text{ex}}$	Recently eroded sediments enriched with ^7Be ; re-	Le Gall et al., 2018

#	Sediment source	Tracers	Indicator	Example
			suspended matter depleted with ⁷ Be	Le Gall et al., 20173
4	Mining impacted soil	¹³⁷ Cs	Sediments depleted with ¹³⁷ Cs and ²¹⁰ Pbex	Sellier et al., 2020
5	Soil after wildfires	²¹⁰ Pb _{ex} , ¹³⁷ Cs	Sediments enriched with ²¹⁰ Pb _{ex} , ¹³⁷ Cs	García-Comendador et al, 2020
6	Fluvial sediment in the sea	²²⁶ Ra, ²³⁸ U	High values of ²²⁶ Ra/ ²³⁸ U indicate river origin; Marine sediments 0.5-1.0	Wang et al., 2021a Du et al., 2021 Lin et al., 2020
7	Water reservoir (river, estuary, lake)	²³⁹ Pu, ²⁴⁰ Pu	²⁴⁰ Pu/ ²³⁹ Pu versus 1/ ²³⁹⁺²⁴⁰ Pu – indicates Pu source and dilution	Liu et al., 2020
8	The sediment of contaminated areas	²³⁹ Pu, ²⁴⁰ Pu, ¹³⁷ Cs, ¹³⁴ Cs	²⁴⁰ Pu/ ²³⁹ Pu: Global fallout (~0.18), Pacific Test Grounds (0.27-0.36), Nevada tests (~0.032) and Chernobyl accident (~0.4); ²³⁹⁺²⁴⁰ Pu/ ¹³⁷ Cs ~ 0.024 (Global fallout); ¹³⁴ Cs as Fukushima accident signal	Salminen-Paatero et al., 2012 Yamada & Zheng, 2020 Pham et al., 2017 Zhang et al., 2019
9	River / coastal	⁷ Be/ ²³⁴ Th	Recent riverine particles in marine water >0.5; Older marine sediments <0.1	Wu et al., 2018

Plutonium mixing model. Plutonium isotopes are widely used for sediment origin studies in seas, oceans (Quiao et al., 2017, Hao et al., 2018, Yamada and Zheng, 2020) and rivers (Zhang et al, 2018, Liu et al., 2020). The unique ²⁴⁰Pu/²³⁹Pu atomic ratio is a useful marker for distinguishing the origin of radionuclides from global fallout of atmospheric nuclear explosions (~0.18), releases of Pacific Test Grounds (PPG) (0.27-0.36), Nevada Tests (0.032) and Chernobyl accident (~0.4). (Yamada and Zheng, 2020).

The expression proposed by (Krey,1976) is used as an end-member mixing model for the mixing of two different isotope ratios:

$$A = \frac{Pu_1}{Pu_2} = \frac{(R_2 - R_{sample})(1 + F \times R_1)}{(R_{sample} - R_1)(1 + F \times R_2)} \quad (1)$$

$$Pu_{PPG} + Pu_{GF} = 1 \quad (2)$$

where **F** – conversion coefficient of atomic ratio to activity ratio (ratio of decay constants 3.674 for ²⁴⁰Pu/²³⁹Pu), **R_i** – ²⁴⁰Pu/²³⁹Pu atomic ratio of the sources 1 and 2. R value is estimated to be between 0.3 and 0.36 for the initial phase of PPG release (Zhang, 2018; Lindahl, 2011). Recent plutonium

releases from PPG were estimated by Pittauer et al. (2017) to be 0.27 based on their studies of coral reefs in Guam.

Plutonium end-member mixing model is used to study sediment transport in marine and ocean waters. Wang et al. (2020) used $^{240}\text{Pu}/^{239}\text{Pu}$ to estimate the contribution of PPG plutonium to bottom sediments in the Bohai Sea and Yellow Sea. The proportions of PPG contribution to bottom sediments varied between 22% and 29%, which was used to build a mass balance model for the Bohai Sea and Yellow Sea. Pittauer et al. (2017) used plutonium isotope ratios to investigate the chronology of plutonium transport in the Indonesian Current. Sediment transport from the Pacific to the Indian Ocean was revealed by the fact that plutonium from the PPG source entered the study area after 1970 and its proportion in the sediment core studied was between 40 and 70%. Corcho-Alvarado et al. (2022) determined plutonium from global fallout and the Nevada Test Site in deep-sea sediments in the Gulf of Mexico. The results indicated that the proportion of plutonium from the Nevada test site increases with depth. Liu et al. (2020) have demonstrated the use of the fingerprints of $^{240}\text{Pu}/^{239}\text{Pu}$ and $1/^{239,240}\text{Pu}$ as indicators of sediment origin. The shift of $^{239}\text{Pu}/^{240}\text{Pu}$ in the sediment mixture towards one of the plutonium sources is caused by their different proportional contributions controlled by different environmental conditions. Sediment dynamics change the absolute contents of $^{239,240}\text{Pu}$ in sediment mixtures due to dilution of the sediment, resulting in differences in the characteristic ranges of plutonium concentrations of river and lake sediments. The combination of these effects is used as a fingerprint to determine the origin of sediments in coastal and marine areas.

Frequency-based approach. Peart and Walling (1986) identified ^{137}Cs as a good tracer that is independent of rock characteristics. Currently, ^{137}Cs is still used in some sediment provenance studies due to its sufficient residual activity and sensitive detection methods. ^{137}Cs is used as a sediment tracer to distinguish surface and subsurface sediments (Chen et al., 2021), forest fire areas (García-Comendador et al., 2020; Muñoz-Arcos et al., 2021), the origin of radionuclides (Zhang et al., 2022) and as a component of composite fingerprints (Lim et al., 2019, García-Comendador et al., 2021). The combination of ^7Be with ^{137}Cs is utilised to distinguish between recent and long-term eroded surface and subsurface sediments (Le Gall et al., 2018). The known characteristics of the distribution of ^{137}Cs and $^{210}\text{Pb}_{\text{ex}}$ in sediment profiles are used to identify areas affected by mining (Sellier et al., 2020). Burnt areas are naturally enriched in ^{137}Cs and $^{210}\text{Pb}_{\text{ex}}$ due to the release of ^{137}Cs and $^{210}\text{Pb}_{\text{ex}}$ by the burnt plants and the reduction of soil mass. Further exposure to atmospheric fallout enriches them with ^7Be and $^{210}\text{Pb}_{\text{ex}}$, and these

features create a specific fingerprint of burnt areas that is used for studies (Chen et al., 2021).

The contributions of sediment sources in the catchments are resolved by various mixing models that suggest some statistics. Because of their relative ease of laboratory analysis, ^7Be , ^{137}Cs and ^{210}Pb can be very useful when large numbers of samples are required. These tracers are used to determine the contributions from three or more sources, e.g., surface, subsurface, fresh and old sediments. There are many models fitted to different sets to determine the contributions of sources to the sediment mixture (Li et al., 2020; Collins et al., 2010; Du et al., 2019; Proshad et al., 2022; Motha et al., 2003; Hughes et al., 2009; Laceby & Olley, 2015). These models are based on the conservation of mass balance and the basic mixing equation:

$$\mathbf{M}_j = \sum \mathbf{X}_k \mathbf{T}_{jk}^s; \sum_k \mathbf{X}_k = \mathbf{1} \quad (3)$$

where \mathbf{M}_j – tracers' mixture; k - number of sources, j – number of tracers; \mathbf{T}_{jk}^s – j -tracers' mean in the source k , \mathbf{X}_k – proportional contribution of source k . The calculation assumes that the equation includes all contributing sources, that the tracers act conservatively and that the concentrations of the tracers do not change during transport from the sources to the target mixture (Stock and Semmens, 2013). The number of sources should not be larger than the number of tracers+1, so that the system can be solved directly.

When the number of tracers is equal to or greater than the number of sources, the system becomes overdetermined and can only be solved numerically using optimization methods. There are two approaches to finding solutions in cases with an overdetermined system. The first is the established frequentist approach and a relatively new probabilistic approach based on the Bayesian' theorem.

The “frequentist” approach utilizes different models (Davis & Fox, 2009; Verduyze & Grabowski, 2018; Collins et al., 2017). The search for optimal solutions based on the sums of the first powers of the absolute or relative errors or their squares (Motha et al., 2003). The best-known method used in studies of sediment sources is that proposed by Collins (Collins et al., 1997). The equation has been modified in various ways. In recent studies the contribution of the sources has been determined by the following equation:

$$\mathbf{R} = \sum_{i=1}^n \left\{ \frac{c_i - (\sum_{s=1}^k K_s P_s S_{si} V_{si})}{c_i} \right\}^2 \times W_i \quad (4)$$

$$\mathbf{RME} = \mathbf{1} - \mathbf{R}/n$$

where: \mathbf{n} - a number of tracers; C_i - distribution of tracer i in the particulate matter; \mathbf{k} – quantity of sediment sources; \mathbf{P}_s – the share of (s) source contribution, modelled as a truncated normal distribution ($0 \leq x \leq 1$), derived with a simulated mixture mean (μ_m) and standard deviation (σ_m), with $\sum P_{s_i} = 1$; S_{si} –distribution of tracer (i) in the source (s); W_i - discriminatory weighting of the tracer determined by the ratio of source samples correctly classified with the tracer (P_i) and with lowest P_i (K_s was not used ($K_s=1$)); K_s – factor to account for particle size, calculated as the ratio of the specific surface areas of the source and stream samples; SV_{si} – weighting factor describing within-source tracer variation (normalised for each tracer), determined as an inverse coefficient of variation (Wilkinson et al., 2013); **RME** – relative mean error (goodness of fit).

The mixing equation is solved using the Monte Carlo algorithm, which enumerates different contributions from sources until the predicted value is as close as possible to the tracer concentrations in the target sediment. The median mixture model provides better accuracy when the distribution of tracers in the samples is related to the distribution of sources than to individual samples (Olley et al. 2013). Normal distributions of tracers and sources in the sediment are determined using their means and standard deviations. The Student's t-distribution is used to model the tracer activities in the samples (C_i) and in the source (S_{si}). The Student's distribution gives better results for a small number of samples because it gives more weight to the tails than the normal distribution (Krause et al., 2003).

The choice of weighting factors is a question of the individual case. Jalowska et al. (2017) attempted to add either tracer-specific correction factors or an individual source element correction factor, but they did not improve the model proposed by Laceby et al. (2015). Le Gall et al. (2018) applied a correction factor for particle size based on thorium concentration for suspended particles only. This correction was based on the assumption that the transported sediments were partially "cleaned" by the flow and were different from the original sediments of the banks and soil. This correction led to an improvement in the overlap of the target and source data ranges of ^{137}Cs activities. The Lamba et al. (2019) model included a correction coefficient for particle size calculated based on the ratio of the specific area of the target sediments to the source sediments. The fraction $< 10 \mu\text{m}$ was used by Rode et al. (2018) to avoid particle size correction. The tracer discriminatory weighting calculated using multivariate discriminant function analysis was added to the formula. The same weighting for each tracer along with $< 63 \mu$ fraction was used by Gellis et al. (2018). The factor was calculated as the ratio

between the number of samples correctly classified by a given tracer and the smallest proportion of correctly classified samples in the group of tracers used.

Bayesian approach. The probabilistic Bayesian approach is an alternative or complement to the frequency-based methods (Moore & Semmens, 2008; Semmens, et al., 2009). The main prerequisite for the use of probabilistic models for sediment source attribution was the inability to solve the basic mixing equation analytically without performing various transformations to limit the number of sources. In contrast to frequentist approaches, the Bayesian method considers the parameter as a random variable rather than an unknown constant. The actual distribution of the parameter depends on the actual data obtained and not on all possible states based on distributions. When investigating sediment sources, this approach determines the probability of contributions from each source, taking into account knowledge of its concentration in the target sediment. Given a vector (\mathbf{g}_q) characterising all possible cases of contributions (\mathbf{g}_i) from sources whose sum is equal to one, it is possible to determine the probability of the contribution vector for each source (q) based on experimental data and a priori information (Moore & Semmens, 2008):

$$P(\mathbf{g}_q | \mathbf{data}) = \frac{L(\mathbf{data} | \mathbf{g}_q) \times p(\mathbf{g}_q)}{\sum L(\mathbf{data} | \mathbf{g}_q) \times p(\mathbf{g}_q)} \quad (5)$$

where $p(\mathbf{g}_q)$ is the prior probability distribution based on prior information; \mathbf{g}_q and \mathbf{q} are the given data and proposed vector, respectively; $L(\mathbf{data} | \mathbf{g}_q)$ is the likelihood of measured tracer value under \mathbf{g}_q ; A key component of Bayesian modelling is the determination of an appropriate prior distribution for variables and hyperparameters (Bolstad & Curran 2016). Hyperparameters are parameters that define uncertainty in prior data - mean and variance.

The approach involves defining a prioritized probability distribution, creating a likelihood function for the statistical model and calculating the resulting probability function by revising prior data based on the measured data (Bolstad & Curran 2016). Since it is impossible to account for all possible variations in the sample area, even if a large number of samples are used, "non-calculated variations" or residual errors are included in the model. Prior information can be derived from the results of modelling the sediment transport of the river system. Bayesian approach utilizes Markov Chain Monte Carlo (MCMC) algorithm. Open-source software such as STAN (Stan Development Team) (Stan Development Team, 2015) and JAGS (Just another Gibbs sampler) (Plummer et al., 2006) are utilized to solve Bayesian models. Radionuclides are not used in the Bayesian approach alone to obtain

contributions from sediment sources. This is because the approach requires a considerable diversity of tracers to obtain a sufficient number of tracers with conservative properties given the number of sources.

There is no universal tracer for the study of sediment sources, but the most usable are stable isotopes and fallout radionuclides, as this set is highly adaptable to the situation. Combinations of different properties, including microelements and stable isotopes (Huang et al., 2020), magnetic and optical properties (Boudreault et al., 2018; Nosrati et al., 2021), physical properties and radionuclides (García-Comendador et al., 2021; Valente et al., 2020) are used. Lizaga et al. (2020) demonstrated the application of ^{137}Cs , ^{40}K , ^{226}Ra , ^{234}Th and ^{238}U in a set of 34 tracers to study spatial and temporal changes in source partitioning in Mediterranean mountainous regions.

Muñoz-Arcos et al. (2021) used geogenic and fallout radionuclides such as ^{137}Cs and $^{210}\text{Pb}_{\text{ex}}$, ^{226}Ra , ^{232}Th , ^{238}U and ^{40}K as tracers to investigate the origin of sediments in burnt environments. In the selection of tracers, ^{226}Ra , ^{232}Th , ^{238}U and ^{40}K were discarded as they did not fall within the threshold range of source concentration. Very few studies use ^{241}Am , $^{239,240}\text{Pu}$ for the statistical approach, as such models require a large number of samples and the treatment in the laboratory is quite expensive and time-consuming. Perich et al. (2022) demonstrated the use of $^{239,240}\text{Pu}$ isotopes to discriminate five watersheds in the USA. A Bayesian approach was used to predict increases in sediment formation from riparian sources due to urbanization. The authors pointed out the advantages of plutonium over geochemical and organic tracers in cases of overlapping sources when these tracers cannot be used.

The similarity of the results obtained with Bayesian and frequentist methods has been observed in several studies. García-Comendador et al. (2021) studied sediment sources and erosive processes in the Es Fangar catchment in Mallorca, Spain. The Bayesian mixing model MixSIAR and end-member mixing analysis led to analogous conclusions throughout the study. The fallout radionuclides ^{137}Cs and $^{210}\text{Pb}_{\text{ex}}$ were used along with a series of colour tracers. Du et al. (2019) compared discriminant function analysis (DFA), Bayesian and Walling-Collins models. The artificial mixture study showed the reliability of both Bayesian and Walling-Collins models, but the DFA analysis showed a moderate result in this experiment with a mean absolute error of 18.5%. As Stock and Brice. (2016) pointed out, although Bayesian models can account for a variety of data sources, they are not a panacea for overdetermined systems. As well as Bayesian approach, the frequency approach should also be used with caution in such cases. Latorre et al. (2021) compared different approaches for selecting a tracer and found significant shortcomings and erroneous solutions for cases where the system

does not follow the $n - 1$ rule. The additional tests of reliability are necessary because faulty tracers can lead to the incorrect result. The respective new systems therefore require tests of the applicability of the tracers, since the models used can produce more than one solution and still be mathematically correct.

The rationale for choosing the size range of the particles under investigation is also necessary in the fingerprinting method, as tracers may have different affinities for different size ranges (Fukai and Yokoyama, 1982; Laceby et al., 2017). The most common practice to avoid particle size is to sample the $< 63 \mu\text{m}$ fraction that can significantly mitigate the effects of particle size during sediment transport (Walling, 2013).

1.4. Sediment transport studies

Sediment dynamics studies aimed to understand the fate of sediments and associated with them particle reactive substances and pollutants in aquatic systems. After release from the source, sediments undergo numerous processes of transportation, deposition, resuspension and burial. Most of the sediment delivered by rivers settles in estuaries and coastal areas and plays an important role in sedimentological and geomorphological processes.

Sediments are an important link between the water column, living organisms and bottom sediments in terms of transport of nutrients and chemical substances (Martin and Whitfield, 1983; Turner and Millward, 2002). Many of the bioactive elements reach the ocean depths with the sinking particles and provide nutrients to pelagic and benthic organisms (De La Rocha and Passow, 2007). Carbon transport is also provided by sinking particles - photosynthetically bound carbon dioxide on particles is transported from the sea surface to the deep sea. To better understand and assess these processes, particle-reactive radionuclides (e.g., ^{234}Th , ^{210}Po , ^7Be , ^{210}Pb , ^{137}Cs , $^{239,240}\text{Pu}$) are used as tracers for sediment dynamics in freshwater and seawater systems. The known source function, high reactivity and radioactive decay make them a very useful tool for tracing sediment fate (Wang et al., 2021b; Benoit et al, 2020; Hong, 2021; Baskaran, 2020).

1.4.1 Sediment transport in catchments

The horizontal transport of sediments in rivers can be characterised by sediment transit time or apparent age. This is the time it takes for sediments to travel from their source to a certain point. The natural radionuclides ^7Be , ^{1210}Pb and ^{210}Po are suitable in this case. Gellis et al. (2019) determined the

short-term age (up to 1 year) of sediments in an agricultural stream by relating ^7Be activities in target and source sediments:

$$\tau_s = \frac{-1}{\lambda_{\text{Be}}} \ln \left(\frac{S_{\text{Be}}}{95S_{\text{Be}}} \times \frac{T_{\text{Be}}}{S_{\text{T}}} \right) \quad (6)$$

where $95S_{\text{Be}}$ - 95th percentile of ^7Be in the surface sediments, λ – decay constant of ^7Be (0.01305/day); T_{Be} – activity ^7Be in the target sample, S_{T} – the share of surface origin sediments in the stream.

The longer scale age (τ_l), up to 85 years, can be calculated using the $^{210}\text{Pb}_{\text{ex}}$ method:

$$\tau_l = \frac{-1}{\lambda_{\text{Pb}}} \ln \left(\frac{S_{\text{Pb}_{\text{ex}}}}{wS_{\text{Pb}_{\text{ex}}}} \right) \quad (7)$$

where $wS_{\text{Pb}_{\text{ex}}}$ - weighted $^{210}\text{Pb}_{\text{ex}}$ activity in the surface sediments, λ – decay constant of ^{210}Pb (0.00008501/day). Sediments containing a negligible amount of $^{210}\text{Pb}_{\text{ex}}$ are considered older than 85 years in this approach. The model assumes that the mixing process has no significant influence on the tracer concentration. Gellis et al. (2019) reported that the ^{210}Pb and ^7Be used in this approach can lead to significantly different results for sediment age. This was explained by the fact that ^{210}Pb better describes the mean age of the surface-derived fraction, while ^7Be only characterises the fraction from sources with recent input.

Since the $^7\text{Be}/^{210}\text{Pb}_{\text{ex}}$ ratio is relatively constant during rainfall in a given area (Wilson et al, 2008) it has been successfully used to estimate sediment transport times that have range up to one year. Because of ^7Be decays faster ($T_{1/2} = 53.12$ d) than ^{210}Pb ($T_{1/2} \approx 8140$ d) their ratio indicates the time elapsed since the rain event. The age of the sediments is calculated using the equation of Matisoff et al. (2005):

$$t = \frac{-1}{\lambda_{7\text{Be}} - \lambda_{210\text{Pb}}} \ln \left(\frac{A}{B} \right)_{\text{sed}} + \frac{1}{\lambda_{7\text{Be}} - \lambda_{210\text{Pb}}} \ln \left(\frac{A_0}{B_0} \right)_{\text{prec.}} \quad (8)$$

where t – age in days, A and A_0 – ^7Be activity in the target samples and precipitation; B and B_0 – ^{210}Pb activity in the target samples and precipitation; λ – decay constant. It is assumed that "old" resuspended particles have a low $^7\text{Be}/^{210}\text{Pb}_{\text{ex}}$ ratio compared to "fresh" recently labelled sediment. The sediment could be dated to an age of up to 1 year using this approach. Schmidt et al. (2021) used this approach to study suspended particles (0.45 μm) in Galveston Bay. It was found that the wave regime creates the conditions for suspended matter and pollutants to remain in the bay for several months.

Migration of fallout radionuclides (^{137}Cs , ^{241}Am , $^{239,240}\text{Pu}$) from the catchment is impeded by the distribution of sedimentary deposits, resulting in

a duration of thousands of years (Smith et al., 1987). Beasley et al. (1984) estimated the residence time of Am and Pu based on the ratio between the radionuclide inventory in the catchment and the amount of radionuclide already released in the catchment. The response time for $^{239,240}\text{Pu}$ and ^{241}Am was estimated to be 6000 years, with annual releases through the catchment assumed to be 0.3 and 0.08 Ci/year, respectively. Based on the Cs/Pu ratio (which was 53), the waters of the Columbia catchment (670000 km²) were found to export about 200 Ci ^{137}Cs with sediment runoff and about 300 Ci with the dissolved phase and by desorption of estuarine sediments. Smith et al. (1987) assumed that the flux of radionuclides is proportional to the integrated inventory in the Saguenay catchment (78000 km²) for times greater than 20 years after fallout. According to the time-dependent two-component model, the estimated residence time of ^{137}Cs was about 1000 years, that of plutonium about 3000 years. The residence time of plutonium corresponds to an annual erosion fraction of 0.023% of its total inventory in the soil.

Considering the annual input of plutonium constant (Beasley et al., 1984) the annual flux of fallout radionuclides (^{137}Cs , ^{241}Am , $^{239,240}\text{Pu}$) that exported from the catchment area can be estimated by the relation between catchment area and fallout radionuclide inventory (Zhang et al., 2019):

$$Q = D \times I \times \ln(2)/t \quad (9)$$

where D is the catchment area of river, I is the reference tracer inventory on the catchment area, t is the plutonium residence time in the catchment area.

1.4.2 Studies of mixing zones of fresh and seawater

The transport of sediments in rivers ends in coastal and estuarine areas, where the waters mix and various physical and chemical processes take place. Abrupt changes in particle and organic matter concentrations, water flow, salinity, pH and other chemical conditions are typical of aquatic systems where freshwater and saltwater mix (Turner and Millward, 2002). Dynamic conditions and high particle concentrations lead to rapid removal of reactive tracers and also favour resuspension processes at these sites.

Studies of particle dynamics in water bodies provide useful information that can serve as a scientific basis for waterway maintenance, estuary management and fisheries management. Important indicators of sediment dynamics are the rate at which particles are removed from the water column and their residence time. The short-lived radionuclides ^7Be , ^{234}Th , ^{210}Po and their ratios $^{210}\text{Po}/^{210}\text{Pb}$, $^7\text{Be}/^{210}\text{Pb}_{\text{ex}}$, $^7\text{Be}/^{234}\text{Th}$ are mostly used to estimate sediment removal pathways and times (Wang et al., 2021b). Waples, (2022)

also showed the possibility of using ^{210}Bi and $^{210}\text{Bi}/^{210}\text{Pb}$ for dynamical systems. The short-lived ^{234}Th ($T_{1/2} = 24.1\text{d}$) is an efficient tool to for studying particle export and dynamics on the scale of days to weeks (Feng et al., 1999). ^{210}Po ($t_{0.5}=138.3$ days) is useful to estimate the integrated flux over several months (Bam and Maiti, 2021).

The atomic ratio $^7\text{Be}/^{210}\text{Pb}_{\text{ex}}$ and $^{137}\text{Cs}/^{210}\text{Pb}_{\text{ex}}$ is used to trace river sediments in the coastal area (Du et al., 2010). Due to the high particle reactivity of ^{137}Cs in freshwater, the presence of riverine particles in estuaries and coastal areas can be identified by the comparatively elevated levels of ^{137}Cs activity (Wang et al., 2016). ^7Be and ^{210}Pb have atmospheric and riverine origins in the coastal area and can be used as indicators of riverine sediment input. Wang et al. (2021b), using $^7\text{Be}/^{210}\text{Pb}_{\text{ex}}$ and $^{137}\text{Cs}/^{210}\text{Pb}_{\text{ex}}$ tracers, found that sediment particles in the northern passage of the Changjiang (Yangtze) estuary were inflowing from the sea. The authors observed a lower $^7\text{Be}/^{210}\text{Pb}_{\text{ex}}$ ratio in the estuarine waters (1.0) compared to the atmospheric deposition ratio (5.2), which was attributed to an additional input of sediment from the sea. In general, ^{234}Th , ^{210}Po , ^{210}Pb , ^7Be , ^{137}Cs and their ratios are suitable for studying particle transport in a range from a few days to a hundred years (Wang et al., 2021b). $^{234}\text{Th}_{\text{ex}}/^{210}\text{Pb}_{\text{ex}}$ is useful for assessing the resuspension process in the estuary. The depletion of the ^{234}Th inventory in suspended solids may indicate that a resuspension process is taking place (Rutgers Van Der Loeff and Boudreau, 1997). Based on the increased $^{234}\text{Th}_{\text{ex}}/^{210}\text{Pb}_{\text{ex}}$ in suspended matter, Wang et al. (2021b) concluded that tides are associated with ocean particle input and resuspension processes. $^7\text{Be}/^{234}\text{Th}$ in surface sediments can be used as an indicator of the relative residence time of fluvial sediments in the marine environment. Wu et al. (2018) distinguished fresh river sediments based on the $^7\text{Be}/^{234}\text{Th}$ ratio in surface sediments in the Rhône River mouth (Gulf of Lions). Younger river sediments contained more ^7Be and $^7\text{Be}/^{234}\text{Th}$ was greater than 0.5. A value of less than 0.1 was attributed to "older" marine sediments. Waples, 2022 suggested the use of ^{210}Bi in dynamic systems with low water residence time. The $^{210}\text{Bi}/^{210}\text{Pb}$ ratio can be used to estimate the particle flux in such systems, while the use of ^{210}Po and ^{234}Th in such conditions is complicated due to the higher removal rate.

The fate of particle-reactive radionuclides is assessed by determining the sources of radionuclide entry into and removal from an aqueous column in dissolved or sorbet form. Based on literature data (Cochran, 2003 ; Feng et al., 1999; Benoit et al, 2020; Wang et al., 2021b; Wang et al., 2020; Wu, 2018), briefly the behaviour of PRR radionuclides in a water column can be described by the simple box model (Figure 2).

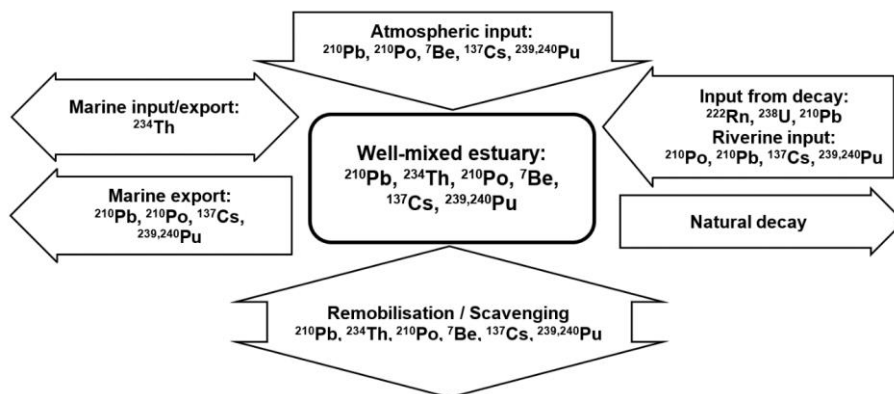


Figure 2. Simplified box model of ^{210}Pb , ^{234}Th , ^{210}Po , ^{137}Cs and ^7Be in a well-mixed estuarine system

With the exception of thorium, radionuclides enter the water column through atmospheric deposition and river flows. The input of ^{210}Pb , ^{234}Th and ^{210}Po into the water column is primarily the result of the radioactive decay of the parent radionuclides ^{222}Rn , ^{238}U and ^{210}Pb . Partially the radionuclides return to the dissolved state by resuspension from sediments. The resuspension process has the most significant impact on the concentration of longer-lived radionuclides (^{137}Cs , ^{210}Pb), as they have time to accumulate in larger quantities (Huang et al., 2010). In estuaries, the removal flux can be negative, which is interpreted as resuspension prevails over removal on particles (Huang et al., 2013). A stable, constant reduction in concentration occurs primarily through the decay of radionuclides (^7Be , ^{210}Po , ^{210}Pb , ^{234}Th , ^{137}Cs), which is more pronounced for the short-lived ^7Be , ^{210}Po and ^{234}Th . Some radionuclides leave the estuary before they decay. By binding to sinking particles, the radionuclides are exported to the seabed.

A simple box model describing the fate of radionuclides in a water column assumes that the radionuclide activity characterises the column well on average and that all imports and exports of radionuclides occur in steady-state mode. *Multi-box models* can take into account the non-steady-state mode and the interaction among different phases of radionuclides, including the dissolved phase, colloidal phase, and particulate phase on suspended or sinking particles (Cochran and Masqué, 2003; Huang et al., 2013). Seo et al., (2021) demonstrated the use of steady-state and non-steady-state scavenging models to estimate the behaviour of ^{210}Pb and ^{210}Po in productive shelf and oligotrophic waters. Total, truly dissolved, particulate and colloidal fractions were considered. Atmospheric deposition was not considered significant because the $^{210}\text{Po}/^{210}\text{Pb}$ ratio in precipitation was low (< 0.2). A non-steady

state model was considered for the East China Sea shelf area invaded by the Northwest Pacific Ocean (NWPO). Lateral transport, atmospheric deposition and removal flux are assumed to be constant in the applied model. The authors found that the removal rate of ^{210}Pb was higher in the productive area, while the removal rate of ^{210}Po was higher in the oligotrophic waters. Non steady state model showed the input ^{210}Po from sinking particles and bottom sediments. The authors concluded, that productive waters are characterised by a high scavenging rate of ^{210}Pb and a high remobilization of ^{210}Po from organic material.

Residence time. Mass balance models are used to assess several parameters: settling/resuspension flux, atmospheric input, horizontal export and residence times (Seo et al., 2021; Benoit et al., 2020; Wang et al., 2021b). In coastal and marine waters, residence time describes the average time required for particles to sink through the water column from the water surface to the bottom of the layer under consideration. Assuming a well-mixed system and neglecting desorption from resuspended particles, the residence time of ^{210}Po and ^7Be in the estuarine system can be estimated using the equation of Baskaran et al. (1997):

$$\tau_{Pb} = 1/(\psi_c^{Pb}) = \frac{A_d}{R+A-\lambda A_d+\lambda A_{Rn}}, \tau_{Be} = 1/(\psi_c^{Be}) = \frac{A_d}{R+A-\lambda A_d} \quad (10)$$

were λ - decay constant; λA_{Rn} - ^{210}Pb production term from ^{222}Rn activity in the water column; A_d - activity of the tracer in the dissolved phase; R - total riverine input of the tracer; A - total atmospheric input of the tracer; ψ_c - first order rate constant for removal on particles.

Residence time is an important parameter in the study of the export of adsorbed pollutants in water systems. Liu et al. (2021) studied the export fluxes of polycyclic aromatic hydrocarbons (PAHs) in the Bering Sea, Chukchi Sea and Canadian Basterin. Using $^{210}\text{Po}/^{210}\text{Pb}$, the residence time of PAHs was estimated to range from 55 to 133 days. The results illustrate a "shelf-sink effect" leading to a sinking of PAH during transport from the Bering Sea to the Chukchi Sea. Wang et al. (2021b) investigated particle dynamics in the North Passage of the Changjiang (Yangtze) Estuary using ^{234}Th , ^7Be , ^{210}Pb , ^{137}Cs . The correlation between the residence time of the tracers (^{234}Th , ^{210}Pb , ^7Be) and physical parameters (SPM concentration and salinity) was observed in the estuary. The residence time of ^7Be is less affected by the resuspension process than that of ^{210}Pb and ^{234}Th because the half-life of ^7Be is shorter and no additional scavenging take place during resuspension. Natural and anthropogenic factors can lead to remobilisation and resuspension

of sediments in shallow waters, which shorten the residence time of the particles (Wang et al., 2021b).

1.4.3 Sediment transport in marine waters

The seasonal transport of particulate organic carbon (POC) (Feng, et al., 2021), the transport and origin of sediments (Du et al., 2021; Wang, et al., 2020), water transport (Stukel et al., 2021) and others processes can be studied by applying non conservative radionuclides in the seas and oceans.

^{234}Th and ^{210}Po are a useful tracer for studying particle export in the upper 500 m of the ocean. They are used as an alternative approach for sediment traps (Hayes et al., 2018; Tang, 2019). The combination of ^{210}Pb and ^{210}Po has been shown to be a good tool for studying particle transport, residence time, vertical and lateral transport, and scavenging processes (Bam and Maiti, 2021). Yang et al. (2021) demonstrated the application of these tracers to track the sinking flux of black carbon in the northern South China Sea. Feng et al. (2021) observed the similarity between the seasonal variations of black carbon and ^{234}Th , that imply the possibility of using ^{234}Th to track the fate of black carbon. Yang et al. (2021) used $^{234}\text{Th}/^{238}\text{U}$ as a tracer to study the transport of particle reactive metals in a newly discovered hydrothermal plume over the Southwest Indian Ridge. The low values of the $^{234}\text{Th}/^{238}\text{U}$ ratio (i.e., 0.73-0.88) were attributed to the intense scavenging of particle reactive metals by the hydrothermal plume. The mutual application of ^{234}Th and ^{210}Po is used to study the POC dynamics on different time scales (Subha Anand et al., 2017).

^{234}Th ^{210}Pb and ^{210}Po approach to tracing sinking particles is based on assessing the shift in secular equilibrium between the parent (e.g., ^{238}U , ^{210}Pb , ^{226}Ra) and daughter (e.g., ^{234}Th , ^{210}Po , ^{210}Pb) radionuclides. Without particle transport, for example, thorium is assumed to be in secular equilibrium with the parent uranium and to increase linearly with depth in a water column (Cochran and Masqué, 2003). Scavenging ^{234}Th from the water column, the sinking particles cause a significant ^{234}Th deficit with the parent ^{238}U because the particle reactivity of ^{234}Th is very high compared to ^{238}U . Feng et al. (2021) found that ^{234}Th is more effectively scavenged by particulate organic matter and silica than by lithogenic particles. ^{210}Po decays faster than ^{210}Pb and has more ways to be scavenged out of the water column. In addition to sinking particles, ^{210}Po is also taken up by phytoplankton cells and becomes a part of the food web (Verdeny et al., 2009). Ma et al. (2021) observed that the scavenging of ^{210}Po by biogenic particles and organisms leads to a significant deficit in the upper 200 m.

Scavenging models, which describe tracer activity changes due to input and export processes, are utilized in studies of particle export. Savoye et al. (2006) demonstrated that ^{234}Th models can vary in complexity and include several boxes. Simple one box model balances for ^{234}Th changes in the water column ($\frac{\partial A_{Th}}{\partial t}$) due to radioactive decay of the parent radionuclide (λA_U), decay of thorium (λA_{Th}) and removal of thorium on particles (scavenging) (\mathbf{P}) as well as removal or inflow by advection and diffusion (\mathbf{V}):

$$\frac{\partial A_{Th}}{\partial t} = \lambda A_U - \lambda A_{Th} - \mathbf{P} + \mathbf{V} \quad (11)$$

Xie et al. (2020) studied ^{234}Th transport in the coastal upwelling system off Peru. The steady-state model found to be more useful in this case because it had fewer errors, which was attributed to the short sampling interval. The sinking fluxes of ^{234}Th were not significantly disturbed by physical processes calculated by (\mathbf{V}) term. Black et al. (2018) emphasized that upwelling processes in the coastal regions should be taken into account when calculating ^{234}Th fluxes, as this could otherwise lead to underestimations by a factor of two out of four. Stukel et al. (2021) studied oceanic carbon export in the Gulf of Mexico two approaches: estimation by sediment traps and $^{238}\text{U}/^{234}\text{Th}$ model with steady state conditions without advection and diffusion term. The U/Th disequilibrium method showed different results than the stationary traps, indicating lateral gradients and horizontal movement of water masses. Hong et al. (2021) found that the contribution of horizontal sediment exchange to the vertical sediment flux in South China Sea is estimated to be 10-33% by $^{238}\text{U}/^{234}\text{Th}$ approach. The author showed that POC transport results obtained for small regions should not be used for interpolation on a global scale. Seasonal variations and limited research coverage can significantly bias the understanding of cross-shelf POC flux.

The similar to $^{238}\text{U}/^{234}\text{Th}$ approach is used to estimate the ^{210}Po flux. Tang et al., (2019) demonstrated one box export model to calculate ^{210}Po balance:

$$\frac{\partial A_{Po}}{\partial t} = \lambda A_{Pb} - \lambda A_{Po} - \mathbf{P} + \mathbf{V} + \mathbf{F}_{Po} \quad (12)$$

This equation balances for ^{210}Po changes in water column ($\frac{\partial A_{Po}}{\partial t}$) due to radioactive decay of the parent radionuclide (λA_{Pb}), decay of polonium (λA_{Po}), atmospheric deposition (\mathbf{F}_{Po}), removal of polonium on particles (\mathbf{P}) as well as removal or inflow by advection and diffusion (\mathbf{V}). In general, steady-state conditions are assumed ($\frac{\partial A}{\partial t} = 0$), when it is not possible to occupy sampling stations to measure spatial gradients and no significant

amount of plankton biomass is observed during the sampling campaign. In some cases, researchers neglect the advection and diffusion term (V), which consists of vertical and horizontal activity gradients and diffusion when considering relative state conditions. For example, in studies of POC and biogenic silica export fluxes in the South China Sea, Cao et al. (2020) estimated vertical transfer and horizontal advection to be less than 1.5%. Steady-state conditions were used in view of the absence of an active plankton bloom. The validity of steady state conditions and absence of physical effects can be estimated by repeating of station occupations or using different tracer (Black et al., 2018).

Seo et al. (2021) studied the atmospheric input of ^{210}Pb in the East Sea (Japan Sea). Based on a mass balance model and assuming steady-state conditions without advection and diffusion, the average annual atmospheric deposition flux ($F_{210\text{Pb}}$) was estimated by:

$$\frac{\partial A_{\text{Pb}}}{\partial t} = \lambda_{210\text{Pb}} \times (A_{210\text{Pb}} - \lambda A_{226\text{Ra}}) - (kA)_{210\text{Pb}} + F_{210\text{Pb}} = 0 \quad (13)$$

where $(kA)_{210\text{Pb}}$ - the first-order scavenging flux, that was measured by sediment traps, $A_{210\text{Pb}}$ and $A_{226\text{Ra}}$ - radionuclides inventory in the water column. The atmospheric flux was estimated at $1.46 \pm 0.25 \text{ dpm cm}^{-2} \text{ y}^{-1}$.

By multiplying the vertical tracer flux (P_t) and the ratio between POC and tracer activity in sinking particles (C_t^p) at the export horizon the vertical POC transport (P_{POC}) can be estimated (Buesseler et al., 2006):

$$P_{\text{POC}} = P_t \times \left[\frac{\text{POC}}{C_t^p} \right] \quad (14)$$

Xie et al. (2020) pointed out that the POC flux should be normalized to the depth of the particle production layer or 100 m. Tang et al. (2019) found that vertical diffusion added 190% of ^{210}Po flux at the shelf station in the in the Pacific. Upwelling processes in the Peruvian coastal area had significant impact on ^{210}Po flux.

The studies of the dynamics of marine particles, the transport and mixing scavenging of particle reactive substances involve application of plutonium isotopes (Yamada et al., 2022). The main sources of plutonium in the ocean are nuclear tests and accidents (Aarkrog, 2003). Currents, biogeochemical cycles and particle dynamics are mainly responsible for the distribution of plutonium in the ocean (Lindahl et al., 2010). $^{240}\text{Pu}/^{239}\text{Pu}$, $^{241}\text{Pu}/^{239}\text{Pu}$ and $^{239}\text{Pu}/^{239+240}\text{Pu}$ are used to study the origin and transport of

sediments in the marine environment (Jinlong et al., 2020; Romanenko et al., 2023).

The ^{241}Am daughter of ^{241}Pu also has the potential to serve as an indicator of sedimentation in studies of sink and export fluxes. Kinoshita et al. (2021) investigated the fate of ^{241}Am in the water column using a scavenging box model in the eastern Pacific. Steady-state conditions without advection and horizontal transport were used. The authors estimated the residence time of ^{241}Am in the region of active deposition to be 550 years.

The applicability of $^{226}\text{Ra}/^{238}\text{U}$ and $^{40}\text{K}/^{238}\text{U}$ and ^{137}Cs for sediment tracing in marine conditions of the Bohai sea were estimated by Du et al. (2021). The authors observed a significant positive correlation between sediment grain size and radionuclide activities. The number of fine particles correlated with ^{226}Ra , ^{40}K , ^{137}Cs while coarse fraction correlated with ^{238}U and ^{210}Pb .

1.5. Applications of radionuclides for study sediments accumulation

Particle-reactive radionuclides have proven their applicability for studying various oceanic processes of water mixing, biological productivity and sediment deposition at different scales (Lindahl et al., 2010). Vertical sediment profiles serve as an additional tool to determine the chronology of sediment transport over the last 70 years. Sediment profiles contain important information on sediment accumulation rates, input of pollutants and their sources. To some extent, accumulated pollutants pose a problem for the water environment, which also underlines the importance of sediment deposit studies. Among the various radionuclides (Foucher et al., 2021; Li et al., 2021) ^{137}Cs , $^{210}\text{Pb}_{\text{ex}}$, $^{239,240}\text{Pu}$ are the most commonly used for the studies combining sedimentation chronology, sediment transport and sediment sources. A series of sediment cores in the area of interest provides information on temporal and spatial changes in the composition of the sedimentary material. These tracers have a wide range of applicability in the sediment chronology: soil and sediment contamination, environmental disasters (e.g., earthquakes, floods), important marine processes (e.g., sedimentation rate, burial rate, bioturbation) (Mulsow et al., 2009; Díaz-Asencio et al., 2009; Avşar et al., 2015; Wang et al., 2021c; Guo et al., 2021; Ciszewski and Łokas, 2019) have been studied using this technique.

The activity of unsupported lead ($^{210}\text{Pb}_{\text{ex}}$) is an effective date marker and has been used for several decades. It is widely used for studies of soil profiles, ice cores, sediment deposits of lakes, rivers, and coastal and shelf areas (Hassen et al., 2019; Guo, 2020; Baskaran & Krupp, 2021; Sawe et al.,

2021; Singh & Vasudevan, 2021). Like any approach, sediment chronology with ^{210}Pb is based on several assumptions. Foucher et al. (2021) specified three assumptions used for ^{210}Pb dating method: a) steady state accumulation ^{210}Pb in closed system, b) effective transfer of ^{210}Pb into the sediments, c) supported ^{210}Pb is in equilibrium with ^{226}Ra . The closer these assumptions are to the real conditions in the individual case, the more accurate the results obtained.

Baskaran et al. (2020) reported application of $^{210}\text{Po}/^{210}\text{Pb}$ to determine the age of the upper layer of bottom sediments in the river. Assuming that all excess lead is of atmospheric origin only, the surface layer of sediments (< 0.5 cm) has an atmospheric $^{210}\text{Po}/^{210}\text{Pb}$ ratio (< 0.1) and the lower layers (> 2 cm) have an age of > 2 years the authors estimated the apparent age using the equation:

$$\tau = \frac{-1}{\lambda_{210\text{Po}}} \ln \left(1 - \left(\frac{^{210}\text{Po}}{^{210}\text{Pb}} \right)_{\text{sed}} + \left(\frac{^{210}\text{Po}}{^{210}\text{Pb}} \right)_{\text{init}} \right) \quad (15)$$

where λ – decay constant ($\lambda = 5.01 \times 10^{-3}\text{d}^{-1}$), $()_{\text{init}}$ – initial activity ratio, $()_{\text{sed}}$ – atomic ratio in the bottom sediment. The authors found that the age of the upper sediment layer (2-3 cm) in the Clinton River in southwest Michigan is ~220 days.

The $^{210}\text{Pb}_{\text{ex}}$ core dating method is often combined and validated with ^{137}Cs and $^{239,240}\text{Pu}$, ^{241}Am , and more sparsely with other radionuclides (Foucher et al., 2021). They are used both as chrono markers and as fingerprints of sediments. Plutonium requires a more complex laboratory procedure but has advantages over caesium in the marine environment. Plutonium is more strongly bound to particles than ^{137}Cs , and normally there are no barriers for particles to the adsorb it from the water (Beasley et al., 1982).

Another alternative chronometer is ^{241}Am . Based on the decay of ^{241}Pu into ^{241}Am , the age of the pollution and associated sediment can be estimated in a sediment profile (Pittauer et al., 2016):

$$t = \frac{1}{(\lambda_{\text{Pu}} - \lambda_{\text{Am}})} \ln \left[1 + \frac{(\lambda_{\text{Pu}} - \lambda_{\text{Am}}) C_{\text{Am}}(t)}{\lambda_{\text{Am}} C_{\text{Pu}}(t)} \right] \quad (16)$$

where λ – radionuclide decay constant, C activity of radionuclide ($C_{\text{Am}}(0) = 0$).

Moros et al. (2017) demonstrated a combination of ^{210}Pb and ^{14}C dating with ^{137}Cs , ^{241}Am , and ^{14}C as chrono markers to determine the history of contamination by lead and PCB (polychlorinated biphenyls). Gardes et al. (2021) employed $^{210}\text{Pb}_{\text{ex}}$ as a dating tool and ^{241}Am and ^{137}Cs as verification

date markers to investigate organochlorine pesticide contamination in the watershed. The data of the artificial radionuclide peaks and sedimentation rates agreed well.

The capabilities of the fingerprint approach and the dating technique can be combined to investigate the chronology of pollution inputs from different sources (Maina, 2019; Wang et al, 2020, Yeager, et al., 2018). Ji et al. (2022) reported on the dating of sediments with ^{137}Cs , $^{239,240}\text{Pu}$ and ^{210}Pb and the use of $^{240}\text{Pu}/^{239}\text{Pu}$, $^{239,240}\text{Pu}/^{137}\text{Cs}$ to determine the origin of radionuclide provenance of sediments in eutrophic lakes. The $^{240}\text{Pu}/^{239}\text{Pu}$ ratio in the sediment profiles showed the global fallout origin of the plutonium. Hernández et al. (2020) studied chronology of sediment pollution caused by mining activities near Lake Izabal, Guatemala. The approach employed ^{210}Pb , ^{14}C , and ^{137}Cs as comparative dating tools to obtain the chronology of Pb, Zn, and Ni delivery.

The assessment of sedimentation rate is an essential part of dating sediment cores with ^{210}Pb models (Foucher et al., 2021). This indicator is a useful tool in the study of spatial sediment distribution, a chronology of sediment accumulation rate and associated pollution input. Zhuang et al. (2019) investigated sediment sources in the Bohai Sea by combining sediment chronology, radionuclide mass balance and fingerprint technique. The peak values of ^{137}Cs and $^{239,240}\text{Pu}$ were used to calculate sediment deposition rate and chronology, indicating anthropogenic influence on sediment supply. Turner et al. (2019) studied the history of plastic pollution in sediment cores from the Hampstead No.1 Pond in North London (UK). In the sediments ^{210}Pb and ^{137}Cs were used for age determination. Calculations for ^{210}Pb dating were performed using the model that assumes a constant rate of ^{210}Pb supply. Belivermiş et al. (2021) showed the results of the accumulation history of microplastics. The studies are based on ^{210}Pb and ^{137}Cs chronology of the estuary sediment profiles. Ivanoff et al. (2021) studied the chronology of sediment distribution in the Lagoa dos Patos lagoon, southern Brazil using the ^{210}Pb and ^{137}Cs . The studies reveal sedimentation load variations linked with dry and wet seasons and intensive land use as favouring factors for increasing sedimentation load.

Various post-depositional disturbances (e.g., bioturbation, mobility/diffusion, physical mixing of sediments due to anthropogenic and natural events) disrupt the vertical distribution of radionuclides in sediment profile of bottom sediments and prevent or complicate interpretation (Foucher et al., 2021). ^{210}Pb dating method solely can't ensure sufficient reliability in every case and it's recommended to use supporting parallel dating techniques. Hung et al. (2021) verified the distribution profile of ^{210}Pb with the distribution

of herbicide spray events with known chronology. The constant initial concentration (CIC) model and the herbicide distribution showed significant discrepancies in the estimates of layer growth. Normally ^{137}Cs is measured to verify ^{210}Pb dating. However, the migration of ^{137}Cs after deposition can cause some problems. In these cases, corrections can be made with ^{241}Am or $^{239,240}\text{Pu}$ to account for broadening, shifting or absence of the ^{137}Cs peak at the expected location of the sediment profile (Ji et al., 2022). Hot particles released from reactor accidents, as well as emissions from spent fuel reprocessing plants and other facilities, can pose a problem for sediment profile studies and also for sediment measurements in general. In the case of doubtful data, the sample is divided into parts and the heterogeneity of the activity is determined. Recently, Appleby et al. (2022) reported such a problem in the study of marine sediment profiles from Veafjord, Norway. The study found hot particles with an activity of 15 mBq and the Chernobyl accident and the UK reprocessing plant were mentioned as possible sources.

1.6. The summary of chapter

Currently, there are numerous applications of particle-reactive radionuclides (^7Be , ^{137}Cs , ^{210}Pb , $^{239,240}\text{Pu}$, ^{241}Am) for various environmental studies. They are used to study sediment transport at different scales: in rivers, estuaries and seas/oceans. More mobile nuclides such as ^{226}Ra , ^{238}U and ^{40}K are useful for studying the particle budget in coastal systems. ^{40}K , ^{226}Ra can be used in some cases as fingerprints in river systems, but their conservatism is not always guaranteed. In coastal areas, $^{226}\text{Ra}/^{238}\text{U}$ is used to distinguish between fluvial and marine sediments, made possible by the greater solubility of uranium compared to radium.

^7Be , ^{137}Cs , ^{210}Pb , $^{239,240}\text{Pu}$ are widely used to estimate the origin of sediments. ^7Be and ^{210}Pb are used to determine the age of sediments up to one year and 85 years accordingly. In coastal regions, ^{234}Th and ^{210}Po are also used to study particle dynamics at different time intervals. Surface sediments and subsurface sediments differ in the caesium content, which is usually higher in surface sediments. The plutonium isotope ratio is an effective tool for determining the origin of radioactive pollution that can be used to identify the origin of sediments and they balance in marine and coastal systems. The simple mixing model of plutonium isotope ratios for Chernobyl accident fallout and global nuclear test fallout is useful to estimate the contribution of sediments sources in the coastal region of the south-eastern Baltic Sea. Radionuclide flux from the catchment area that accumulated fallout radionuclides (^{137}Cs , $^{239,240}\text{Pu}$) can be estimated by the radionuclide inventory,

catchment area and the eroded fractions. This model is applicable for the radionuclide flux calculations from the catchment of Neman River to the Curonian lagoon.

Box models that describe the behaviour of radionuclides in the water column are valuable tools for studying various parameters such as particle export to the water column, residence time, deposition flux, and more. These models utilize tracers such as ^{234}Th , ^7Be , ^{210}Pb , ^{210}Po , $^{239,240}\text{Pu}$ to investigate these processes. Estimation of the flux of sinking particles and resuspension is often determined by the radionuclide equilibrium change method ($^{210}\text{Pb} : ^{210}\text{Po}$; $^{238}\text{U} : ^{234}\text{Th}$, $^{222}\text{Rn} : ^{210}\text{Pb}$). In coastal areas and estuaries, ^{137}Cs , ^7Be , ^{234}Th are used to assess river and marine water balance, resuspension and deposition. The plutonium isotopes ^{239}Pu and ^{240}Pu are useful tools for estimating sediment balance and sources in water bodies. They have proven to be favourable for studying particle transport under different conditions. It is worth noting that plutonium isotopes have been used more extensively to estimate sediment transport in river-dominated marginal seas, such as a combination of $1/^{239,240}\text{Pu}$ and $^{240}\text{Pu}/^{239}\text{Pu}$.

Sediment accumulation zones are a good repository of ecological information. ^{210}Pb , ^{137}Cs , $^{239,240}\text{Pu}$ are used to study the accumulation history of sediments and pollutants and to distinguish their sources. The conventional models for the input of ^{210}Pb differ in their diversity. The approach using anthropogenic Cs and Pu is simpler and assumes a uniform sediment supply, with the year of maximum precipitation associated with the depth of the peak. Interpretation of sediment profiles can be significantly complicated by mixing of sediments due to activities of biota, diffusion of radionuclides, disturbance of sediments by anthropogenic activities and sediment dynamics. The distribution of americium and plutonium is least influenced by such factors. Sediment dating is often used to study the response of aquatic environments to human activities. The dating technique using ^{241}Pu and ^{241}Am activity changes is useful for assessing sediment cores in the Baltic Sea and Curonian Lagoon. This approach can elucidate the origin of pollution and estimate the purity of the pollution source signal based on the date. It is assumed that only two sources are present, dating from 1963 and 1986.

2. MATERIALS AND METHODS

2.1 Study area

The Baltic Sea is an inland sea in northern Europe, that has a volume of about 21500 km³. The sea covers the area of about 370000 km² (Figure 3a) and its catchment area is about four times the size of the sea itself. Because of its location, the sea can be considered a huge estuarine system, with the inland basins divided into smaller areas. Water circulation in the sea is relatively slow, with an average rate of a few centimetres per second (Kullenberg et al., 1981). The water exchange rate of the sea is about 4000 km³ per year and the residence time of the water is about 35 years. The weak connection with other seas and the strong inflow of fresh water result in a good stratification of the sea, characterized by layers of dense, salty water and slightly salty water. Seasonal anoxic conditions are typical for the sea when organic material accumulates in sufficient quantities in the deep layers (Anderson et al., 1985). Over 85 million people live in the Baltic Sea catchment area, resulting in extremely high anthropogenic pollution (Bollmann et al., 2019). The sea is one of the most chemically polluted seas in the world (Szymczycha et al., 2019).

More than 250 rivers flow into the Baltic Sea of which the Neman is one of the largest, located in the south-eastern part of the sea. The catchment area of the Neman River (Figure 3a) is located to the east and southeast of the Lagoon, covering an approximate area of 105 km² (Manton et al., 2021). The Neman River, which rises in the Minsk region of Belarus (~462 km), is the largest river in Lithuania with a length on its area of about 359 km. The river's catchment area covers about 0.5×10^5 km² (~72%) of Lithuania's territory.

The Curonian Lagoon is intermediate reservoir between Neman River and the Baltic Sea (Figure 3 a, b). The Neman River provides about 90% of the total inflow to the Curonian Lagoon. The catchment area of the Curonian Lagoon is 100458 km², of which 98% is the Neman catchment area. The Curonian Lagoon has an area of 1555 km² and is a semi-enclosed area that is in a fragile ecological state due to its shallow depth and limited water exchange, which makes it vulnerable to harmful factors (Vaikutienė et al., 2017). The quality of the water and sediments flowing into the rivers is closely related to the ecological condition of the lagoon. One of the identified problems of the lagoon is the high incidence of blue-green algae blooms (up to 100 g/m³) and eutrophication, leading to a decrease in oxygen levels and fish kills (Aleksandrov et al., 2018). According to Mėžinė et al. (2019), the Curonian Lagoon delivers about 1.9×10^8 kg of sediment annually to the coast

of the southwestern part of the Baltic Sea. The catchment of Neman River is characterized by a high level of industrial and agricultural activities, which contribute significantly to the eutrophication of the Curonian Lagoon and the Baltic Sea (Knuuttila et al., 2011).

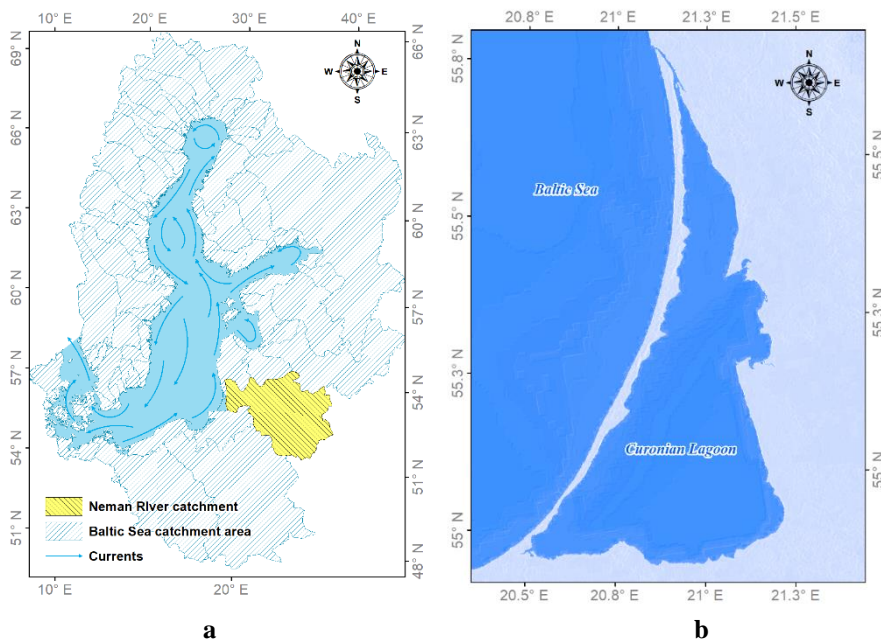


Figure 3. Baltic sea – a (The currents were drawn after the European Environment Agency (European Environmental Agency, 2009), Curonian Lagoon - b

The main sources of radionuclides that have contaminated the Baltic Sea and its catchment area are global fallout from atmospheric nuclear testing and fallout from the Chernobyl accident. The ^{137}Cs contamination of the Baltic Sea water is estimated at 5.7 PBq, and the contributions from the various sources are: Chernobyl fallout - 82% (4700 TBq), global fallout from nuclear testing - 14% (800 TBq), emissions from nuclear waste processing plants - 4% (230 TBq) and emissions from nuclear facilities in the Baltic Sea - 0.1% (6 TBq). About 70% of caesium is found in bottom sediments, of which 5% is in hard bottom and the rest in soft bottom (Ikäheimonen et al., 2009). The heterogeneity of the caesium distribution in the sea is due to the very different sediment accumulation rates (SAR) (0.2-29 mm/year in areas with soft seabed). According to Mattilia et al. (2006), the intensity of sedimentation in the Baltic Sea ranges from 0.06 to 103 g/(m²yr). The highest SAR was observed in the northern part of the Bothnian Sea (2345 g/(m²yr)), lower values in the Gulf of Finland (754 g/(m²yr)) and in the Baltic Sea proper (374

g/(m²yr)). In the areas with the highest sedimentation intensity - in the coastal areas and in the Gulf of Bothnia and the Gulf of Finland - higher activities are observed (Ikäheimonen et al., 2009), which can be attributed to more intensive scavenging of caesium from the water.

According to Holm, (1995), global fallout from nuclear tests ^{239,240}Pu entered the Baltic Sea in amounts of 40-50 Bq/m² (16-18 TBq). The caesium input from nuclear tests is estimated at 0.93 PBq (Nielsen et al., 1999). In 1982, the inventory of ¹³⁷Cs and ^{239,240}Pu in bottom sediments of the Baltic Sea was 290 TBq and 24 TBq, respectively. The inventories in the Gulf of Bothnia were estimated at 110 TBq (¹³⁷Cs) and 9.4 TBq (^{239,240}Pu), in the Gulf of Finland - 51 TBq (¹³⁷Cs) and 1.9 TBq (^{239,240}Pu), in the Baltic Proper - TBq (¹³⁷Cs) and 0.86 TBq (^{239,240}Pu) (Salo et al, 1986). The activity values of the radionuclides in the bottom sediments were: in the Gulf of Bothnia 73 Bq/kg (¹³⁷Cs) and 6.2 Bq/kg (^{239,240}Pu), in the Gulf of Finland 133 Bq/kg (¹³⁷Cs) and 5.0 Bq/kg (^{239,240}Pu), in the Baltic Sea Proper 83 Bq/kg (¹³⁷Cs); and 3.9 Bq/kg (^{239,240}Pu) (Salo et al, 1986). The calculations assume an accumulation rate of bottom sediments of 0.3 mm/year for the Baltic Sea proper and 4 mm/year for the Gulf of Finland and the Gulf of Bothnia. Before the Chernobyl accident, plutonium levels in the water were estimated to be 4-8 µBq/l and caesium levels 0.6-6 µBq/l (Holm, 1995).

Of the major bodies of water, the Mediterranean Sea, the Black Sea and the Baltic Sea were most affected by Chernobyl fallout, with the latter posing the greatest risk of radioactive accumulation, which is related to the long residence time of the water. The Chernobyl fallout is the largest contributor of ¹³⁷Cs to the Baltic Sea. The total amount of caesium (¹³⁷Cs) released into the sea as a result of the Chernobyl accident is estimated at 4.7 PBq (Nielsen et al., 1999), which is about five times more than the global fallout from nuclear testing. The ¹³⁷Cs load from Chernobyl fallout is unevenly distributed across the catchment area of the sea, with the highest values located in the northern and north-eastern parts of the sea. Currently, the Baltic Sea is the main source of Chernobyl-derived caesium in the NE Atlantic (Povinec et al., 2004). It is estimated (HELCOM, 1996) that the inventories of ¹³⁷Cs and ^{239,240}Pu in bottom sediments increased by 400% and 20%, respectively, between the early 1980s and 1991 as a result of the Chernobyl fallout. Holm, 1995 estimated the inventories of ²⁴¹Pu and ^{239,240}Pu from Chernobyl fallout in the Baltic Sea to be 88 TB (23 TB in 2023) and 1.5 TBq, respectively, with ²⁴¹Pu accounting for 64% of the total plutonium activity and ^{239,240}Pu about 9%. Radioactive nuclides that have entered the Baltic Sea area are in constant dynamics due to the mixing of water masses by currents and waves, the

varying intensity of sediment transport and sedimentation rates, which gives a complex picture of their spatial distribution.

2.2 Sampling

Neman river and Curonian Lagoon. To investigate the activities of ^{137}Cs and $^{239,240}\text{Pu}$, four stations in the Curonian Lagoon and three stations in the Neris River (Figure 4) were selected to collect samples of suspended particles. In summer 2020, three samples of suspended matter were collected at stations N1, N2 and N3. In summer 2021, suspended matter was sampled at stations N1, N2, N3, CL1, CL2, CL3 and CL4.

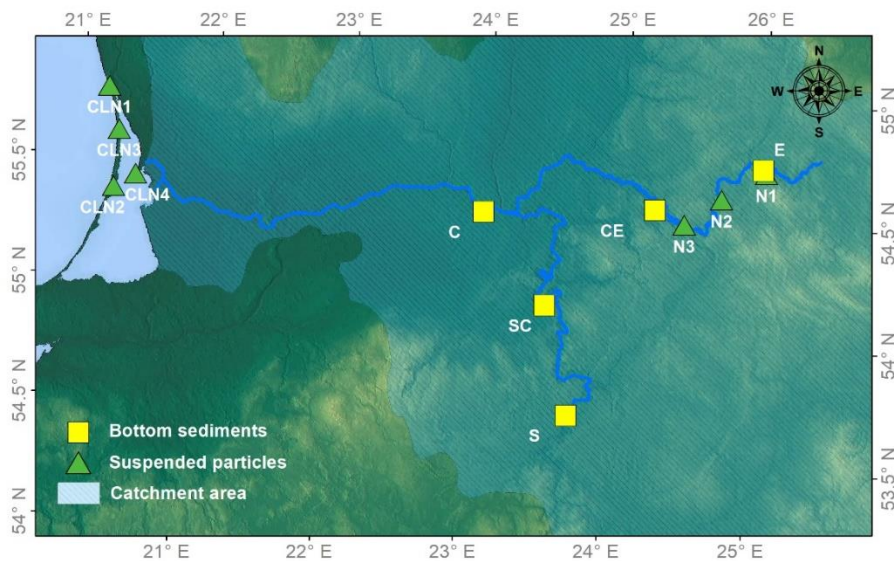


Figure 4. Sampling design: the Curonian lagoon and the Neris River

The same method of suspended particle sampling was used during expeditions. The samples in the Curonian Lagoon were taken in the coastal waters at the moorings, while in the river they were collected at the deepest point of the water flow.

Baltic Sea area. In order to assess the influence of different factors (sediment size, location, depth and content of other radionuclides ^{210}Pb , ^{214}Pb , ^{40}K) on the distribution of $^{239,240}\text{Pu}$, ^{137}Cs and ^{241}Am , the samples taken during the last expeditions (Figure 5) were analysed and the previous data were used for estimations.

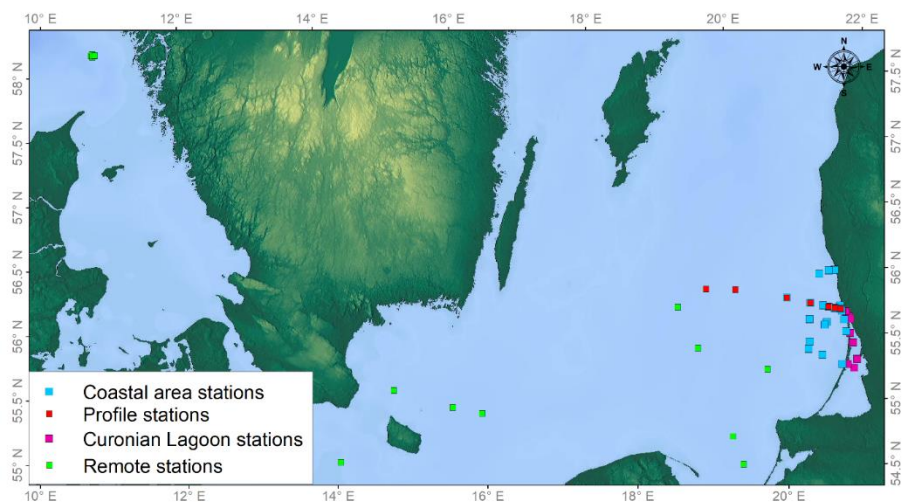


Figure 5. Scheme of sampling stations in the Baltic Sea

The sampling stations can be divided into two groups. The first group (sampling campaign 2011-2015) of stations in the Curonian Lagoon and the coastal area of the Baltic Sea was analysed for the spatial activities (Bq/m^2) of $^{239,240}\text{Pu}$, ^{241}Am and ^{137}Cs at the 30 stations. The profile of 8 stations with a length of 120 km, starting at the coast and ending in the deep sea, was studied. The second group of remote stations was sampled in 2018 and shows considerable spatial dispersion. Bottom sediment sampling was carried out by Environmental Protection Agency (Klaipėda, Lithuania) and the collaboration team. In the the Skagerrak Bay were taken 7 bottom sediment samples and 9 samples were taken from the southern part of the Baltic Sea. In the second group of samples such parameters as sampling depth, distribution particles by size and activities of ^{137}Cs , ^{210}Pb , ^{214}Pb , ^{40}K were determined.

Sampling of suspended solids. A set of three consecutive philtre cartridges (US Filter Plymouth Products) with pore sizes of $0.2\ \mu\text{m}$, $1\ \mu\text{m}$ and $25\ \mu\text{m}$ were used to philtre the water. A volume of $\sim 1\ \text{m}^3$ of water was pumped through the system and the volume of water was measured using a conventional water metre.

Sampling of bottom sediments. The surface layer (0-5 cm) of bottom sediments in the Neman and Neris rivers was sampled at five locations. Samples were taken from the water about 1 m from the shore. In the Baltic Sea, the bottom sediment samples were taken with a Van Veen grab sampler. In the shallower Curonian Lagoon, the bottom sediments were collected with the Ekman-Birge sampler. The sampling depth in the Curonian lagoon and Baltic Sea ranged from 4 to 220 m.

2.3. Samples preparation

Samples of suspended matter. After sampling, the philtres with the samples were dried at 25°C for one week to stabilise the mass. The philtres were melted and dried into the hard state at ~250°C. The samples were then ashed overnight in an oven at 450°C.

The concentration of suspended particles was determined by filtration through the 0.2 µm membrane. Prior to filtration, the membrane was dried at 60° C for 24 hours and weighed to the nearest 0.01 g. The sample volume was then divided into two parts. Then the sample volume (about 20 litres) was filtered through the membrane using the vacuum pump system.

After the second drying and weighing, the concentration of suspended solids was calculated:

$$C = (w_2 - w_1)/V_{water} \quad (17)$$

where V_{water} is the volume of water filtered through the membrane, w_2 and w_1 is the weight of the membrane after and before filtration.

Preparation of bottom sediments. The samples that were taken in the Neris river were heated at 60°C for 24 hours until the weight stabilized and then sieved through a 63 µm sieve in order to study the mobile fraction. The bottom sediment samples from the Baltic Sea and Curonian Lagoon were subjected to a drying process at a temperature of 100°C for one day. Through this process, the samples lost about 20-30% of their total weight, including water and volatile substances.

Then the samples of suspended matter and bottom sediments were weighed and then incinerated at 550°C for about 16 hours. After the combustion process, internal standards such as ^{242}Pu and ^{243}Am were added to each sample. The samples were treated with a concentrated mixture of HCl and HNO₃ (40 g of the mixture per 10 g of sample) and then boiled for 30 minutes. The cooled mixtures were filtered and the insoluble residues were washed with distilled water. The resulting solutions were then evaporated and redissolved in 50 ml of 6M HNO₃ + 0.5M NaNO₂.

Radiochemical isolation of Pu. Liquid extraction of Pu⁴⁺ from an acidic solution containing 0.2M TOPO in cyclohexane (10:1, twice) for 15 minutes. After extraction, the combined organic phases were washed three times with a 3M HCl solution for 5 minutes. Pu was re-extracted from aqueous phase the with 0.5 M ascorbic acid/1M HCl with shaking twice for 15 minutes. The resulting aqueous phase was then washed several times with a few millilitres of CCl₄ solution. This completely separated the plutonium from the nuclides Po, Ra, Am, Cm and Cf and left it in the original aqueous phase from

which Am was extracted. In addition, Pu was partially separated from the nuclides U, Th and Np in this procedure, which interfere with the detection of Pu. Plutonium was purified from uranium by precipitating Pu with NdF_3 . A 10 mg/ml Nd solution was added to the extraction solution, mixed and then a concentrated hydrofluoric acid solution was added, mixed again and the resulting precipitate centrifuged. The solution was not used further and the resulting precipitate was subjected to a washing step with a 1.5M solution of HF, followed by centrifugation. The precipitate was then dissolved in a mixture of hot boric acid and concentrated HNO_3 acid. Then 15 ml of concentrated ammonia was added to the solution until the pH reached 9. The solution was cooled and the resulting precipitate was separated by centrifugation and washed with water. The resulting precipitate was further treated by mixing with a drop of concentrated ammonia and then centrifuged again. The resulting precipitate was dissolved in concentrated HNO_3 acid, then evaporated and processed on UTEVA columns. Further purification of Pu was carried out according to the CFE method using Eichrom UTEVA columns. The columns were first washed with a mixture of 6M nitric acid and hydrogen peroxide. The sample was then dissolved in 2 ml of the same acid mixture. The sample solution was then passed through the column and then washed with 20 ml of 6M $\text{HNO}_3 + \text{H}_2\text{O}_2$. The columns were then washed with 9M HCl and the Pu fraction was collected by elution with a mixture of 2M nitric acid, ascorbic acid and hydroxylamine hydrochloride.

Radiochemical isolation of Am. Radiochemical isolation of Am was carried out by separating Am^{3+} from the matrix elements in the aqueous phase obtained after Pu extraction with TOPO in cyclohexane. The pH of the solution was adjusted to 1.2 with concentrated NH_3 . Am was extracted into the organic phase with TOPO in cyclohexane, twice for 15 minutes at a ratio of 1:10. The organic phase was washed twice with 5 mol/L HNO_3 (1:1), pH 1.2. Am was then extracted into the aqueous phase with a 2 mol/L nitric acid solution in a 1:1 ratio, shaking twice for 15 minutes. The aqueous phase was washed twice with a few millilitres of carbon tetrachloride solution per minute. To minimize the matrix effects, an organic mixture consisting of 0.05 mol/L TOPO/cyclohexane and PMBP (1-phenyl-3-methyl-4-benzoyl-5-pyrazolone) was utilized. In order to mitigate the adverse effects of Fe^{3+} on the release of Am^{3+} , Fe^{3+} was reduced to Fe^{2+} . Ascorbic acid (200-800 mg) was added to the samples depending on the quantity of iron present, to facilitate the reduction reaction. The amount of iron in the samples and the completion of the reduction reaction were estimated visually by monitoring for any changes in colour. Following the separation of Am from other matrix elements, additional purification of americium was performed via liquid-

liquid chromatography using Eichrom TRU and TEVA columns. Prior to passing the samples through the columns, the extracted solutions were evaporated to dryness by treatment with a mixture of 1:3 nitric and hydrochloric acid, nitrogen, hydrogen peroxide, and nitrogen once again. The TRU columns were rinsed with 2 mol/L nitric acid, then the dry residue in the test samples was dissolved in a solution of 2 mol/L nitric acid/ascorbic acid. The column was then rinsed with 0.5 mol/L nitric acid solution. The fractions of 9 mol/L and 4 mol/L hydrochloric acid solution were collected. The collected solution was evaporated to dryness and the dry residue was evaporated with nitrogen, hydrogen peroxide and concentrated nitric acid to prepare the samples for further analysis with TEVA columns. The columns were first rinsed with a solution of 2 mol/L ammonium thiocyanate/0.1 mol/L formic acid. Then the samples were added to the solution and the dry residue was dissolved in a similar solution. The columns were rinsed with a solution of 1 mol/L ammonium thiocyanate/0.1 mol/L formic acid. The fraction was collected by adding 4 mol/L hydrochloric acid (Lujaniene, 2013).

Sample preparation for alpha-spectrometric measurements. Sample preparation for the spectrometric measurements was carried out as follows. The fraction containing radionuclides was isolated and purified and then evaporated to dryness. The dry residue was further evaporated in a few millilitres of concentrated acid in the following order: twice with a 1:3 mixture of nitric acid and hydrochloric acid, once with nitric acid, hydrogen perchlorate, three times with nitric acid, once with hydrochloric acid and twice with hydrochloric acid. The dry residue was then dissolved in a few millilitres of 0.4M HCl / 4.0% (NH₄) C₂O₄ / deionized water and transferred to a Teflon electrolysis cell. The cathode was a polished stainless-steel disc and the anode was a platinum wire spring. Electrolysis was carried out for 2 hours at a current density of 300 mA/cm². A few drops of concentrated ammonia were added 1 minute before the end of electrolysis. All radionuclides present in the solution were deposited quantitatively and qualitatively on the cathode cover. The steel disc with the radionuclides deposited on it was washed with deionized water and acetone and dried. The activity of the obtained steel disc with an ultra-thin coating was analysed with an alpha spectrometer.

2.4. Samples analysis

Gamma-spectrometry. Gamma ray emitting radionuclides were analysed using an ORTEC gamma ray spectrometer with an HPGe GWL-120-15-LB-AWT detector. The detector has a resolution of 2.25 keV at 1.33 MeV. The gamma line of Ba-137m (661.66 keV) was used to estimate the parental

Cs-137 activities. The activities of K-40 were measured with a gamma energy of 1462 keV. The duration of the measurements varied from 80000 to 450000 s. The relative error of gamma-spectroscopic measurements does not increase 10%.

Alpha-spectrometry. The alpha spectrometry measurements were performed with a system of passivated implanted silicon detectors (PIPS) manufactured by AMETEK in Oak Ridge, Tennessee, USA. The PIPS detectors used had an active area of 450 mm². The relative uncertainties of ^{239,240}Pu and ²⁴¹Am measurements were not higher than 5% and 7%. The ²⁴¹Pu was determined by the increase of the ²⁴¹Am peak (5.49 MeV) in the sample spectra after 10 years of storage (Lujanienė et al., 2022).

Plutonium atomic mass spectrometry. The recovery of plutonium in the samples prepared for accelerated mass spectroscopy (AMS) was ~95%. The atomic ratio ²⁴⁰Pu/²³⁹Pu was analysed by a 1.0MV HVE Tandem AMS.

Grain-size distribution. The grain size of the bottom sediments that were sampled in the southern Baltic Sea was measured with a laser particle analyser (ANALYSETTE 22 MicroTec-plus).

The Analysette 22 Microtec Plus laser particle sizer from Fritsch GmbH is used to measure suspensions, emulsions and solids by means of laser diffraction. The device consists of a central measuring unit and a dispersion module with two lasers (7 mW, 532 nm and 940 nm) and a measuring range from 0.008 micrometres to 2000 micrometres in one unit with a resolution of up to 108 channels. Measurements are made using an optically transparent measuring cell with an ultrasonic water bath for the use of the dispersion liquid. The particle size is measured in a range from 0.08 to 2000 micrometres (Analysette 22 manual).

3. RESULTS AND DISCUSSION

3.1 The studies of the radionuclide export to the Curonian lagoon with the Neman River

3.1.1. Activity levels

According to the data obtained, the average content of suspended matter in the water of the Neris River and the Curonian Lagoon was 0.008 and 0.04 kg/m³, respectively. The activity values of ¹³⁷Cs in the suspended matter of the Neris River ranged from 4.2 ± 1.3 Bq/kg to 49 ± 15 Bq/kg, with an average value of 20.3 Bq/kg (0.17 Bq/m³, N=6). The highest value was measured at station N1. In the first year, the activity levels were lower with an average of 8.4 Bq/kg (0.07 Bq/m³) (N=3), while in the second year the average activity was more than three times higher with 32.1 Bq/kg (0.26 Bq/m³) (N=3).

Caesium-137. In the Curonian Lagoon, the activity values of ¹³⁷Cs in suspended particles were lower than in the river and ranged from 3.4 ± 1.1 Bq/kg to 17.0 ± 2.2 Bq/kg, with an average value of 9.3 Bq/kg (0.37 Bq/m³, N=4) (Table 3). The highest specific activity was characteristic of station CL1, located in the strait connecting the lagoon to the sea. The lowest concentration of caesium and suspended solids was observed at station CL4, where the water from the Neman River flows into the lagoon. It should be noted that the volumetric activity of caesium was higher in the lagoon, while the massic activity in suspended matter was lower due to the higher concentration of particles.

Table 3. Radionuclide activity levels in the bottom sediments and suspended particles

Location	¹³⁷ Cs, Bq/kg		^{239,240} Pu, mBq/kg	
	Bottom sediments	Suspended particles	Bottom sediments	Suspended particles
Neris r.	6.4 ± 0.5	4.2(± 1.3) – 49(± 15)	90 ± 5	60(± 3) - 190(± 10)
Neman r.	7.3 ± 0.6	-	80 ± 4	-
Curonian lagoon	-	9.3 ± 0.7	10.0 (± 0.5) – 20 (±1) *(1350 (± 68))	30 ± 2

* - single value at station CL10

The measured values are comparable to those of Lujanienė et al. (2012), which range between 15-170 Bq/kg, taking into account the correction for caesium decay. The activity values of ¹³⁷Cs in suspended particles are also comparable with previous studies from 1998-2000 (Lujanas et al., 2002). According to the published data, ¹³⁷Cs activities in suspended particles

between 60.6 and 75 Bq/kg were observed at the Buivydžiai station during the summer. A comparison of the data is shown in Figure 6. The values determined in this study are somewhat lower than expected, even taking into account the decrease in caesium activity due to radioactive decay alone.

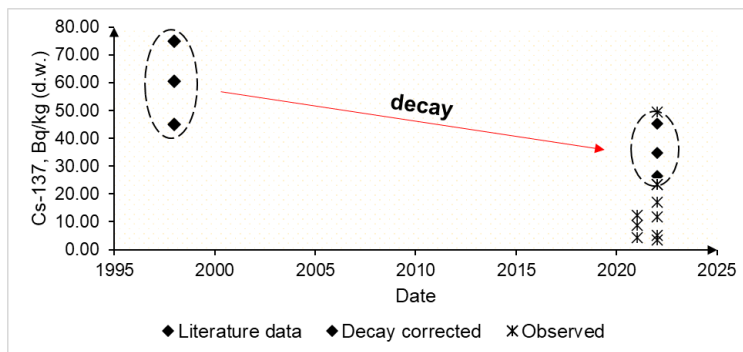


Figure 6. Data comparison of Lujanias et al. (2002) and measured values

The specific activity of ^{137}Cs in bottom sediments of the Neman River (0-5 cm, fraction $< 63 \mu\text{m}$) had an average value of 6.5 Bq/kg (5 stations). At the southern site (Neman River), activities were 5.8 Bq/kg and 8.8 Bq/kg. At the eastern site (Neris River), the activities were 5.4 Bq/kg and 7.4 Bq/kg, and at the central site below the confluence of the tributaries, the measured activity was 5.3 Bq/kg. Overall, the observed activities were within a narrow range of 5.3 to 8.8 Bq/kg. This range was slightly lower than the measured activities in suspended matter, but the limits of the determined values were comparable. In general, the determined activities of ^{137}Cs in the Neman River are in agreement with the data for the Curonian Lagoon and with literature data.

Plutonium-239,240. $^{239,240}\text{Pu}$ activity values in suspended matter in the Neris River determined by alpha spectroscopy were 0.06 and 0.19 Bq/kg (0.5 and 1.6 mBq/m³) with an average value of 0.13 Bq/kg dry weight (dr.w.). In the Curonian Lagoon, the values were even lower, and after combining four samples, the average content in suspended solids was 0.03 Bq/kg (1.2 mBq/m³). In previous studies by Lujanienė et al. (2014), the activity levels of $^{239,240}\text{Pu}$ in suspended solids in the Klaipėda Strait ranged from 0.13 Bq/kg to 1.3 Bq/kg, which is an order of magnitude higher than the levels observed in this study.

The mean activity of $^{239,240}\text{Pu}$ in the $< 63 \mu\text{m}$ fraction of bottom sediments in the Neris and Neman rivers was 0.08 Bq/kg (N=6), with a maximum of 0.15 Bq/kg at station CE and a minimum at station C, located downstream from the confluence of the Neris and Neman rivers. The contents of $^{239,240}\text{Pu}$ in the bottom sediments of the Curonian Lagoon were in the range

of 10 to 20 mBq/kg (Table 3). An anomalous value of 1350 mBq/kg is located in the south-eastern part of the study area, near the shore opposite the tributary of the Neman River. The elevated activity values at CL10 can be attributed to the presence of "hot" particles or a local accumulation zone for radionuclides.

Particle fractions. The analysis of three fractions of suspended particles (0.2-1 μm , 1-25 μm , > 25 μm) showed that the largest share of total activity of studied radionuclides was found in the coarsest (C) fraction (> 25 μm) (Figure 7, Table 4). The mean values of measured activities were 65% and 55% in the Curonian Lagoon and the Neris River respectively. The average share of radionuclide activity (^7Be , ^{40}K , ^{137}Cs , ^{210}Pb , ^{214}Pb) in the finest (F) fraction (0.2-1 μm) was 7% in both the Curonian Lagoon and the Neris River. The activity of ^7Be and ^{137}Cs in the finest fraction was below the detection limit. In this fraction, the highest activity fractions, 22% (1.2 Bq/m³) and 29% (0.23 Bq/m³), were found for ^{40}K and ^{214}Pb , respectively, the former in samples from the Neris River and the latter in samples from the Curonian Lagoon. These radionuclides exhibited a relatively even distribution among the different fractions.

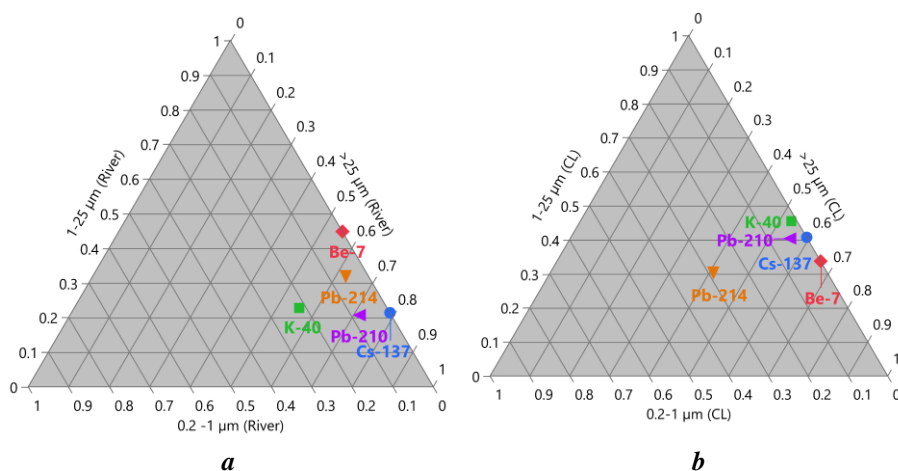


Figure 7. The shares of radionuclides activities in the sediment fractions (0.2-1 μm , 1-25 μm , > 25 μm) Neris river (on the left), Curonian Lagoon (on the right)

The activity of caesium dominated in the coarsest fraction (Table 4). The distribution of caesium activity (0.26 Bq/m³ and 0.37 Bq/m³) between the middle (M, 1-25 μm) and the coarsest fraction in the Neris River and the Curonian Lagoon, respectively, was 20% and 80% and 40% and 60%.

Table 4. Radionuclide distribution between fractions of suspended sediments (C->25 μm ; M- 1-25 μm ; F-0.2-1 μm), n/d – not detected

Location	Fraction	^7Be , Bq/m ³	^{40}K , Bq/m ³	^{137}Cs , Bq/m ³	^{210}Pb , Bq/m ³	^{214}Pb , Bq/m ³
Neris r.	C	1.6 ± 0.1	3.0 ± 0.2	0.21 ± 0.01	1.12 ± 0.08	0.38 ± 0.03
	M	1.27 ± 0.09	1.21 ± 0.08	0.060 ± 0.004	0.32 ± 0.02	0.19 ± 0.01
	F	n / d	1.15 ± 0.08	n / d	0.120 ± 0.008	0.030 ± 0.002
Curonian Lagoon	C	1.18 ± 0.08	2.4 ± 0.2	0.22 ± 0.02	0.95 ± 0.07	0.34 ± 0.02
	M	0.60 ± 0.04	2.0 ± 0.1	0.15 ± 0.01	0.69 ± 0.05	0.25 ± 0.02
	F	n / d	0.070 ± 0.005	n / d	0.100 ± 0.006	0.23 ± 0.02

The activity values of ^{210}Pb were 1.12 Bq/m³ and 0.95 Bq/m³ in the coarsest fraction and 0.32 Bq/m³ and 0.69 Bq/m³ in the middle fraction of suspended sediments. The activity values of ^{214}Pb were 0.38 Bq/m³ and 0.34 Bq/m³ in the coarsest fraction and 0.19 Bq/m³ and 0.25 Bq/m³ in the middle fraction for the Neris River and the Curonian Lagoon, respectively. The activity values of the radionuclides considered in the coarsest fraction (> 25 μm) were approximately the same, while in the middle fraction they differed by a factor of two in most cases.

3.1.2. Radionuclide flux

Based on literature data and the measurements, the annual export of caesium and plutonium from the catchment area of the Neman River (Figure 8) were estimated.

Caesium. According to the three-year monitoring by Lujanas et al. (2002), the activity levels of ^{137}Cs in suspended matter in the Neris River are similar to those in the Neman River into which it flows (68 Bq/kg and 60 Bq/kg averaged over three years). Jakimavicius (2012) estimated that the catchment of the Neman River carries an average of 21.8 km³ of water annually. Assuming that the average activity of ^{137}Cs in suspended particles is 0.17 Bq/m³, the annual flux with these particles into the Curonian Lagoon is estimated at 3.6 GBq. Assuming that about 80% of the caesium in the Neman River is in dissolved form (Monte et al., 2002), the total flux is estimated to be 18.2 GBq/year, which is close to the previous estimate (Lujanas et al., 2002) of 41±34 GBq/year (decay corrected to 2021). The sources of caesium could be either the Chernobyl accident or global fallout. This is because the proportion of Chernobyl fallout in suspended particles varies due to uneven distribution and deposition in the watersheds. The southern part of the Neman has a higher proportion of Chernobyl-derived caesium than the western part,

where the proportion is 2-4 times lower. However, on average 47% of the river's total caesium activity originates from Chernobyl fallout (Marčiulionienė et al., 2017). Therefore, the expected contribution of these sources to the caesium flux into the Curonian Lagoon is about the same.

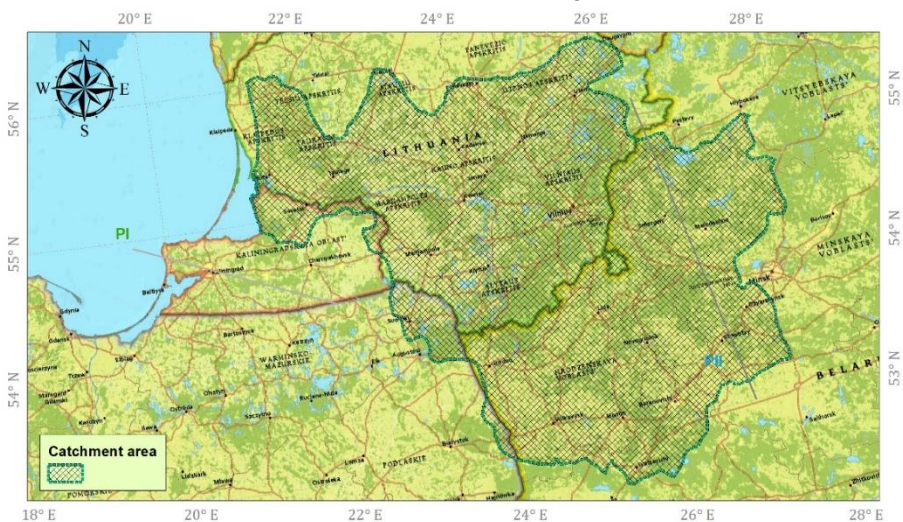


Figure 8. The catchment area of the Neman River

Water flux-based approach. The annual input of plutonium with suspended matter can be estimated similarly to caesium. The average activity of plutonium in suspended solids is 1.0 ± 0.5 mBq/m³, so the total flux to the lagoon is estimated to be 23 ± 12 MBq/year.

Sediment-based approach. Another method for estimating the plutonium flux is to use plutonium activity in suspended particles (0.13 Bq/kg) and estimates of the sediment budget in the Curonian Lagoon. Mežine et al. (2019) estimated the average annual sediment input to the lagoon from the Neman River to be $4.8 \times 10^8 \pm 3.8 \times 10^8$ kg/year. On this basis, the annual input of ^{239,240}Pu can be estimated to be 62 ± 49 MBq/year.

Catchment runoff-based approach. For comparison, the annual input of ^{239,240}Pu by the Vistula River was estimated to be 89.0 MBq by Skwarzec et al. (2011) (unfiltered water with low SPM content). This estimate shows the input of plutonium during the observed period. Over a longer period, the average plutonium input can be estimated based on the catchment area and the plutonium inventory in the area.

The catchment area of the Neman River, which supplies the Curonian Lagoon with suspended particles, is 10⁵ km². The annual input of ^{239,240}Pu from the catchment was estimated based on the data on plutonium deposition in the considered area (I), the mean residence time of plutonium in the catchment (t) and its area (S) according to Equation 9.

The estimated inventory of $^{239,240}\text{Pu}$ fallout in the 50-60 latitude range was $1.3 \pm 0.5 \text{ mCi/km}^2$ ($48.1 \pm 18.5 \text{ Bq/m}^2$) (Hardy et al., 1973). According to UNSCEAR (1982), 39 Bq/m^2 of plutonium was deposited in the Northern Hemisphere. Chernobyl fallout contribution to total plutonium in soil could be as high as 96% (Ketterer et al., 2004). Mietelski (2001) reports that the contribution of Chernobyl-derived plutonium in soil in Poland is about 5% (centre), 15% (east) and in some cases 100% (north-east). The leachable $^{239,240}\text{Pu}$ of global fallout ranged from 40 to 59.8 Bq/m^2 , and Chernobyl-derived plutonium was up to $1.2 \pm 0.3 \text{ Bq/m}^2$. Lukšienė et al. (2015) studied undisturbed Lithuanian meadow soils and found that Chernobyl-derived plutonium accounted for between 6.5 and 59.1% of the total plutonium. The average $^{239,240}\text{Pu}$ inventory in the southwestern transect was $26 \pm 4 \text{ Bq/m}^2$ and in the north-eastern transect $19 \pm 3 \text{ Bq/m}^2$. Thus, it can be concluded that the range of the $^{239,240}\text{Pu}$ inventory is between 16 and 60 Bq/m^2 .

Due to the high reactivity to the particles, plutonium is mainly removed from the soil surface by erosion. The amount of plutonium removed from the catchment can be affected by land use and changes in soil erosion rates (Foster and Hakonson, 1984). To roughly estimate long-term processes, it is usually assumed that the erosion rate remains constant at its average value (Beasley et al., 1984). The amount of plutonium eroded in a catchment is determined by the residence time of the plutonium ($\ln(2)/[\text{eroded fraction}]$). In the studied literature (Beasley et al., 1984; Smith et al. (1987); Zhuang et al., 2019; Wang et al., 2021a) various values are reported for the residence time of plutonium in the catchments, as illustrated in Figure 9.

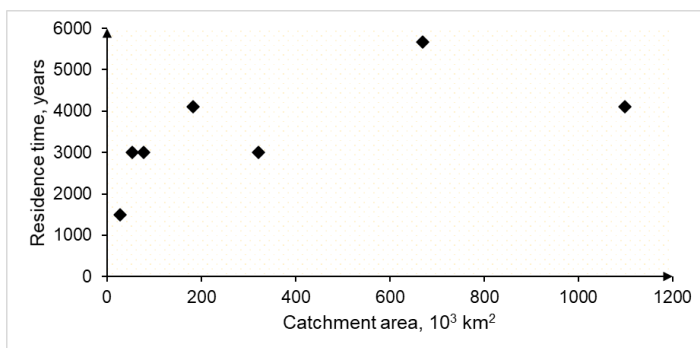


Figure 9. Residence time of plutonium depending on catchment area

Several studies have estimated the residence times of different catchments in relation to plutonium removal. Smith et al. (1987) studied the transport of fallout radionuclides in the Saugenay catchment (78000 km^2). The time-dependent two-component model used to simulate radionuclide transport

showed that the residence time of $^{239,240}\text{Pu}$ of 3000 years agreed well with the other soil erosion model. Beasley et al. (1984) found that erosive processes remove transuranic radionuclides over a period of around 6000 years based on the removal rate of plutonium from the Columbia catchment (670000 km²). Meanwhile, Zhuang et al. (2019) estimated a residence time of 3000 years for the Haihe River catchment, and Wang et al. (2021a) assigned residence times of 800, 1500, and 4100 years to catchments with an area of less than 5200, between 5200 and 78000 and more than 78000 km², respectively, based on their study of the plutonium inventory in the Bohai and Yellow Seas. Of these publications, only approaches based on experimental data were considered (Smith et al. 1987; Beasley et al., 1984). Compared to the catchment size of 0.78×10^5 km² used in the calculations of Smith et al. (1987) a residence time of 3000 years was considered more appropriate for the 10^5 km² catchment. Based on the Equation 16, the total contribution of the flux of $^{239,240}\text{Pu}$ was 882 ± 510 MBq per year.

The different calculation methods used yielded varying results: 23 ± 11 MBq/year, 62 ± 49 MBq/year, and 882 ± 510 MBq. The first two methods are based on measured activity results, and their confidence intervals overlap, with values close to the reported estimate of 89 MBq/year for the Vistula River (Skwarzec et al., 2011). As the catchment-based approach is widely used, it is worth considering it as a conservative scenario.

Plutonium in the Curonian lagoon. Using sediment budget calculations Mežine et al. (2019) estimated that approximately 62% of the sediment entering the Curonian Lagoon remains trapped within its boundaries. According to the amount of plutonium that settles in the lagoon, this retention amounts to about 39 MBq per year, while the remaining 24 MBq per year enter the Baltic Sea. In other words, the input from the rivers contributes to the 25 mBq/m². This inflow is assumed to continue for more than 40 years, resulting in 1 Bq/m². The reported average spatial activity of $^{239,240}\text{Pu}$ in the bottom sediment of the Curonian Lagoon was 2.6 Bq/m² (Lujanienė et al., 2022), so the estimate is closer to the actual situation. The total inventory in the bottom sediments of the Curonian Lagoon can be estimated at 1.56 GBq.

3.1.3. Chapter conclusions

Plutonium activity in bottom sediments fraction $< 63 \mu\text{m}$ of the Neman River was on average 0.08 Bq/kg, while the suspended matter contained 0.13 Bq/kg (1 mBq/m³). In the Curonian Lagoon, significant variations in the concentration of suspended matter and the activity values of $^{239,240}\text{Pu}$ were found, but no significant dispersion of the activity data of $^{239,240}\text{Pu}$ in the

bottom sediments. Analysis of particle fractions (0.2-1 μm , 1-25 μm , > 25 μm) showed that > 93% of the total radionuclide activity (^7Be , ^{40}K , ^{137}Cs , ^{210}Pb , ^{214}Pb) was contained in the fraction > 1 μm . The activity values of ^{137}Cs in the fraction > 25 μm were about the same in the Curonian Lagoon and Neris river waters ($\sim 0.21 \text{ Bq/m}^3$), while the activity in the fraction 1-25 μm in the Curonian Lagoon was more than twice as high than in the fraction 1-25 μm of the river.

Based on the assessment of ^{137}Cs activity in suspended particles, it was estimated that about 3.6 GBq of caesium (as of 2022) flow into the Curonian Lagoon with the Neman River, which is consistent with previous observations. Three approaches were used to estimate plutonium transport, based on water flow, sediment flow and catchment runoff model data, resulting in estimates between 23 MBq/year, 62 MBq/year and 882 MBq/year. The result of sediment flux approach is closer to the estimates for the Vistula, and the value of 882 MBq/year can be used as a conservative estimate.

The annual riverine contribution of $^{239,240}\text{Pu}$ to the bottom sediments of the Curonian lagoon estimated 1 Bq/m^2 for the period of 40 years. Taking in account the uneven distribution of plutonium in the lagoon area and reported values at 2.6 Bq/m^2 the assessment is close to the actual situation. Based on the value of 62 MBq/year, the annual amount of $^{239,240}\text{Pu}$ retained in the lagoon area is about 39 MBq/year.

3.2. The study of factors influencing the distribution of radionuclides in the Baltic Sea

3.2.1. Curonian Lagoon

The distribution of the ^{137}Cs , $^{239,240}\text{Pu}$, ^{241}Am shows that the activities in the bottom sediments of the Curonian Lagoon were higher near the coast on the opposite side of the river inflow (station 10) and at the narrows of the Klaipeda Strait (Figure 10, Figure 11).

The average activity values of $^{239,240}\text{Pu}$ and ^{241}Am in the bottom sediments of the Curonian Lagoon are 1.51 and 0.81 Bq/m^2 , respectively. The median activity of $^{239,240}\text{Pu}$ was 2.6 Bq/m^2 with the range from 0.13 to 15 Bq/m^2 . Relatively higher activities were observed in the Klaipeda strait, Neman River with the highest activity recorded at the station CL10 in the southwestern part of the studied area. The measured activity values of $^{239,240}\text{Pu}$ and ^{241}Am at this station were 15 and 13.3 Bq/m^2 , respectively.

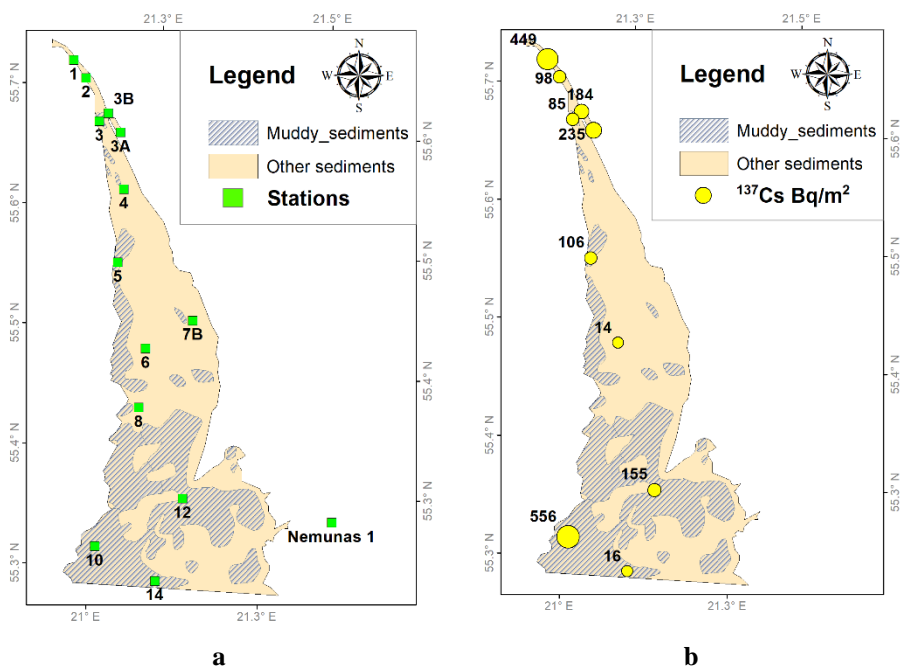


Figure 10. Plots of the station's setup and ^{137}Cs distribution in the bottom sediments of the Curonian Lagoon. The muddy sediments zones plot based on data Vaičiūtė et al. (2021)

Except for one anomalous value, it can be concluded that the majority of activities of $^{239,240}\text{Pu}$ and ^{241}Am at all stations were not higher than 1.8 Bq/m^2 .

The activities of ^{137}Cs in the bottom sediments of the Curonian Lagoon are shown in Figure 10b. The median activity is 131 Bq/m^2 and is in the lower half of the observed range of values from 14 to 556 Bq/m^2 . The highest values were observed in the southern part of the study area at the Nida station (556 Bq/m^2) and in the Klaipėda Strait (449 Bq/m^2).

Previous studies show that the highest activities of ^{137}Cs in this area are associated with the finest particles ($0.2\text{-}1 \mu\text{m}$) and have positive correlation with sediments with of high total organic carbon (0.75) and clay minerals (0.95) (Lujanienė et al., 2013). Thus, the areas with muddy sediments are the potentially radionuclide enriched zones in the lagoon area.

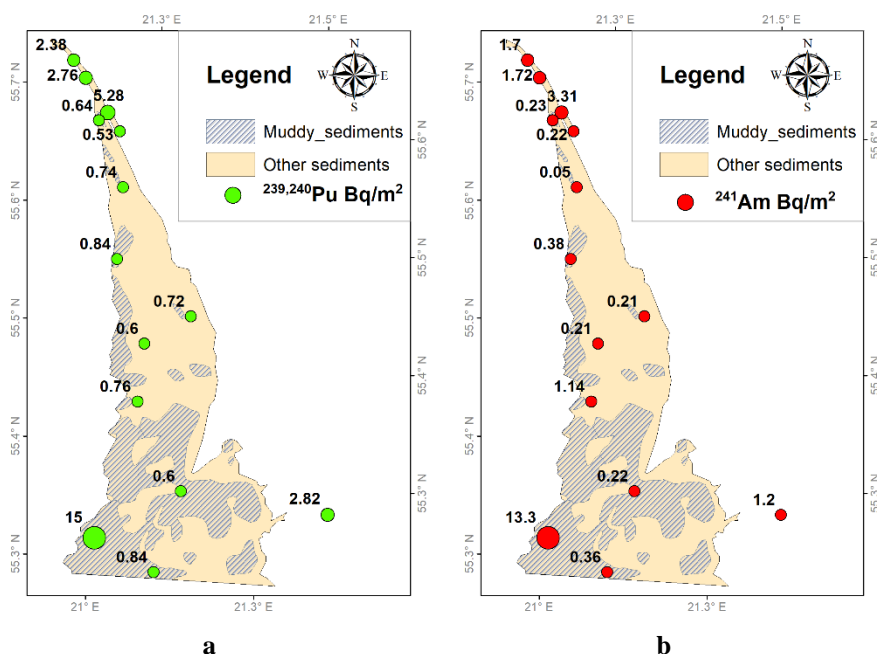


Figure 11. Plots of $^{239,240}\text{Pu}$ (a) and ^{241}Am (b) in the bottom sediments of the Curonian Lagoon. The muddy sediments zones plot based on data Vaičiūtė et al. (2021)

The areas of fine silty mud sediments (50-10 μm) reported by Vaičiūtė et al. (2021) (Figure 10,11) are characterised by both low and high values of activities of ^{137}Cs , $^{239,240}\text{Pu}$, ^{241}Am . From this we can draw the preliminary conclusion that the areas with mud sediments in the Curonian Lagoon play a minor role in the accumulation of radionuclides ^{137}Cs , in the Curonian Lagoon area. The data of $^{239,240}\text{Pu}$ and ^{241}Am distribution led to the same conclusion.

3.2.2. Coastal region of the south-eastern part of the Baltic Sea

3.2.2.1. Activity levels of $^{239,240}\text{Pu}$, ^{137}Cs , ^{241}Am

East to west profile. In the research profile of stations (Figure 5, red squares), measurements were made at eight stations, with a range of $^{239,240}\text{Pu}$ activity from 0.42 to 8.94 Bq/m^2 , ^{137}Cs activity from 546 to 2188 Bq/m^2 and ^{241}Am activity from 0.19 to 3.36 Bq/m^2 (Figure 12). The depth difference between station 4 and ChG2 is 86 metres, with a distance of 120 kilometres. The profile shows an exponential slowdown in the depth decrease with a sharp change at the furthers station (ChG2). $^{239,240}\text{Pu}$ and ^{241}Am show a linear trend of increasing activity from east to west (as well as with increasing seabed

depth), with approximately equal regression coefficients ($R^2 = 0.8$). The average increase in activity of $^{239,240}\text{Pu}$ and ^{241}Am towards the coast is $0.07 \text{ (Bq/m}^2\text{)/km}$ and $0.025 \text{ (Bq/m}^2\text{)/km}$, respectively.

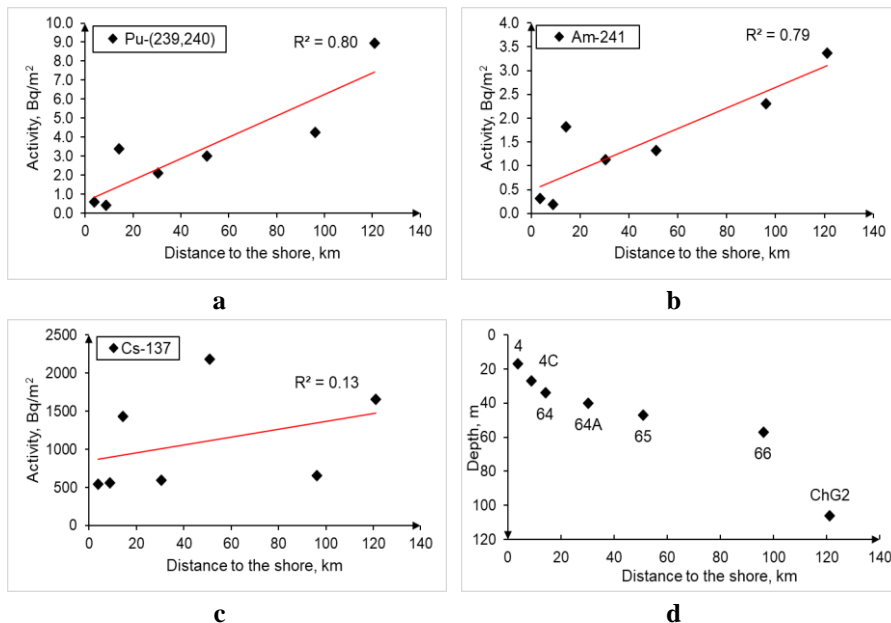


Figure 12. Average radionuclide activities (Bq/m^2) (a,b,c) and depth profile (d)

As can be seen from the depth profile (Figure 13), the trend of increasing activity of $^{239,240}\text{Pu}$ with depth is 0.82, while for ^{241}Am it is 0.64. It should be noted that the measurement at station ChG2 provides a sufficiently high correlation coefficient for $^{239,240}\text{Pu}$ without exceeding 0.5 in the coastal zone (stations 4 to 66). Since the trend only appears on a sufficient scale, this could indicate the weakness of the effect of "sediment focusing" on the studied profile, despite the relatively high correlation coefficient. Furthermore, the limited number of measurements in the profile should be taken into account. The distribution of ^{137}Cs in the profile shows no trend with increasing depth, and an alternation of increases and decreases in activity is observed with increasing depth.

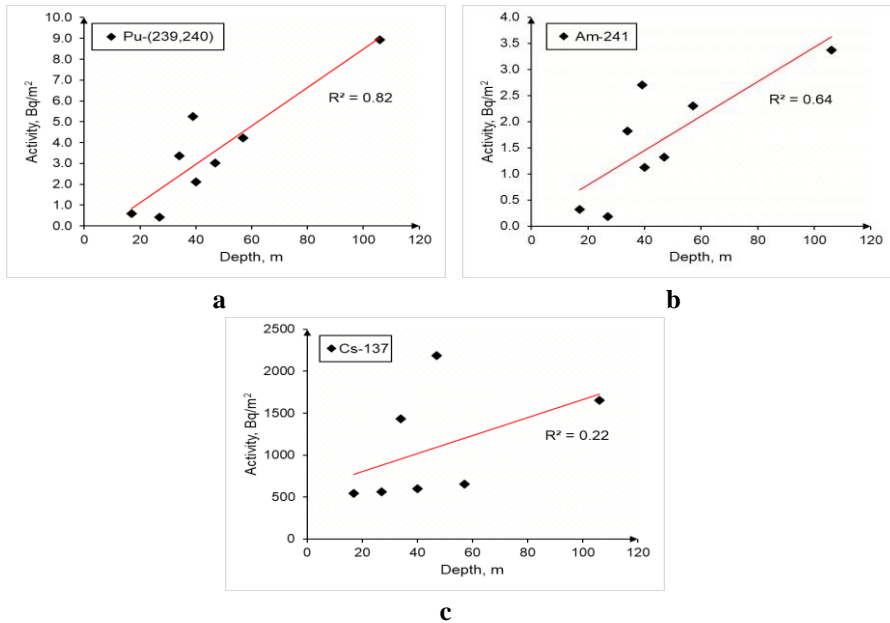


Figure 13. General trends of $^{239,240}\text{Pu}$ (a), ^{241}Am (b) and ^{137}Cs (c) activities depending on depth

Coastal area. The studied area has a size of 45×82 km and borders on the Curonian Lagoon in the west. The spatial distributions of depth and radionuclide activities were interpolated using the Kriging algorithm (Cressie, 2015). The layout of the station is shown in Figure 14. The area is characterised by the weak slope to the west and the local depression at station 6b. The input of sediments from the Curonian Lagoon occurs in the area of stations 4 and 5. The spatial distribution of $^{239,240}\text{Pu}$ and ^{241}Am activities in the coastal area of the outflow from the Curonian Lagoon is shown in Figure 15 and Figure 16. The scheme shows the shape of the seabed and the colour represents the radionuclide activity. The distribution is characterised by two spots with $^{239,240}\text{Pu}$ activities of 5.2 (station 64B) and 4.2 Bq/m² (station N-6) in the northern and southern parts, respectively. The spatial distribution of ^{241}Am corresponds to the pattern of $^{239,240}\text{Pu}$ with two spots of high activities of 2.7 (station 64B) and 2.5 Bq/m² (station N-6) in the northern and southern parts, respectively.

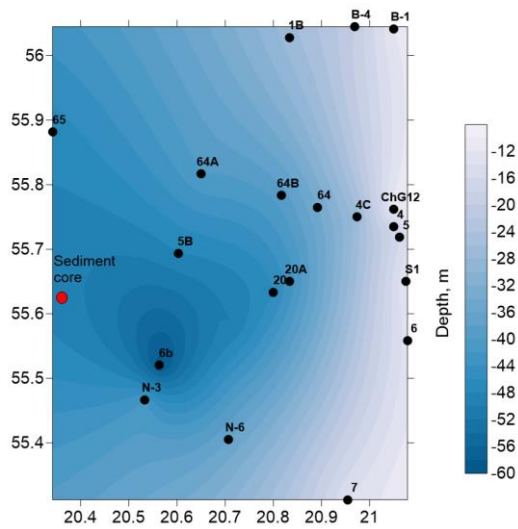


Figure 14. Station setup and kriging interpolation model of depth distribution of the coastal area of Curonian Lagoon sediment discharge (The coastal area and lagoon that are located on the eastern part are not shown)

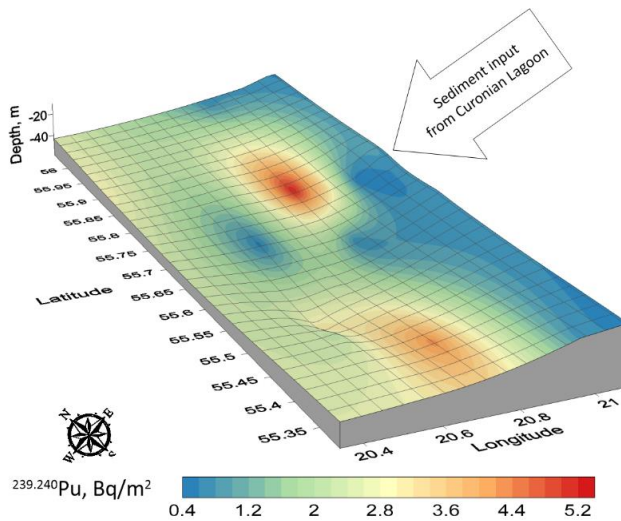


Figure 15. Kriging interpolation model of $^{239,240}\text{Pu}$ distribution of the coastal area of Curonian Lagoon sediment discharge (longitude and latitude is in degrees, z axis (depth, m) is enlarged ~ 1000 times for representativeness)

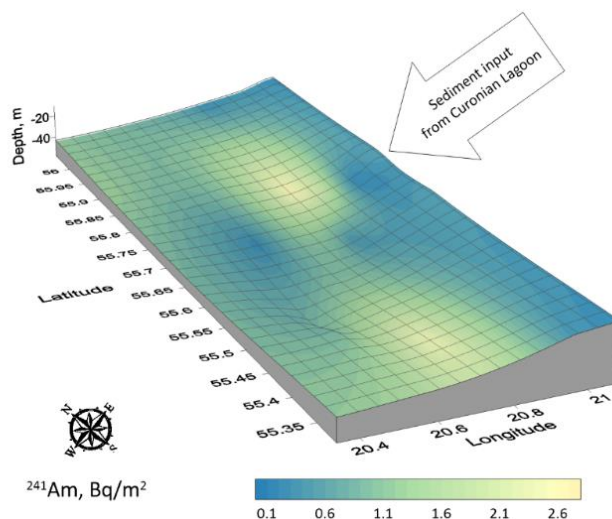


Figure 16. Kriging interpolation model of ^{241}Am distribution of the coastal area of Curonian Lagoon sediment discharge (longitude and latitude is in degrees, z axis (depth, m) is enlarged ~ 1000 times for representativeness)

The average activity values for $^{239,240}\text{Pu}$ and ^{241}Am in this area were 1.6 and 0.82 Bq/m² (N=20), respectively (Table 5). The median value of $^{239,240}\text{Pu}$ is 0.71 Bq/m² and is closer to the minimum activity values between 0.42 and 5.25 Bq/m². The median value of ^{241}Am is 0.44 Bq/m² and is also closer to the minimum activity values between 0.19 and 2.7 Bq/m².

Table 5. The comparative data of radionuclide activities in the studied areas

Nuclide	$^{239,240}\text{Pu}$, Bq/m ²				^{241}Am , Bq/m ²				N
	Area	High	Low	Mean	Median	High	Low	Mean	
Lagoon	5.3 ± 0.3	0.13 ± 0.01	1.8 ± 0.1	0.84 ± 0.06	3.3 ± 0.2	0.050 ± 0.004	0.9 ± 0.1	0.37 ± 0.03	14
Coastal	5.3 ± 0.3	0.42 ± 0.03	1.6 ± 0.1	0.71 ± 0.05	2.7 ± 0.2	0.19 ± 0.01	0.8 ± 0.1	0.44 ± 0.03	20
Profile	8.9 ± 0.4	0.42 ± 0.03	3.5 ± 0.2	3.2 ± 0.2	3.4 ± 0.2	0.19 ± 0.01	1.6 ± 0.1	1.6 ± 0.1	8

Disregarding the anomalous value in the lagoon (15 Bq/m²), the maximum values $^{239,240}\text{Pu}$ in the coastal region and in the lagoon area are approximately the same (5.25 Bq/m² and 5.28 Bq/m²), which is also true for the average values (1.61 Bq/m² and 1.78 Bq/m²). A similar conclusion can be drawn for ^{241}Am . Thus, the activity of $^{239,240}\text{Pu}$ and ^{241}Am is approximately the same in the lagoon area and in the coastal region.

3.2.2.2. Estimation of the share of Chernobyl-derived radionuclides

The $^{241}\text{Pu}/^{239,240}\text{Pu}$ ratio is a unique signature of the major sources of radioactive contamination. Due to the large difference in half-lives between the daughter nuclide ^{241}Am ($T_{1/2} = 432.2$ years) and ^{241}Pu ($T_{1/2} = 14.35$ years) (NuDat 3, n.d.), the $^{241}\text{Pu}/^{239,240}\text{Pu}$ ratio decreases and the $^{241}\text{Am}/^{239,240}\text{Pu}$ ratio increases over time until the complete decay of ^{241}Pu . Thus, knowing the initial $^{241}\text{Pu}/^{239,240}\text{Pu}$ ratios for the global and Chernobyl fallout, we can use the $^{241}\text{Am}/^{239,240}\text{Pu}$ ratio to assess the contribution of these sources to bottom sediments in the Curonian Lagoon area and the south-eastern coastal zone of the Baltic Sea.

According to Kashparov et al. (2003), the release of $^{239,240}\text{Pu}$ from Unit 4 of the Chernobyl reactor was estimated to be 18-52 TBq, while the release of ^{241}Pu and ^{241}Am was estimated to be 1530-3990 TBq and 1.3-3 TBq, respectively. Using these values, the initial $^{241}\text{Pu}/^{239,240}\text{Pu}$ ratios ranged from 29 to 216 and the $^{241}\text{Am}/^{239,240}\text{Pu}$ ratios ranged from 0.02 to 0.16 (for 1986). The value 82 for $^{241}\text{Pu}/^{239,240}\text{Pu}$ was given by the (IAEA, 1986) as characteristic for fallout from Chernobyl. Strumińska et al. (2006) and Paatero et al. (2004) reported values for $^{241}\text{Pu}/^{239,240}\text{Pu}$ between 54 and 94.8 in aerosol samples. Lujanienė et al. (2009) reported $^{241}\text{Am}/^{239,240}\text{Pu}$ ratios between 0.08 and 0.19 (average - 0.11) in aerosol samples collected during the first days of the Chernobyl fallout (28 April - 01 May 1986) in the Lithuanian area (Vilnius). Holm et al. (1986) reported $^{241}\text{Pu}/^{239,240}\text{Pu}$ ratios of 12.0-13.9 (corrected to 1963) for marine and terrestrial samples contaminated by global nuclear weapons test fallout. Salminen et al., 2005 reported a $^{241}\text{Pu}/^{239,240}\text{Pu}$ ratio of 16 in nuclear weapons test fallout (1963) on the territory of Finland.

The activity ratios of the selected samples were adjusted for analysis. We assumed that the Curonian Lagoon and the south-eastern part of the Baltic Sea have only two main sources of ^{241}Am and $^{239,240}\text{Pu}$ - the global and Chernobyl fallout, with a combined contribution of 100%. The initial value of ^{241}Am in the global fallout was assumed to be zero. According to literature data, the selected ratios of $^{241}\text{Pu}/^{239,240}\text{Pu}$ and $^{241}\text{Am}/^{239,240}\text{Pu}$ in the Global fallout were $R_{\text{Pu}(0)}^{\text{GF}} = 12$ and $R_{\text{Am}(0)}^{\text{GF}} = 0$ (1963), while in the Chernobyl fallout they were $R_{\text{Pu}(0)}^{\text{Ch}} = 82$ and $R_{\text{Am}(0)}^{\text{Ch}} = 0.11$ (1986). The ratio of $^{241}\text{Pu}/^{239,240}\text{Pu}$ was chosen to be 12 to ensure that the measured ratio of the samples without contribution from the Chernobyl fallout is not lower than that of the global fallout, as is the case when a value above 12 is used. The ratio of $^{241}\text{Am}/^{239,240}\text{Pu}$ ($R_{\text{Am}(t)}$) changes due to the decay of these isotopes and the formation of ^{241}Am from ^{241}Pu . Since the activities of ^{239}Pu and ^{240}Pu change

only insignificantly during the calculation period (by 0.1% and 0.3%, respectively), we did not take these changes into account. Therefore, the ratio for global fallout was determined by the following equation:

$$R_{Pu(t)}^{GF} = R_{Pu(0)}^{GF} \times \text{Exp}(-\lambda_{Pu}t) \quad (18)$$

where $t_{GF}=51$ years, time from the beginning of the countdown, $\lambda_{Pu}=0.0483 \text{ y}^{-1}$. Similarly, for the Chernobyl fallout ($t_{Ch}=28$ years) we obtain $R_{Pu(t)}^{Ch} = 21.2$.

The ratio for ^{241}Am will be determined from the decay of the formed ^{241}Am and the ^{241}Am that was already present at the time of the release:

$$R_{Am(t)} = R_{Pu(0)} \times \left(\frac{\lambda_{Am}}{\lambda_{Am} - \lambda_{Pu}} \right) \times (\text{Exp}(-\lambda_{Pu}t) - \text{Exp}(-\lambda_{Am}t)) + R_{Am(0)} \times \text{Exp}(-\lambda_{Am}t) \quad (19)$$

where, $\lambda_{Am} = 0.0016 \text{ y}^{-1}$. For Chernobyl ($R_{Am(0)}^{Ch} = 0.11$) and Global fallout ($R_{Am(0)}^{GF} = 0$) and for the year 2014 it equals $R_{Am(t)}^{GF} = 0.34$, a $R_{Am(t)}^{Ch} = 2.07$.

According to the obtained data, in the considered profile and coastal zone, the ratios of $^{241}\text{Am}/^{239,240}\text{Pu}$ are shown in Figure 17. As can be seen from the diagram (Figure 17a), the ratios are in the Global fallout area, indicating a low proportion of Chernobyl-derived ^{241}Am and $^{239,240}\text{Pu}$ in most samples.

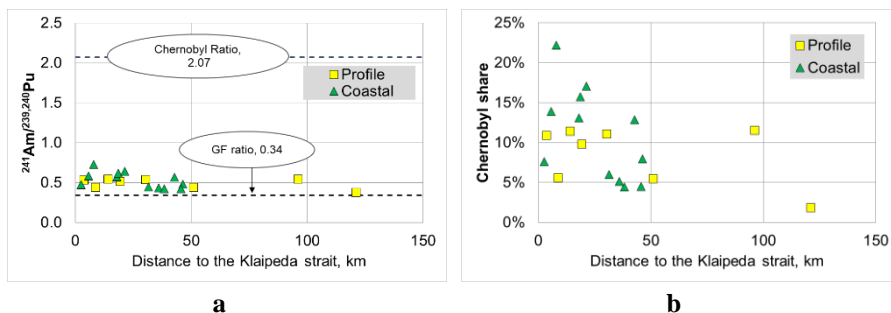


Figure 17. Radionuclide activity ratios (a) and Chernobyl fallout contribution (b)

The Figure 17b shows the estimated contribution of the Chernobyl fallout. The values range from 2% to 22%, with an average of 10%. With increasing distance from the coast, the maximum values decrease to 5.5%, but a higher value (11.5%) is again observed at station 66 in a more distant area.

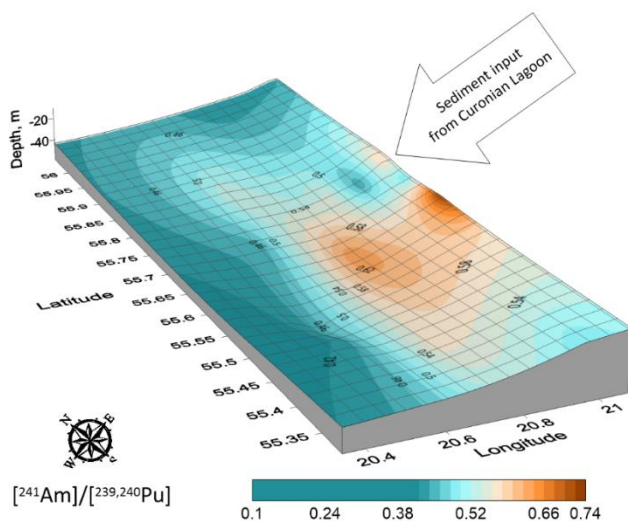


Figure 18. The spatial distribution (Kriging interpolation model) of $^{214}\text{Am} / ^{239,240}\text{Pu}$ ratio in the coastal region of the south-eastern Baltic Sea (longitude and latitude is in degrees, z axis (depth, m) is enlarged ~ 1000 times for representativeness)

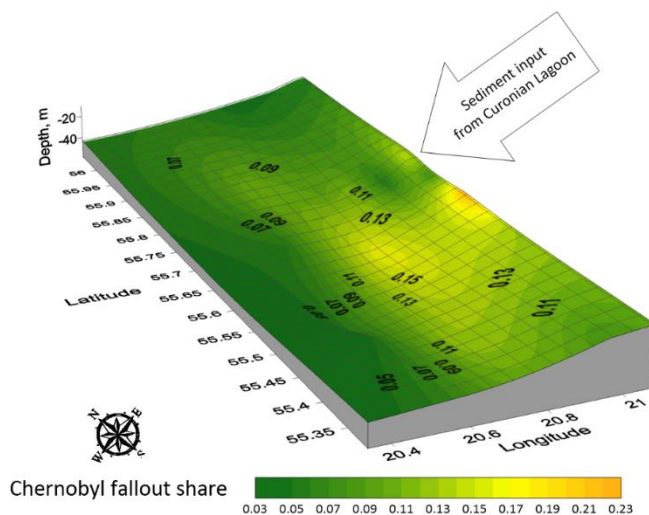


Figure 19. The spatial distribution (Kriging interpolation model) of the Chernobyl fallout contribution in the coastal region of the south-eastern Baltic Sea (longitude and latitude is in degrees, z axis (depth, m) is enlarged ~ 1000 times for representativeness)

The average of $^{241}\text{Am}/^{239,240}\text{Pu}$ activity ratios in the bottom sediments of the Curonian Lagoon lied within a range from 0.35 to 0.89 with the mean

value 0.49. In the coastal area nearby to the lagoon (Figure 18) the ratios were within a range from 0.42 to 0.73 with mean and average values at 0.52. Thus, the range of values in the Lagoon is inside the range of the coastal area and both distributions are approximately symmetric.

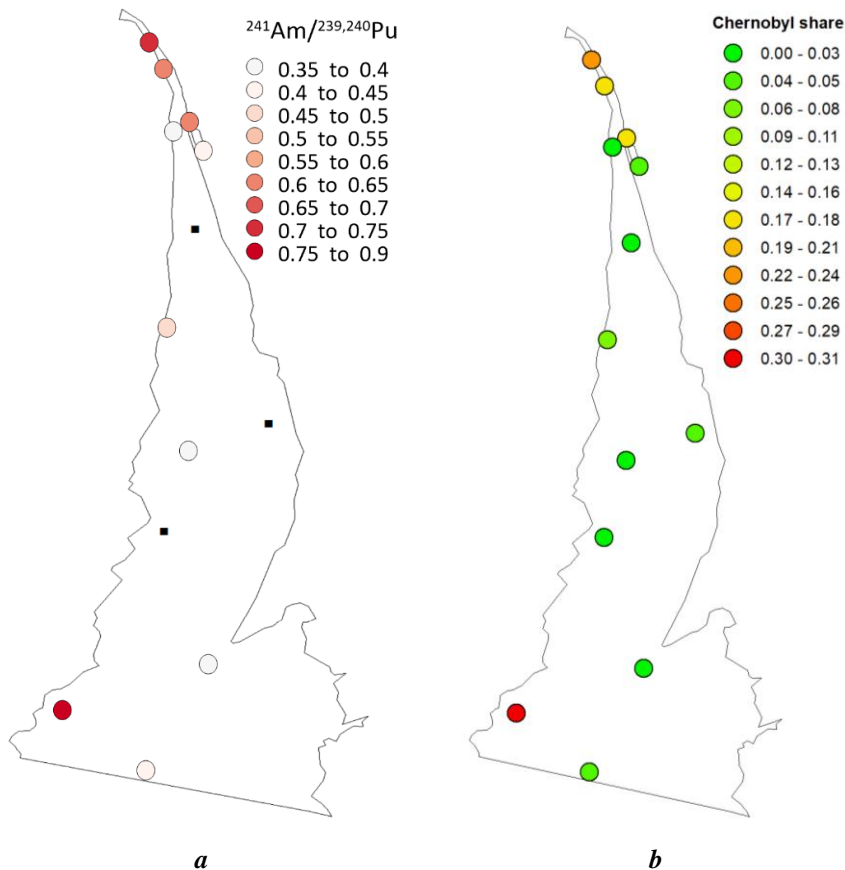


Figure 20. Plots of the $^{241}\text{Am}/^{239,240}\text{Pu}$ (a) and Chernobyl share (b) in the bottom sediments of the Curonian Lagoon.

The estimated by the $^{239,240}\text{Pu}/^{241}\text{Am}$ ratio contribution of the Chernobyl fallout in the coastal area (Figure 19) adjacent to the Curonian Lagoon ranged from 4% to 22%. The mean and median values were 10%. The spatial pattern is characterised by higher contributions of Chernobyl fallout off the coast of the Curonian Lagoon and low values on the deep sea side, indicating the probable result of discharge from the lagoon area. A higher contribution of Chernobyl fallout (30%) was also observed in the bottom sediments of the Curonian Lagoon (Figure 20) at station 10 (south-western part of the study area), where higher activities of $^{239,240}\text{Pu}$ and ^{241}Am were detected. The

contribution of Chernobyl fallout to the bottom sediments of the Curonian Lagoon is estimated within a range from 0.3% to 31.4% with an average and median value 8.7% and 4.9% (N=13) accordingly.

Figure 20 demonstrates the estimated values $^{240}\text{Pu}/^{239}\text{Pu}$ atomic ratios of bottom sediments sampled in the Curonian Lagoon and the Baltic Sea. The values were within a range from 0.17 to 0.20 and this is around the value (0.18) of the plutonium ratio of global fallout of nuclear explosions. Based on these values and the Equation 1 and Equation 2 the contribution of the Chernobyl fallout was estimated (Table 6). It was assumed that there are only two sources of plutonium in the area - the global fallout with $^{240}\text{Pu}/^{239}\text{Pu} = 0.18$ and the Chernobyl fallout with a ratio of 0.40 (Salminen-Paatero et al., 2012).

The estimated impact of the Chernobyl fallout in the Curonian Lagoon ranges from 0% to 34% at station 10, where anomalous values of radionuclide activities are observed. Station 5 (Figure 14), located in the area where sediments are discharged from the Curonian Lagoon, shows a range from 0% to 37%, similar to the values observed in the lagoon. Station 7, which is located in the sea near the Curonian Lagoon, shows a lower range of values between 4% and 21%. At station 65 (~50 km), which is far from the coast, the contribution is almost non-existent.

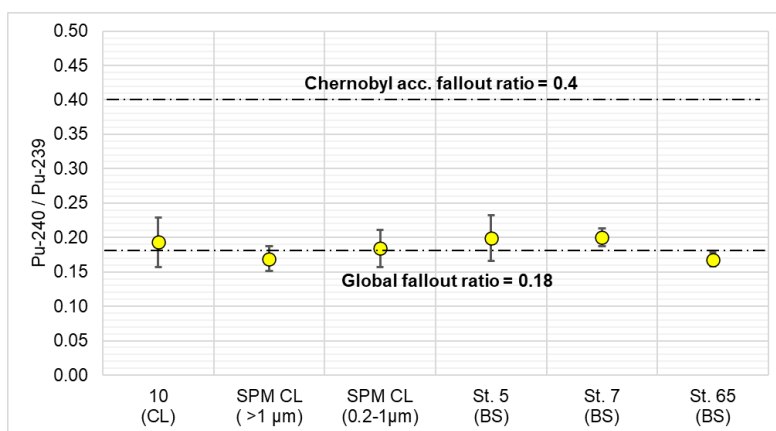


Figure 21. The values of $^{240}\text{Pu}/^{239}\text{Pu}$ atomic ratio for bottom sediments. BS – Baltic Sea, CL – Curonian Lagoon, suspended matter samples: SPM CL, bottom sediments: 10, st.5, st.7, st.65

The study of suspended matter in the Curonian Lagoon reveals the presence of a global fallout signal of plutonium. The Chernobyl fallout signal is estimated to be less than 5% in suspended particles of > 1 μm and less than 19% in suspended particles in the range of 0.2-1 μm (Table 6). This phenomenon can be attributed to the source of the plutonium (Choppin and

Morgenstern, 2001) and requires additional research for a better understanding.

Table 6. The comparative data of Chernobyl fallout contribution

#	Sample	Place	Chernobyl share
1	Station 10	Lagoon	0 - 34%
2	SPM >1 μm	Lagoon	0 - 4%
3	SPM 0.2-1 μm	Lagoon	0 - 19%
4	Station 5	Sea	0 - 37%
5	Station 7	Sea	4 - 21%
6	Station 65	Sea	0%

It can be assumed that a large proportion of the particles containing Chernobyl fallout are deposited in the lagoon at specific accumulation sites that correspond to the locations of sediment deposition in the model of Mežine et al. (2019). Consequently, the hydrodynamic conditions of the lagoon lead to an uneven distribution and concentration of radionuclides originating from the Neman River catchment. This process has the potential to lead to an accumulation of ecologically significant amounts of radionuclides.

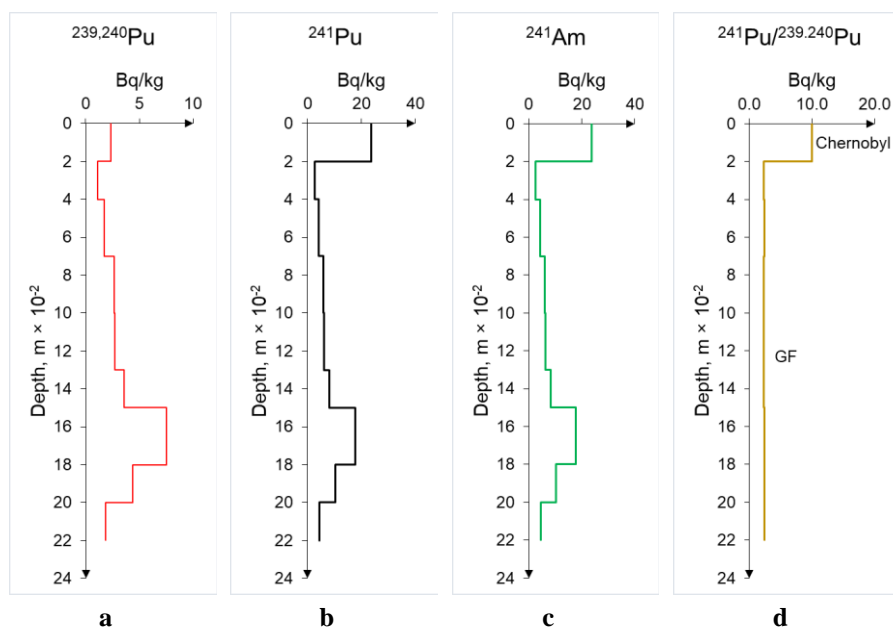


Figure 22. The vertical distribution of the radionuclides and the ratio $^{241}\text{Pu}/^{239,240}\text{Pu}$ in the sediment core, located in the western part of coastal area (figure 14)

In the western coastal region of the study area (Figure 14), a sediment core was taken in 2001, the data of which were recalculated and evaluated. The depth distribution of the radionuclides ($^{239,240}\text{Pu}$, ^{241}Pu and ^{241}Am) shows a very similar pattern (Figure 22). In the upper layer of 0-2 cm there is a layer with elevated values, followed by a layer with minimal values and an increase in values to a depth of 15-18 cm, where the maximum is observed for $^{239,240}\text{Pu}$ and the second largest peak for ^{241}Am and ^{241}Pu . The $^{241}\text{Am}/^{241}\text{Pu}$ ratio is also in a narrow range of 0.14 to 0.15, and in the upper layer of 0-2 cm it decreases to 0.05. The age of the sediment layers was calculated based on the decay of ^{241}Pu and the formation of ^{241}Am using Equation 16 indicating that most of the deposits date back to 1965, which corresponds to the global fallout. The estimated origin of pollution in the upper layer (0-2 cm) is from 1981. Since the upper layer is a mixture of signals from the global fallout and the fallout from Chernobyl, the calculated age may be biased by the addition of "fresh" ^{241}Pu . The ratio of $^{241}\text{Pu}/^{239,240}\text{Pu}$ is also in a narrow range of 2.30 to 2.45 in the 2-22 cm layer, confirming the origin of the global fallout. Therefore, the layer with the increased concentration (0-2 cm) reflects the presence of signals from the Chernobyl fallout, and based on this layer, the sedimentation rate in the upper layer (0-2 cm) can be estimated to be about 1.3 mm/year. Similarly, based on previous calculations, we assume that the ratios of $^{241}\text{Am}/^{239,240}\text{Pu}$ and $^{241}\text{Pu}/^{239,240}\text{Pu}$ are 0 and 12, respectively, for the global fallout and 0.11 and 82, respectively, for the Chernobyl fallout. Using Equation 17 and 18, we estimated that the contribution of Chernobyl fallout in the 0-2 cm thick layer is ~20%. With the calculated sedimentation rate, the layer with mixed contamination from Chernobyl and global fallout will reach 5 cm by 2023.

3.2.2.3. Chapter conclusions

It was found that the activities of $^{239,240}\text{Pu}$ and ^{241}Am in the bottom sediments of profile increase with sampling depth and distance from the sampling station to the shore. The distribution of $^{239,240}\text{Pu}$ and ^{241}Am in the bottom sediments compared to sampling depth of the research profile reveals an upward trend in activity towards the west from the Klaipeda Strait with correlation estimated at 0.82 for $^{239,240}\text{Pu}$ and 0.64 for ^{241}Am . A strong linear regression ($R^2 \sim 0.8$) with distance to the shore observed for the both radionuclides. The increase in activity per kilometre was found to be 0.07 Bq/m² for $^{239,240}\text{Pu}$ and 0.025 Bq/m² for ^{241}Am . This increase in activity can be attributed to the effect of fine particles increasing with depth, which are the main carriers of radionuclides, also known as the effect of "sediment focusing".

The spatial distribution of the $^{239,240}\text{Pu}$ and ^{241}Am activities in the coastal area (45×82 km) of the outflow from the Curonian Lagoon is characterised by two areas of high activities with peak at the station 64B and N-6. The observed average activities of $^{239,240}\text{Pu}$ and ^{241}Am (1.8 Bq/m^2 and 0.9 Bq/m^2 , respectively) in the Curonian Lagoon were close to the values of the adjacent coastal area (1.6 Bq/m^2 and 0.8 Bq/m^2 , respectively). This can be result of the natural and anthropogenic (dredging of Klaipeda Strait) transport Curonian Lagoon sediments to the coastal area.

At the station CL10, located in the Curonian Lagoon, anomalous activity values of $^{239,240}\text{Pu}$ and ^{241}Am were detected, amounting to 15 and 13.3 Bq/m^2 , respectively, 31% of which were due to the Chernobyl fallout signal. The study has not revealed a pronounced connection between the spatial distribution of muddy sediments and the activities of ^{137}Cs , $^{239,240}\text{Pu}$ and ^{241}Am in the bottom sediments of the Curonian Lagoon. The high radionuclide activities in the bottom sediments at the station CL10 could be due to the presence of “hot” particles as well as to an accumulation of radionuclides, which requires further investigation.

The analysis of the radionuclide origin shows that the predominant pollution with $^{239,240}\text{Pu}$ and ^{241}Am in the bottom sediments (0-5 cm) in the south-eastern area of the Baltic Sea is related to the global fallout. The areal contour with an increased signal of Chernobyl fallout (from 10% to 20%) was interpreted as an effect of sediment input from the catchment area of the Neman River through the Curonian Lagoon by natural and anthropogenic activity (dredging). In the Curonian Lagoon area, the contribution of the Chernobyl fallout ranged from 0.3% to 31% with an average value of 9%, which could indicate the significant spatial non-uniformity of $^{239,240}\text{Pu}$ and ^{241}Am .

The studies of vertical distribution of ^{241}Pu , $^{239,240}\text{Pu}$, ^{241}Am in the sediment core taken in the south-eastern part of the Baltic Sea shows that the contribution to the plutonium activity of the Chernobyl fallout in the upper layer (0-2 cm) of sediments is about 20%. The plutonium found in the deeper layers of the sediment core is attributed to the global fallout resulting from atmospheric nuclear explosions. By utilizing the ^{241}Pu – ^{241}Am dating model, it has been determined that this plutonium originates from 1965. The sedimentation rate of the upper layer of the sediment core has been estimated to be 1.33 mm/year .

3.2.3. Southern Baltic Sea area and Skagerrak Bay area

3.2.3.1 Grain size distributions

The setups of sampled stations have shown on a Figure 23-a, b. The samples from all the areas studied consisted of sediments rich in silt and sandy mud. The grain sizes of these sediments showed a bimodal distribution with a mean value of 14-45 μm (Figure 24 a-c).

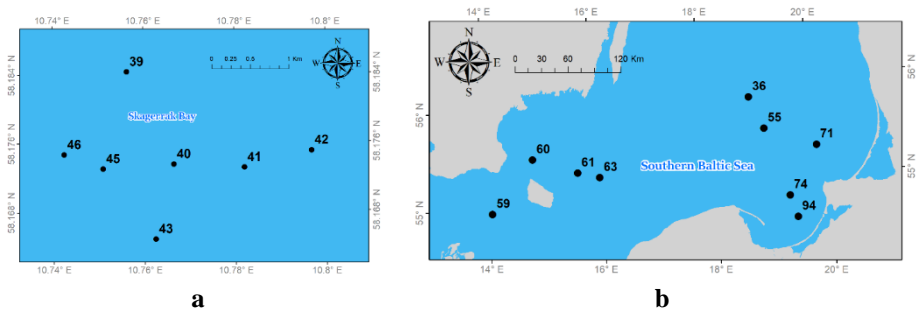


Figure 23. Sampling stations setup: Skagerrak – a; Southern Baltic Sea stations – b

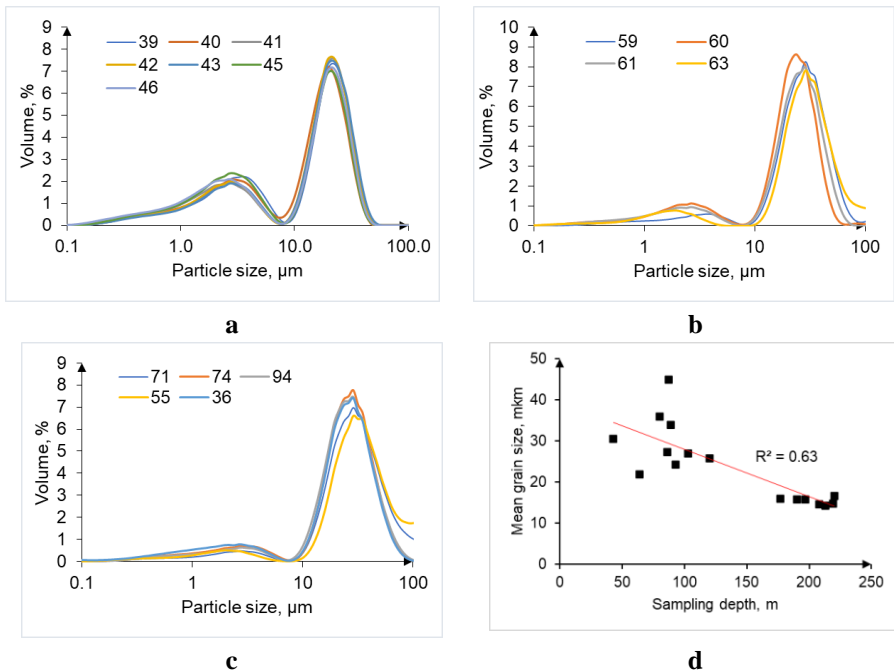


Figure 24. Grain size distributions (a, b, c) and plot of sampling depth and mean grain size (d)

The larger mode ranged from 7 to 216 μm and was mostly found in the 7-50 μm range. The lower tail mode had limits of 0.2-6 μm in most cases. Most samples have a minimum within the size range between 7 and 8 μm , with the exception of Station 39, where the minimum shifted to a slightly larger size range of 8.5-9.0 μm .

On average, the modes peaked at 26 and 3 microns, but certain sample groups deviated from this pattern. Specifically, the sediment samples collected from the stations in Skagerrak Bay showed a tendency to have a higher concentration of finer particles (belonging to the first mode) compared to the other stations. At station 40, the peak value for larger particle fractions was in the range of 21-22 micrometres, while at station 60 it was in the range of 19-20 micrometres. However, at the other stations (46, 45, 39, 43, 41, 42, 59, 61, 63, 36, 55, 74, 94, 71) the peak value was in the range of 28-30 micrometres. In Skagerrak Bay, the relative peak area of the smaller mode was between 4.9 and 7.6 %, which is more than double the range of 0.4-1.9 % at the other stations. Mean grain size has a weak tendency to decrease with sampling depth (($P=0.8$, $\alpha<0.05$)) as shown on Figure 24d.

3.2.3.1 Radionuclides activities

The measured activity range of ^{137}Cs in the sediment samples was between 8 Bq/kg and 220 Bq/kg, with an average value of 53 Bq/kg (Table 7). Upon comparing the studied sites, it was observed that the eastern part of the southern site (SE) exhibited lower activity levels of ^{214}Pb , ^{40}K and ^{137}Cs that were estimated at 49 Bq/kg, 929 Bq/kg and 116 Bq/kg, respectively. A gradual increase in activity levels of this nuclides was observed from the south-eastern part to the south-western part and further to the Skagerrak Bay. Compared to other radionuclides, ^{210}Pb levels were lower in the western part (SW) with a value of 112 Bq/kg, while the highest levels were found in the eastern section.

Table 7. The activities of ^{137}Cs , ^{210}Pb , ^{214}Pb , ^{40}K in the bottom sediments at the studied areas

Area		Skagerrak Bay	South-Western BS (SW)	South-Eastern BS (SE)	TOTAL
Stations		39, 40, 41, 42, 43, 45, 46	59, 60, 61, 63	36, 55, 74, 94, 71	All
^{137}Cs , Bq/kg	Min	8.0 \pm 0.4	17 \pm 0.9	62 \pm 3.1	8 \pm 0.4
	Max	11 \pm 0.6	80.0 \pm 4	220.0 \pm 11	220 \pm 11
	Mean	9 \pm 0.5	52 \pm 3	116 \pm 6	59 \pm 3
	Min	94 \pm 4.7	83 \pm 4.2	133 \pm 7	83 \pm 4

Area		Skagerrak Bay	South-Western BS (SW)	South-Eastern BS (SE)	TOTAL
Stations		39, 40, 41, 42, 43, 45, 46	59, 60, 61, 63	36, 55, 74, 94, 71	All
²¹⁰ Pb, Bq/kg	Max	164 ± 8	133 ± 7	171 ± 9	171 ± 8.6
	Mean	121 ± 6	112 ± 6	151 ± 8	128 ± 6
²¹⁴ Pb, Bq/kg	Min	25 ± 1	25 ± 1	30 ± 2	25 ± 1
	Max	30 ± 2	52 ± 3	80 ± 4	80 ± 4
	Mean	28 ± 1	38 ± 2	49 ± 2	38 ± 2
⁴⁰ K, Bq/kg	Min	706 ± 35	447 ± 22	827 ± 41	447 ± 22
	Max	783 ± 39	1012 ± 51	1093 ± 55	1093 ± 55
	Mean	746 ± 37	812 ± 41	929 ± 46	829 ± 41
Depth, m	Min	177 ± 9	64 ± 3	43 ± 2	43 ± 2
	Max	220 ± 11	93 ± 5	120 ± 6	220.0 ± 11
	Mean	203 ± 10	82 ± 4	88 ± 4	124 ± 6

Skagerrak Bay. Seven stations (39, 40, 41, 42, 43, 45 and 46) were sampled in Skagerrak Bay, an area with an average sampling depth of 203 metres, significantly deeper than the southern site, which was 82-88 metres deep (as shown in Table 5). These stations were located in west-east direction and showed increasing depth towards the east (Figure 25).

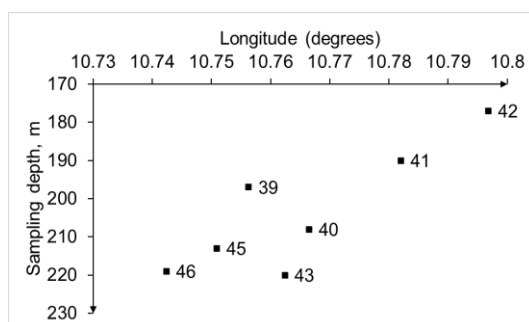


Figure 25. Schematic of the depth profile along longitude (from West to East direction)

The activity levels of ¹³⁷Cs, ²¹⁴Pb and ⁴⁰K were relatively low compared to southern Baltic Sea area with an average of 9 Bq/kg, 28 Bq/kg and 783 Bq/kg, respectively. The values of the ²¹⁴Pb/[sample depth] ratio in this area were in a narrow range between 0.13 and 0.14, while the ratios in the other areas were between 0.35 and 0.57. This suggests that ²¹⁴Pb activities increased at a slower rate with increasing sampling depth in this site relatively southern Baltic Sea stations. The ²¹⁰Pb/¹³⁷Cs ratio was also significantly different from

the other areas, ranging between 8.6 and 19.0, while the rest of the study area (SW and SE) had values between 0.8 and 5. Taking in account small activities of ^{137}Cs this ratio is reasonably higher. This may be result of a smaller number of riverine particles that bring ^{137}Cs from contaminated catchments to this area from the inner part of the Baltic Sea.

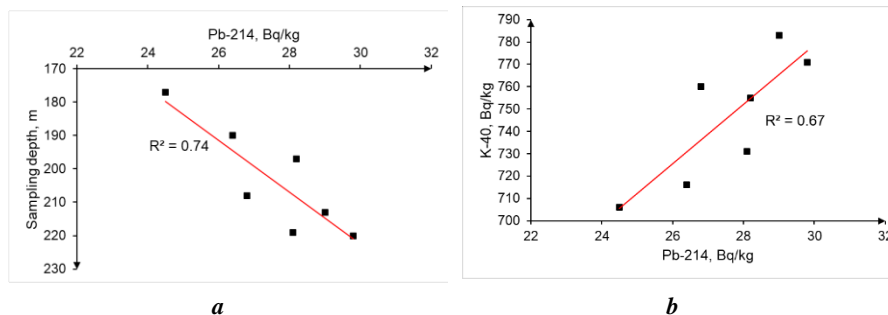


Figure 26. Plots of ^{214}Pb activities with sampling depth (a) and ^{40}K (b)

The study found that there was a strong positive correlation between the activity of ^{214}Pb and depth in the sampled area ($R = 0.86$, $p < 0.05$) as shown in Figure 26.

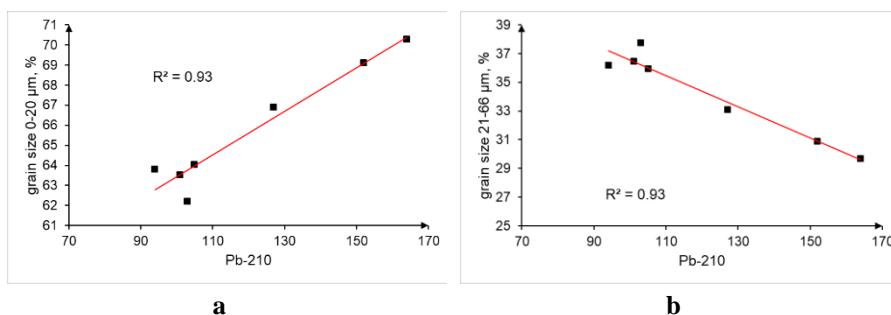


Figure 27. Plots of ^{210}Pb activities with a volume of fractions 0-20 μm (a) and 21-66 μm (b) in the Skagerrak Bay

It is likely that the increase in ^{214}Pb activity with depth may be due to the fact that particles that reach greater depths have a longer residence time in seawater, which increases their likelihood of scavenging more ^{226}Ra . This is consistent with Le Roy et al. (2018) results, which showed that ^{226}Ra acts as a partial conservative in seawater.

Additionally, the study found that there was a high positive correlation between the activity of ^{214}Pb and ^{40}K ($R = 0.82$, $p < 0.05$), which also supports the hypothesis that the increasing ^{214}Pb activity is due to the particle residence time (Figure 26b).

The analysis of the correlations between the activities of the radionuclides (^{137}Cs , ^{40}K , ^{214}Pb , ^{210}Pb) and the relative amounts of the grain size fractions (0-10 μm , 10-20 μm , 21-40 μm , 42-66 μm , 69-120 μm , 125-196 μm) in the collected samples showed that there is a statistically significant dependence between the content of the fraction 21-66 μm and ^{210}Pb ($R = -0.97$, $p < 0.05$) at the Skagerrak Bay (Figure 27a). The decrease of the 21-66 μm fraction means that the volume of the other fraction increases. As can be seen in Figure 27b, the 0-20 μm fraction shows a strong positive correlation with ^{210}Pb ($R = 0.97$, $p < 0.05$). Accordingly, the fraction $< 21 \mu\text{m}$ plays an important role in the transport mechanism of ^{210}Pb at this site. This is consistent with the conclusions of Ravichandran et al. (1995), who observed a positive correlation between fine-grained sediments and ^{210}Pb in the Sabine-Neches estuary.

Southern Baltic Sea stations. Nine stations (Figure 23b) were studied in the southern part of the Baltic Sea, that located in the Arkona Basin (St. 59), the Bornholm Basin (St. 60, 61, 63), the eastern Gotland Basin (St. 36, 55, 71) and the Gdansk Basin (74, 94). Figure 28 (a, b) shows the depths levels of the sampled stations.

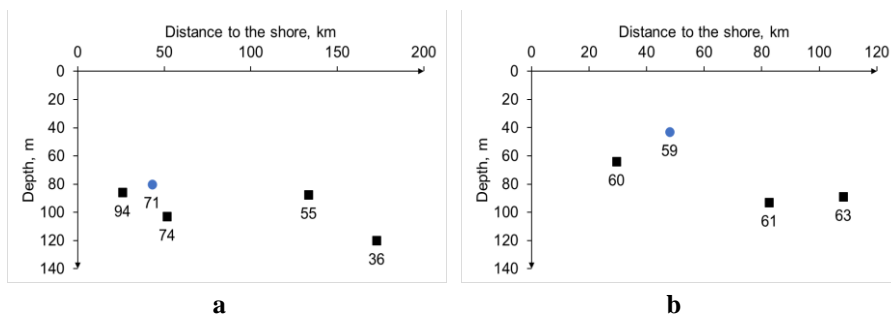


Figure 28. Depth levels at the stations

The stations in the *Arkona and Bornholm* basins (stations 59, 60, 61, 63) were located at depths from 64 to 93 m. The mean radionuclide activities for these stations were 52 Bq/kg, 112 Bq/kg, 38 Bq/kg and 812 Bq/kg for ^{37}Cs , ^{210}Pb , ^{214}Pb , ^{40}K , respectively. The ^{137}Cs activities ranged from 16.5 to 79.6 Bq/kg. Station 61 was located in the deepest area (93 m depth) and the activities of ^{137}Cs in the bottom sediments were highest at this station. The average caesium activity at the site is more than five times higher than at the Skagerrak site.

At the *Eastern Gotland and Gdansk basin* the deepest sampling depth of 120 m was recorded at the station 36, where the highest values of ^{214}Pb (80 Bq/kg) and ^{40}K (1093 Bq/kg) were measured. In contrast, station 74, which is

located at a depth of 103 m and lies in a seabed depression compared to stations 94, 55 and 71 (86, 87.5 and 80 m, respectively), has the lowest values of ^{210}Pb (42 Bq/kg). The activities of ^{137}Cs at this site varies between 62 Bq/kg and 220 Bq/kg, with an average value of 116 Bq/kg. This average value of is more than twice as high as that at the Arkona and Bornholm Basin stations and more than 10 times as high as that at the Skagerrak site.

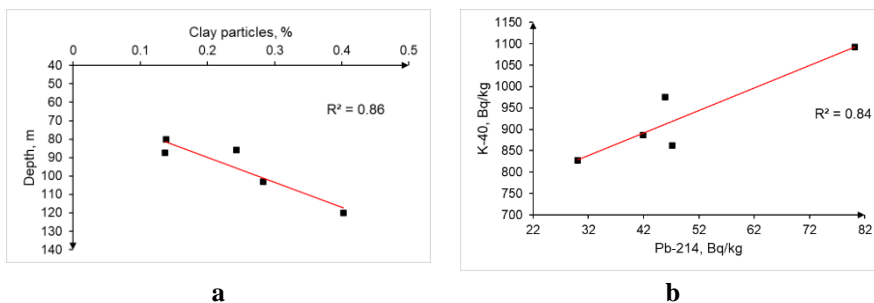


Figure 29. Plots of depth distribution of clay particles share (%) in the samples (a) and ^{214}Pb activities with ^{40}K (b)

At this site a significant correlation ($R=0.93$; $p < 0.05$) between clay content ($< 1.95 \mu\text{m}$) and sampling depth was found (Figure 29a). As at the Skagerrak site, a significant positive correlation ($R=0.92$, $p < 0.05$) between ^{40}K and ^{214}Pb was observed (Figure 29b), which may indirectly indicate similar mechanism of their scavenging from the seawater.

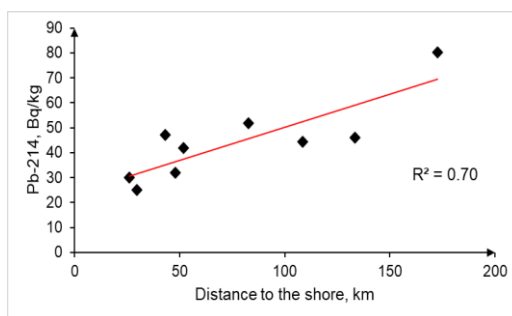


Figure 30. Plot of relation distance to the shore with ^{214}Pb activity in the bottom sediments of the southern Baltic Sea region

In contrast to Skagerrak stations the correlation between ^{210}Pb or $^{210}\text{Pb}/^{137}\text{Cs}$ with grain size at the Southern Baltic Sea stations was not observed. Positive correlation with distance to the shore demonstrated ^{214}Pb (Figure 30). This can be related to the increase of particle residence time with distance to the shore (since more ^{226}Ra can be scavenged by particles).

3.2.3.3. General trends

Figure 31 shows the distributions of correlation coefficients for different particle sizes, radionuclide activities and depths of sampling at the studied sites (Figure 23). Based on the data, it can be seen that the content of particles with grain sizes within ranges 0.4-0.75 μm , 2.0-7.5, 11-18 μm increases positively with the depth of sampling, while the number of particles of the range from 30 to 59 μm decreases with increasing depth.

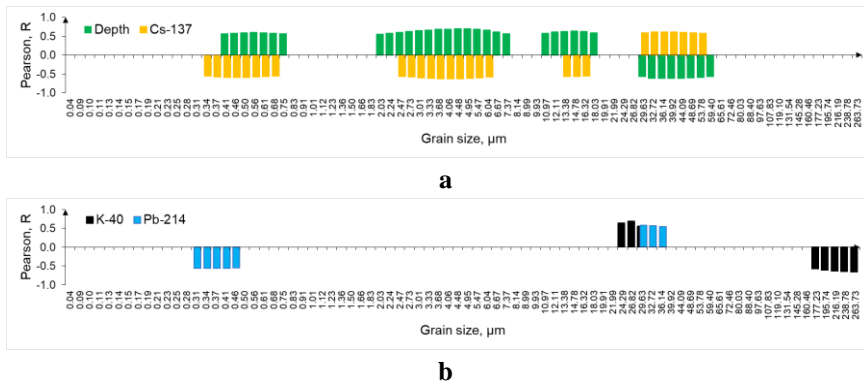


Figure 31. Plots of Pearson correlation coefficients (>0.55 , $\alpha < 0.05$) of grain size and radionuclide activities (^{137}Cs)-a, (^{40}K , ^{214}Pb)-b and sampling depth – a

The results show that caesium activities have three size ranges of particles where they show negative average correlation: 0.34-0.68 μm , 2.5-6.0 μm , 13.4-16.3 μm . Meanwhile the average positive correlation was found within a range from 30 to 54 μm and that is in agreement with caesium distribution in suspended particle fractions (Table 4). The activity of ^{40}K decreases in particles from 177 to 264 μm and has positive correlation with range of 24-30 μm . The activities of ^{214}Pb have overlapping range (30-36 μm) of positive correlation with ^{40}K , while in the range of 0.31-0.46 μm showed negative correlation. The negative correlation of radionuclide with a particular particle size fraction suggests that the specific radionuclide may not be present in that fraction and that as the fraction increases, the specific activity naturally decreases.

A weak positive correlation was observed between mode ratio and caesium activity (Figure 32a), indicating that the particles with mean size around 26 μm have a more influence on caesium transport in the Baltic Sea compared to particles with a size of around 3 micrometres. This is differed from result obtained by Charlesworth et al. (2006) in their study of sediments

at the bottom of the eastern Irish Sea. In their studies, Charlesworth et al. demonstrated a linear relationship between the proportion of the 15 μm fraction and the activity of ^{137}Cs and ^{241}Am . However, the sampling area was densely sampled at the stations with similar hydrodynamic conditions, which may have resulted in preferential sorption of radionuclides by certain fractions of particles. Laceby et al. (2017) reported that the specific surface area of particles typically correlates with the activity of particle-reactive radionuclides. However, this pattern is not universal and depends on the origin of the radionuclide. For example, radionuclides on sinking particles may be scavenged of the water or enter the particles in sorbet form from other areas.

The $^{210}\text{Pb}/^{137}\text{Cs}$ ratio decreases as the number of particles containing ^{137}Cs increases, indicating an increase in the influence of riverine input due to the transport of ^{137}Cs from contaminated catchments. On the other hand, the increase in the $^{210}\text{Pb}/^{137}\text{Cs}$ ratio can be linked to the higher accumulation of ^{210}Pb on particles due to longer residence times of particles in seawater. Therefore, the increase in this ratio can be attributed to areas that are less affected by the riverine input of ^{137}Cs and have longer residence times, such as more distant and deeper areas. The $^{210}\text{Pb}/^{137}\text{Cs}$ ratio showed an inverse distribution (Figure 32b) with grain size mode ratio. This suggests that the small particles from the first mode ($< 6 \mu\text{m}$) influence on lead scavenging in the seawater.

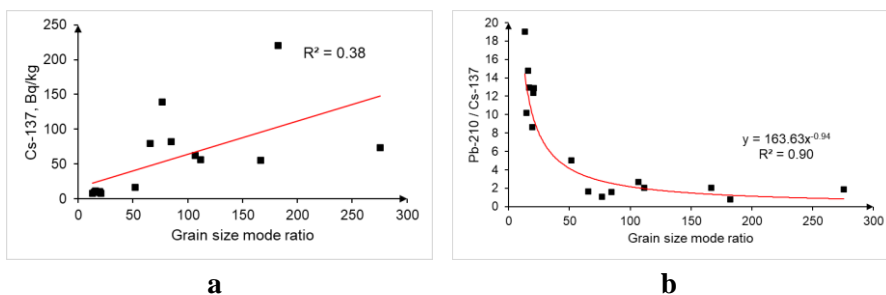


Figure 32. Plots of grain size mode ratio relationships with ^{137}Cs (a) and $^{210}\text{Pb}/^{137}\text{Cs}$ ratio in the bottom sediments of southern Baltic Sea and Skagerrak Bay

The interpretation of the $^{214}\text{Pb}/^{137}\text{Cs}$ ratio is similar to that of the $^{210}\text{Pb}/^{137}\text{Cs}$ ratio, with the exception that the increase in ^{214}Pb can be attributed to the scavenging of more ^{226}Ra from seawater. This scavenging process is likely facilitated by the increased residence time of particles in the water column, which is linked to depth and distance from the shore. The ratios of $^{210}\text{Pb}/^{137}\text{Cs}$ and $^{214}\text{Pb}/^{137}\text{Cs}$ showed high positive correlation ($R \sim 0.92$, $\alpha < 0.05$) with the amount of the 0-20 μm fraction in the sediment samples (Figure

33a,b). This implies that the variations in this ratio originate primarily from marine sources rather than from rivers. Thus, the observed correlations could indirectly indicate the scavenging features of ^{210}Pb and ^{226}Ra from seawater and the dominance of the 0-20 μm fraction in these processes. Furthermore, the positive correlation of these ratios with depth (Figure 34a,b) may also indicate the influence of particle residence time in seawater, affecting the probability of sorption of the aforementioned radionuclides.

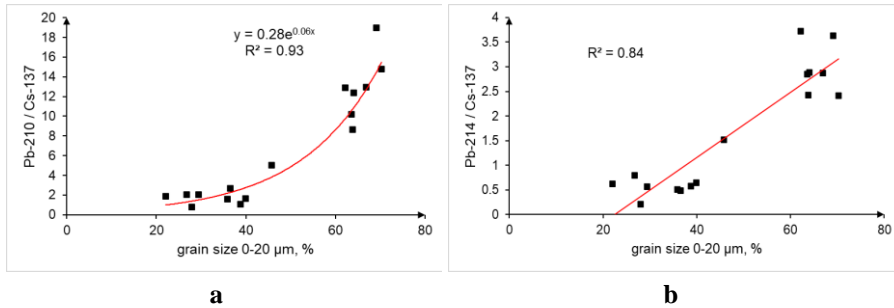


Figure 33. Plots of 0-20 μm grain size share with radionuclide ratio $^{210}\text{Pb}/^{137}\text{Cs}$ (a) and $^{214}\text{Pb}/^{137}\text{Cs}$ (b) in the bottom sediments of southern Baltic Sea and Skagerrak Bay

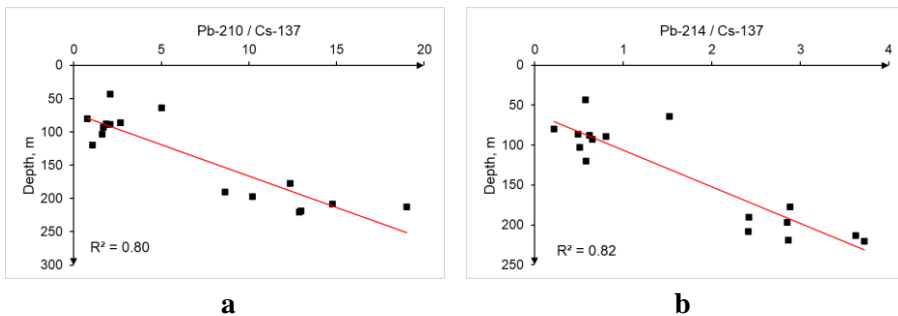


Figure 34. Depth distributions of cesium ratios: $^{210}\text{Pb}/^{137}\text{Cs}$ (a), $^{214}\text{Pb}/^{137}\text{Cs}$ (b) in the bottom sediments of southern Baltic Sea and Skagerrak Bay

The relationship between the parent isotope ^{214}Pb and the daughter isotope ^{210}Pb is shown in Figure 35a. As can be seen in the figure, the general trend shows that the dominance of the daughter isotope ^{210}Pb in this ratio increases with depth. However, when the data are divided into small segments, local decreases in ^{210}Pb activity and an increase in the dominance of ^{214}Pb with depth can be observed. The general trend can be explained by the significantly longer half-life of ^{210}Pb and the presence of more sources than ^{214}Pb . Local conditions may depend on various factors, such as the sinking flux (^{210}Pb scavenging rate) and the type of material on the seabed (^{226}Ra content).

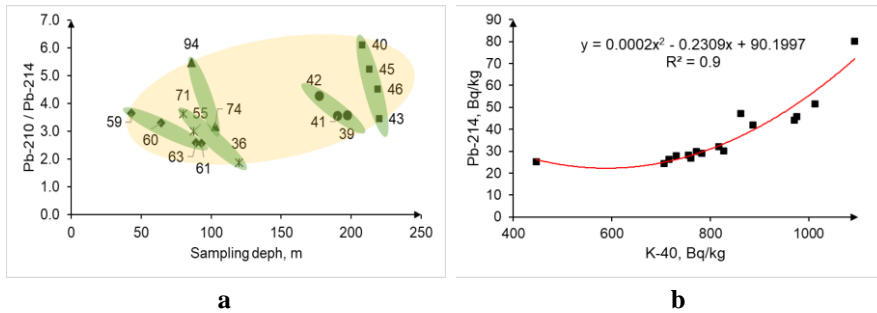


Figure 35. Plot of the sampling depth and $^{210}\text{Pb}/^{214}\text{Pb}$ ratio (a) and of ^{40}K with ^{214}Pb (b) in the bottom sediments of southern Baltic Sea and Skagerrak Bay

In the general data set (Figure 35b), an increase in ^{214}Pb activity is also observed with an increase in ^{40}K activity, which is consistent with known patterns of radionuclide behaviour. The increase in ^{214}Pb activity could be attributed to the presence of ^{40}K , which may have been scavenged from seawater along with ^{226}Ra . It is also possible that the observed correlation is due to the radionuclide composition of the parent rock. Further studies would be required to confirm the exact mechanisms that condition this relationship.

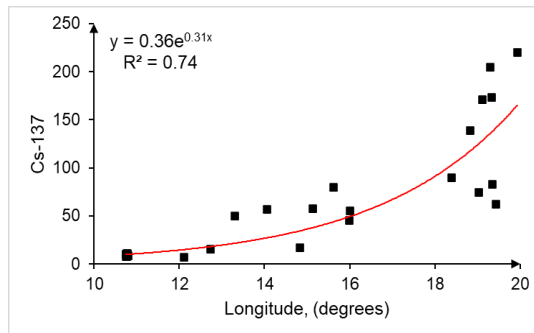


Figure 36. The longitudinal distribution of ^{137}Cs in the bottom sediments of southern Baltic Sea and Skagerrak Bay

To give further context to the data, we have also included 2018 results from the HELCOM database (ICES, 2020), which helps to increase the overall representativeness of the analysis. The observed trend ($R=0.83$) (Figure 36) suggests that the origin of caesium is within the Baltic Sea, as activity levels decrease as they move further out to sea boundaries. This pattern is consistent with the results documented in (Povinec et al., 2004).

Several factors can influence the transport of caesium in suspended matter in seawater, including the physical properties of the sediment (such as size, density and shape), the strength and direction of the current, as well as

water temperature and salinity, the density of particles in the water column and others (Lujanienė et al., 2014). Regardless of these factors, the probability of dilution by caesium-free particles and release of caesium from contaminated particles increases with residence time, which in turn increases with distance from the river sources, especially for the finest particles. The general trend of increase in caesium levels in the easterly direction (about 0.27 Bq/km) on the way from Skagerrak Bay to the Gotland Basin could be due to the decreasing residence time of riverine particles and the increasing number of particles carrying caesium from catchments contaminated by Chernobyl and global fallout.

3.2.3.4. Chapter conclusions

The mean grain size exhibited a bimodal distribution with a mean value of 14-45 μm and indicated a decreasing trend with greater sampling depth. The sediments obtained in Skagerrak Bay had the deepest sampling depth (177-220 m) in comparison to the other stations (43-120 m). These sediments comprised a higher proportion of smaller particles ($<6 \mu\text{m}$) and showed the lowest levels of ^{137}Cs activities (8-11 Bq/kg) and $^{137}\text{Cs}/^{210}\text{Pb}$ ratio (8.6-19). This can be attributed to the limited impact of rivers with catchments contaminated by ^{137}Cs .

In the context of the Skagerrak Bay the correlation between ^{210}Pb and particle size ranges indicates that particles smaller than 20 μm play a significant role in the accumulation of ^{210}Pb in the bottom sediments. However, the general data set (stations of Skagerrak Bay and southern part of Baltic Sea) did not show a significant correlation between ^{210}Pb and the 0-20 μm particle size range. Instead, the $^{210}\text{Pb}/^{137}\text{Cs}$ ratio demonstrated a strong trend with 0-20 μm particle size range. This also suggests that the ratio of $^{210}\text{Pb}/^{137}\text{Cs}$ is more indicative of the sorption process of ^{210}Pb in the specific marine conditions, rather than reflecting the initial variations of ^{210}Pb sorbet onto particles in riverine conditions.

The $^{214}\text{Pb}/^{137}\text{Cs}$ ratio in the bottom sediments of studied sites (southern Baltic Sea and Skagerrak Bay) showed a strong correlation with the grain size 0-20 μm and sampling depth. This was attributed to the dominating scavenging of ^{226}Ra from seawater by particles of $<20 \mu\text{m}$ size. And the amount of scavenged ^{226}Ra increase with depth, because of longer residence times of particles that reached greater depth.

The noted rise in ^{214}Pb levels as the sampling depth increases and as the activities of ^{40}K increase in the bottom sediments of Skagerrak Bay was attributed to that fact that the particles in the deeper regions spending more

time in seawater. This prolonged duration enhances their chances of scavenging higher amounts of ^{226}Ra and ^{40}K that may have the single source. A similar mechanism is likely to explain the increase in ^{214}Pb activity in the bottom sediments with distance from the shore in the southern part of the Baltic Sea.

The analysis reveals that the radionuclides exhibit varying affinities to different grain size ranges. As a result, the activities of ^{40}K are positively correlated with the fraction ranging from 24-30 μm , while ^{214}Pb shows a positive correlation with the fraction of 30-36 μm . The average positive correlation was also observed between ^{137}Cs activities and the grain size fraction of 30-54 μm , which aligns with the distribution of caesium in suspended particle fractions of the Neris River and the Curonian Lagoon. Consequently, it appears that the sediment fraction of 30 μm is a common factor influencing the accumulation of these radionuclides in the bottom sediments of the Baltic Sea.

Furthermore, the analysis of the data obtained in this work and the HELCOM database revealed that over the course of approximately 800 km, from Skagerrak Bay to the Kattegat and Gotland basins, there was an average increase of 0.27 Bq/km in caesium activity in the bottom sediments. This was attributed to the growing presence of particles carrying caesium originating from catchments contaminated by Chernobyl and global fallout.

CONCLUSIONS

The study provides new data on the transport, distribution and flux of radionuclides ($^{239,240}\text{Pu}$, ^{241}Pu and ^{241}Am) in the aquatic environment of the Neman River, the Curonian Lagoon and the Baltic Sea in the Lithuanian economic zone.

The Neman River basin is a long-term source of $^{239,240}\text{Pu}$ with an average annual rate of 62 MBq/year. The flux of ^{137}Cs , estimated at 3.6 GBq, is consistent with previous observations. Most of the activity is transported to the Curonian Lagoon by the particles $> 1 \mu\text{m}$ in the Neman River.

The suspended particles of 25 - 63 μm dominate in the the transport of ^{137}Cs and natural radionuclides (^7Be , ^{40}K , ^{210}Pb , ^{214}Pb) with the water of the Neman River into the Curonian Lagoon. Nevertheless, particles with a size of 30 μm play an important role in the distribution of ^{137}Cs , ^{40}K and ^{214}Pb , while suspended particles with a size of $< 20 \mu\text{m}$ influence the transport of ^{210}Pb in the Baltic Sea.

The obtained data on the spatial distribution of $^{239,240}\text{Pu}$ and ^{241}Am in the Curonian Lagoon and in the Baltic Sea of the Lithuanian Economic Zone indicate a characteristic pattern supporting the use of these radionuclides to trace pollutants in the studied area.

4. SANTRAUKA

ĮVADAS

Pakibusių dalelių bei nuosėdų transportacija paveikia radioaktyviųjų medžiagų ir įvairių teršalų sklaidą. Tuo pačiu paveikiamas ir vandens telkinių ekologinis statusas. Pastaraisiais metais Europos jūrų, o tarp jų ir Baltijos jūros užteršimas radionuklidais tapo esmine problema. Šios teritorijos tarša radionuklidais kilo iš branduolinių ginklų testavimo atmosferoje bei Černobylio katastrofos bei vėlesnės tokios pačios kilmės radionuklidų transportacijos iš šių regionų per upes iš užterštųjų baseinų (Povinec et al., 2003). Šie šaltiniai prisidėjo prie bendrojo kenksmingų medžiagų kiekio jūrinėje ekosistemoje. Tai kelia pavojų tiek gamtinei aplinkai, tiek ir žmonių sveikatai (Winkler, P. ir Roider, 1997; Livingston ir Povinec, 2002). Baltijos jūros radiologinę situaciją reikšmingai paveikia iš upių patenkančios šio pobūdžio medžiagos. Į Baltijos jūrą vandenį atnešančių vandens telkinių baseinai sudaro didžiulę $1,6 \times 10^5$ km² teritoriją (Matthäus ir Schinke, 1999), o upės atneša didžiausią tiek vandens, tiek ir nuosėdų dalį. Į Baltijos jūrą įteka daugiau nei 250 upių, kuriomis per metus į jūrą vidutiniškai patenka 446 km³/metai gėlo vandens (Graham ir Bergstrom, 2001). Tuo pačiu į jūrą patenka ir dideli kiekiai kietųjų dalelių bei teršalų, galintys neigiamai paveikti gamtą ir žmonių sveikatą. Labai svarbu žinoti apie potencialius ekologinius pavojus, susijusius su teršalais, kuriuos gabena kietosios dalelės bei dugno nuosėdos. Tokiu būdu galima įgyti esminį Baltijos jūros ekologinio statuso pokyčių suvokimą.

Pakibusios kietosios dalelės (PKD) yra itin svarbus teršalų keliavimo, sklaidos ir persiskirstymo vandens ekosistemose faktorius. Iš tikrųjų vandens srautai yra susiję su maždaug 90% mikroelementų, kurie aptinkami sąsajos su kietosiomis dalelėmis jūrinėje aplinkoje. Baltijos jūros seklumas prisideda prie bangų sukeltos resuspensijos, dėl kurios teršalai persiskirsto didelėje šios jūros dalyje (Almroth-Rosell et al., 2011).

Pagrindiniai pakibusių nuosėdų šaltiniai pietrytinėje Baltijos jūros dalyje yra Visos ir Nemuno upės, kurių baseino teritoriją sudaro $1,9 \times 10^5$ km² ir $0,98 \times 10^5$ km², atitinkamai. Šioje teritorijoje plutonis, americis ir radiocezijs yra svarbiausi ilgai išsilaikantys radionuklidai, keliantys grėsmę aplinkai. Manoma, kad Baltijos regione tipinė ^{239,240}Pu siekia apie 40–50 Bq/m² (Holm, 1995).

Palyginus su plutoniu, cezijs vandens sistemose yra mobilesnis ir tirpesnis (Michel et al., 2002). Ši savybė leidžia ceziui keliauti didesnius atstumus ir prasiskverbti į gyvuosius organizmus. Monte et al. (2002) atliktas

tyrimas atskleidė, kad ^{137}Cs depozicija Nemuno baseine siekia iki 100 kBq/m^2 . Smith et al. (1987) pateikė vertinimą, kad $^{239,240}\text{Pu}$ ir ^{137}Cs gali išlikti upių baseinuose atitinkamai 3000 ir 1000 metų. Atsižvelgiant šiuos didžiulius radionuklidų išsilaikymo upių baseinuose periodus bei Nemuno baseino užteršimą radioaktyviųjų dulkių radionuklidais, galima nuspėti, kad ši baseino teritorija gali tapti ilgalaikiu radionuklidų šaltiniu Kuršių marioms bei Baltijos jūrai. Panaši situacija susidarė ir gretimame Vyslos baseine. Pasak Skwarzec ir Bojanowski, R. (1992), Vyslos upė per metus atneša vidutiniškai $192\text{ MBq/metai }^{239,240}\text{Pu}$ kietųjų dalelių ($> 0,45$ mikronai) į Gdansko baseiną, kurių vidutinis aktyvumas įtekančiame vandenyje siekia $6,5 \pm 2,8\text{ mBq/m}^3$. Skwarzec et al. (2011) pranešė, kad Vysloje buvo rasta nuo 2 iki 52% plutonio, kuris buvo paskleistas per Černobylio katastrofą, o vidutinė metinė koncentracija siekė apie 3 mBq/m^3 . Skwarzec et al. (2003) vertina, kad 78% $^{239,240}\text{Pu}$ nusėdusio Gdansko baseine kilo iš upių, o dugno nuosėdų suma sudaro $3,8\text{ TBq}$.

Ankstesnieji vertinimai, kokie kiekiai $^{239,240}\text{Pu}$ patenka į Nemuno baseino vandens srautus, regimai buvo kilę iš Vyslos upės tyrimų. Tuo pačiu susidaro įspūdis, kad nebuvo atlikta jokių nuoseklių tyrimų, siekiančių nustatyti, koks realus $^{239,240}\text{Pu}$ kiekis patenka į Nemuno upę. Neatrodo, kad į šiandieninius duomenis patektų išsami informacija apie $^{237,239}\text{Pu}$ bei ^{137}Cs kiekį bei pasitaikymo dažnį Nemuno upės baseine, o duomenys apie Kuršių marias taip pat pateikiami itin nenuosekliai. Publikacijų apie radionuklidų transportaciją su kietosiomis dalelėmis Nemuno upe – tokių kaip Lujanas et al. (2002), Lujanienė et al. (2014) yra itin nedaug. Reikia tolimesnių tyrimų, kuriais būtų galima užpildyti žinių spragas apie konkrečius radionuklidų transportavimo iš Nemuno upės baseino aspektus, radionuklidų aktyvumo lygį bei srautus.

Nemuno upė yra pagrindinis pakibusių nuosėdų šaltinis Kuršių mariose. Hidrologinės marių sąlygos yra paveikiamos daugybės faktorių, tokių kaip vandens gylis, krituliai, upių tekėjimas, garavimas, vėjo sukeltas judėjimas bei vandens apytaka per Klaipėdos sąsiaurį. Sąsiaurio laidumą gali paveikti tokie faktoriai kaip dugno gilinimas ar vandens lygio skirtumai tarp Kuršių marių ir Baltijos jūros (Jakimavičius ir Kovalenkovicienė, 2010).

Dinamiškos Kuršių marių gamtinės sąlygos atsispindi įvairių parametru svyravime – tokių kaip pakibusių nuosėdų koncentracija, druskingumas bei radionuklidų pasiskirstymas. Pavyzdžiui, Lujanienė et al. (2013) nustatė, kad pakibusių dalelių koncentracija Kuršių mariose pasižymi didžiule įvairove nuo 2 iki 304 mg/L , o vidutinės vertės yra tris kartus didesnės nei Baltijos jūros pietrytinės pakrantės regione. Pranešama apie ^{137}Cs aktyvumą

pakibusiose kietosiose medžiagose bei dugno nuosėdose. Šie skaičiai taip pat pasižymi didžiule įvairove, atitinkamai nuo 20 iki 250 Bq/L ir nuo 0,4 iki 208 Bq/kg. Pažymėtina, kad maždaug 62% nuosėdų medžiagų nusėda Kuršių marių teritorijoje (Mėžinė et al. (2019)). Tokiu būdu Kuršių marios tampa nuosėdinių medžiagų ir teršalų tiekėju ir kaupykla-saugykla (Davulienė et al., 2006; Stakenienė et al., 2019; Jokšas et al., 2016; Lujanienė et al., 2014).

Dėl didžiulio Kuršių marių ir Nemuno upės baseinų dydžių skirtumo (daugiau nei 30 kartų), kuomet radionuklidai transportuojami iš jų pradinės vietos į Kuršių marias, jų aktyvumas proporcingai didėja lyginant su atitinkamomis jų pradinėmis buvimo vietomis. Kasmetinis radionuklidų inventoriaus patekimas iš baseino teritorijos į Kuršių marias sukelia radionuklidų inventoriaus 30 kartų padidėjimą Kuršių mariose. Svarbu pažymėti, kad ilgai išliekančių radionuklidų, tokių kaip $^{239,240}\text{Pu}$ ir ^{241}Am kaupimasis tam tikrose marių vietose gali atvesti prie tam tikrų aplinkosaugos grėsmių ateityje. Jei žinosime, koks yra radionuklidų likimas jiems keliaujant per Kuršių marias, tai leis įgyti esminį nuosėdų dinamikos suvokimą bei supratimą, kokį poveikį teršalai turi šiai jautriai ekosistemai.

Atlikta keletas plutonio ir cezio tyrimų Kuršių marių bei pietrytinės Baltijos jūros pakrančių teritorijos vandenyje ir dugno nuosėdose. Buvo tiriamas pakibusių dalelių pernešimas. Kaip nustatė Lujanienė et al. (2004) ir Lujanienė et al. (2010), tyrusi ^{137}Cs elgesį pakibusiose nuosėdose bei dugno nuosėdose (0,2–50 μm), cezio veiklos variacijos yra susijusios su metų laikų įvairovės sukelta pakibusių nuosėdų cheminės sudėties įvairove. Lujanienė et al. (2014) nustatė aiškų gradientą tarp ^{137}Cs aktyvume lyginant Baltijos jūros pakrančių teritorijas bei Kuršių marias, o ^{137}Cs koncentracija dugno nuosėdose buvo panaši abiejuose regionuose. Siekiant nustatyti plutonio kilmę pakibusioje medžiagoje bei dugno nuosėdose, šie autoriai naudojo atominius $^{238}\text{Pu}/^{239,240}\text{Pu}$ ir $^{240}\text{Pu}/^{239}\text{Pu}$ santykius. Jų tyrimas atskleidė, kad didžiausi iš Černobylio katastrofos kylančių 0,2–1 μm diapazono dalelių kiekiai Klaipėdos sąsiauryje buvo pastebėti 2011–2012 metais. Plutonio santykiai taip pat suteikė įrodymų, kad iš Černobylio kilusias radioaktyvias dulkes upė gabena į Kuršių marias po to, kai šios dalelės yra išplaunamos baseino teritorijoje. Lujanienė et al. (2013) nustatė stiprią koreliaciją tarp ^{137}Cs aktyvumo ir masės santykio bei visos organinės anglies (TOC) Baltijos jūroje ($r=0,75$) ir su molio mineralais ($r=0,95$). $^{239,240}\text{Pu}$ aktyvumo ir masės santykis buvo nuo 0,03 iki 7,5 Bq/kg, o didelė koreliacija su VOA buvo aptikta tiek $^{239,240}\text{Pu}$ ($r=0,98$) tiek ir ^{241}Am ($r=0,96$). Lujanienė et al. (2017) nustatė, kad plutonis kilęs iš likusio pasaulio kilmės radioaktyvių dulkių dominuoja

gilesnėse pietrytinės Baltijos jūros vietose, o tokie šaltiniai kaip Černobylio dulkės gali labiau paveikti pakrančių teritorijas.

Aukšti mėginių rinkimo kaštai bei atliekamos americio ir plutonio analizės sudėtingumas labai riboja tyrėjų galimybes pietrytiniame Baltijos jūros regione. Informacija apie jūros dugno topografijos poveikį, vandenyno sroves, sūrumo gradientus, bangų procesus bei kitus faktorius, įtakančius šių radionuklidų elgesį Baltijos jūroje vis dar išlieka nepakankama. Tolimesni tyrimai suteikia galimybę aptikti naujus dėsningumus bei įgyti naujų įžvalgų apie radionuklidų judėjimą ir persiskirstymą ir ištirti galimą jų pritaikymą žyminiams tyrimams.

TYRIMO TIKSLAS IR UŽDAVINIAI

Dalelių reaktyviųjų radionuklidų transportavimo ir pasiskirstymo tyrimas Nemuno upės, Kuršių marių ir Baltijos jūros pakibusiose ir dugno nuosėdose tyrimas siekiant jas pritaikyti kaip aplinkos tyrimo žymenis.

Pagrindiniai tyrimo uždaviniai buvo:

1. Nustatyti radionuklidų pasiskirstymą įvairiuose dalelių dydžių diapazonuose pakibusiose Nemuno upės nuosėdose (intake Neryje) bei Kuršių mariose.

2. Technogeninių radionuklidų (^{137}Cs ir $^{239,240}\text{Pu}$) patekimo per Nemuno upės baseiną į Kuršių marias nustatymas.

3. Erdvinio $^{239,240}\text{Pu}$, ^{241}Am ir ^{137}Cs pasiskirstymo nustatymas Kuršių marių dugno nuosėdose bei pietrytinėje Baltijos jūros pakrantės teritorijoje.

4. $^{239,240}\text{Pu}$ ir ^{241}Am kilmės įvertinimas Kuršių marių dugno nuosėdose bei pietrytinės Baltijos jūros pakrančių teritorijoje.

5. Faktorių tokių kaip grūdelio dydis, mėginio gylis, kitų radionuklidų, tokių kaip ^{210}Pb , ^{214}Pb , ^{40}K , bei artumas prie kranto linijos poveikio įvertinimas $^{239,240}\text{Pu}$, ^{241}Am , ^{137}Cs poveikio pasiskirstymui Baltijos jūros dugno nuosėdose.

TYRIMO NAUJUMAS

Šis tyrimas pristato išsamiausiai ^{241}Am ir Pu izotopų tyrimo pakibusioje medžiagoje ir dugno nuosėdose, atlikto pietrytinėje Baltijos jūros dalyje, rezultatus. Tikėtina, kad ^{241}Pu vertės Kuršių marių bei Baltijos jūros Lietuvos ekonominės zonos teritorijose buvo įvertintos pirmą kartą. Santykis $^{241}\text{Am}/^{239,240}\text{Pu}$ buvo panaudotas, kad įvertinti natūralių ir antropogeninių nuosėdų transportacijos poveikį pakrantės teritorijai, esančiai šalia Kuršių marių. Be to, buvo įvertintas nuosėdų susidarymas pakrantės zonoje, esančioje šalia Kuršių marių. Buvo įvertinta, kad plutonio izotopai Nemuno baseine generuoja 62 MBq/metai vertę, o plutonis, besikaupiantis Kuršių mariose kasmet sudaro 39 MBq/metai vertę.

REZULTATŲ MOKSLINIS IR PRAKTINIS REIKŠMINGUMAS

Šiuo metu dėl klimato kaitos gausėja gamtinių katastrofų ir potvynių bei kyla vandens lygis. Dėl šių priežasčių didėja dirvožemio erozija bei resuspensija, kad, galiausiai, auga ir įvairių teršalų bendrasis kiekis bei persiskirstymas. Šis tyrimas suteiks žinių apie įrankius, kuriais galima įvertinti aplinkos taršą bei poveikį klimato kaitai.

Įgyti duomenys apie ^{137}Cs ir $^{239,240}\text{Pu}$ lygį pakibusioje kietojoje medžiagoje bei dugno nuosėdose praplėtė žinias apie teršalų transportaciją upėje tekančiu vandeniu. Šiuos rezultatus galima įtraukti į modelius, kuriais vertinama teršalų transportacija atskirų vandens telkinių baseinuose.

Be to, duomenys apie $^{239,240}\text{Pu}$ ir ^{241}Am pasiskirstymą bei duomenys apie jų kilmę iš pakrantės zonos gali pasitarnauti tolesniems tyrimams apie upių nuosėdų dispersiją bei teršalus upės nuotėkio teritorijose. Taip pat bus galima kurti prognozių modelius.

Duomenys apie radionuklidų pasiskirstymą įvertinant skirtingų dalelių dydžių grupes gali būti naudingi modeliuojant teršalų transportaciją upių ir jūrinėse sistemose.

Šio tyrimo rezultatus galima pritaikyti ateities pokyčių gamtoje, susijusių su teršalų sklaida ir transportacija, įvertinimui.

AUTORIAUS INDĖLIS

Autoriaus indėlį į šį tyrimą galima apibūdinti šiais teiginiais: Išsamios literatūros apžvalgos tyrimo tema parašymas ir publikacija, mėginių ėmimo Neries upėje ir kuršių mariose suplanavimas ir įgyvendinimas, mėginių parengimas laboratorinei analizei, radiocheminis $^{239,240}\text{Pu}$ ir ^{241}Am atskyrimas laboratorijoje. Radionuklidų aktyvumo verčių nustatymas, duomenų apdorojimas, skaičiavimų atlikimas, žemėlapių parengimas, rezultatų vizualizacija ir interpretavimas. Atlikto tyrimo parengimas publikacijai.

GINAMIEJI TEIGINIAI

1. 25–63 μm pakibusių nuosėdų frakcija yra pagrindinis ^{137}Cs ir natūraliai gamtoje esančių radionuklidų (^7Be , ^{40}K , ^{210}Pb , ^{214}Pb) pernešėjas į Baltijos jūrą Nemuno upe.

2. $^{239,240}\text{Pu}$ ir ^{137}Cs dalelių transportacija iš Nemuno upės baseino į Kuršių marias siekia, atitinkamai, 62 MBq ir 3.6 GBq vertes. Šie radionuklidai kaupiasi tam tikrose teritorijose, ir, laikui bėgant, $^{239,240}\text{Pu}$ kiekis gali pasiekti ekologiškai reikšmingą lygį.

3. Erdvinis radionuklidų ($^{239,240}\text{Pu}$ ir ^{241}Am) pasiskirstymo lygis Baltijos jūros pakrantės teritorijoje bei akumuliacijos zonoje atskleidžia dėsningumą ir tendencijas, leidžiančias šiuos radionuklidus panaudoti kaip gamtinės aplinkos tyrimo žymeklius.

4. 30 μm dydžio dalelės atlieka svarbų vaidmenį transportuojant ^{137}Cs (o taip pat ir ^{40}K , ^{214}Pb), o $< 20 \mu\text{m}$ dydžio dalelės paveikia ^{210}Pb transportavimą Baltijos jūroje.

4.1. MEDŽIAGOS IR METODAI

4.1.1 Tyrimo erdvė

Baltijos jūra yra vidinė jūra Šiaurės Europoje, užimanti maždaug 21 000 km² dydžio teritoriją. Šios jūros paviršiaus plotas siekia maždaug 370 000 km², o jos baseino dydis yra apytiksliai keturis kartus didesnis už pačios jūros plotą. Dėl geografinės padėties šią jūrą galima laikyti didžiule estuarijų sistema, kurioje vidiniai baseinai padalina aprėpti į mažesnes teritorijas. Į Baltijos jūrą įteka daugiau nei 250 upių, ir Nemunas yra viena didžiausių iš jų. Nemunas įteka į pietrytinę jūros dalį. Nemuno upės baseinas yra į Rytus ir Peryčius nuo Kuršių marių. Kuršių marių baseinas sudaro maždaug 105 km² teritoriją (Manton et al., 2021). Kuršių marios yra tarpinis vandens rezervuaras tarp Nemuno upės ir Baltijos jūros. Nemuno upė atneša maždaug 90% vandens, įtekančio į Kuršių marias. Kuršių marių baseino teritorija siekia 100 458 km², iš kurių 98% sudaro Nemuno baseinas. Pagrindiniai radionuklidų, teršiančių Baltijos jūrą ir jos baseino teritoriją, šaltiniai yra viso pasaulio kilmės radioaktyviosios dulkės, patekusios iš atominio ginklo bandymų atmosferoje bei Černobylio katastrofos radioaktyviosios dulkės. ¹³⁷Cs Baltijos jūros vandens užteršimas vertinamas 5,7 PBq, o šio dydžio struktūra atsižvelgiant į konkrečius šaltinius yra: Černobylio katastrofa – 82% (4700 TBq), pasaulinės branduolinių testų dulkės – 14% (800 TBq), emisijos iš branduolines atlieka apdorojančių gamyklų – 4% (230 TBq) bei emisijos iš branduolinių įrengimų, esančių Baltijos jūroje – 0,1% (6 TBq). Pasak Holm, (1995), radioaktyvių ^{239,240}Pu dulkių iš visame pasaulyje vykdomų branduolinių testų kiekis, patekęs į Baltijos jūrą, sudaro 40–50 Bq/m² (16–18 TBq).

4.1.2 Mėginių ėmimas bei tyrimas

Siekiant ištirti ¹³⁷Cs ir ^{239,240}Pu aktyvumą, pakibusių dalelių mėginių surinkimui buvo pasirinktos 4 stotys Kuršių mariose ir 3 stotys Neris upėje. 2020 metų vasarą buvo surinkti trys pakibusių dalelių mėginiai stotyse N1, N2 ir N3. 2021 metų vasarą pakibusios medžiagos mėginiai buvo surinkti stotyse N1, N2, N3, CL1, CL2, CL3 ir CL4.

Siekiant įvertinti įvairių faktorių poveikį (nuosėdų dydis, vieta, gylis bei kitų radionuklidų ²¹⁰Pb, ²¹⁴Pb, ⁴⁰K kiekis) ^{239,240}Pu, ¹³⁷Cs ir ²⁴¹Am pasiskirstymui dugno nuosėdose, buvo surinkti mėginiai Kuršių mariose, pietrytinės Baltijos jūros pakrantės zonoje, pietinėje Baltijos jūros dalyje bei Skagerako įlankoje.

Pakibusių kietųjų dalelių mėginių ėmimas. Vandens filtravimui buvo naudojamas trijų nuoseklaus tyrimo filtrų kasečių rinkinys (US Filter Plymouth Products) su 0.2 μm , 1 μm ir 25 μm porų dydžiu. $\sim 1 \text{ m}^3$ vandens tūris buvo pumpuojamas per sistemą, o vandens tūris buvo matuojamas naudojant standartines vandens tūrio matavimo priemones.

Dugno nuosėdų mėginių ėmimas. Dugno nuosėdų paviršaus lygis (0–5 cm) Nemuno ir Neries upėse buvo matuojamas 5 vietose. Mėginiai buvo imami iš vandens 1 m nuo kranto. Baltijos jūroje dugno mėginiai buvo surinkti Van Veen griebtuvų mėginių ėmikliu. Seklesnėse Kuršių mariose dugno nuosėdos buvo surinktos su Ekman-Birge mėginių ėmikliu. Mėginių ėmimo gylis Kuršių mariose ir Baltijos jūroje svyravo nuo 4 iki 220 m.

Gama spektrometrija. Gama spindulius skleidžiantys radionuklidai buvo analizuojami pasitelkiant ORTEC gama spindulių spektrometrą su HPGe GWL-120-15- LB-AWT detektoriumi. Detektoriaus raiška buvo 2,25 keV esant 1,33 MeV. Ba-137m (661,66 keV) gama linija buvo panaudota siekiant įvertinti jo šaltinio Cs-137 aktyvumą. K-40 aktyvumas buvo matuojamas su 1462 keV gama energija. Matavimų trukmė svyravo tarp 80 000 ir 450 000 s. Santykinis gama spektroskopijos matavimų neapibrėžtumas neviršijo 10%.

Alfa spektrometrija. Alfa spektrometrijos matavimai buvo atliekami su pasyvintais implantuoto silicio detektoriais (PIPS), pagamintais AMETEK (Oak Ridge miestas, Tenesio valstija, JAV). Naudojami PIPS detektoriai turėjo 450 mm^2 aktyvųjį plotą. $^{239,240}\text{Pu}$ ir ^{241}Am matavimų santykinės paklaidos buvo ne didesnės nei 5% ir 7%. ^{241}Pu buvo nustatytas pagal ^{241}Am viršūnės išaugimą (5,49 MeV) mėginių spektruose po 10 metų saugojimo (Lujanienė et al., 2022).

Plutonio atominės masės spektrometrija. Mėginiuose, parengtuose akceleruotos masės spektroskopijos (AMS) tyrimams, buvo išgauta $\sim 95\%$ plutonio. Atominis $^{240}\text{Pu}/^{239}\text{Pu}$ santykis buvo ištirtas su 1.0MV HVE Tandetron AMS prietaisu.

Grūdelių dydžio pasiskirstymas. Dugno nuosėdų mėginių, surinktų pietinėje Baltijos jūroje, pasiskirstymas buvo matuojamas lazeriniu dalelių analizės prietaisu (ANALYSETTE 22 MicroTec-plus).

Analysette 22 Microtec Plus lazerinis dalelių dydžio nustatymo prietaisas, pagamintas Fritsch GmbH, buvo naudojamas matuoti suspensijoms, emulsijoms bei kietiesiems kūnams, remiantis lazerine difrakcija. Matavimai buvo atlikti naudojant optiškai permatomą matavimo erdvę su ultragarsine vandens vonėle naudojant dispersijos skystį. Buvo matuojamas dalelių dydis nuo 0,08 iki 2000 mikrometrų (Analysette 22 manual naudojimo instrukcija).

4.2. REZULTATAI IR APTARIMAS

4.2.1 Radionuklidų patekimo iš Nemuno upės į Kuršių marias tyrimas

4.2.1.1. Aktyvumo lygis

Pasak surinktųjų duomenų, vidutinis pakibusios medžiagos kiekis Neris upės bei Kuršių marių vandenyje atitinkamai buvo $0,008$ ir $0,04 \text{ kg/m}^3$. ^{137}Cs aktyvumo lygis pakibusioje Neris upės medžiagoje svyravo nuo $4,2 \pm 1,3 \text{ Bq/kg}$ iki $49 \pm 15 \text{ Bq/kg}$ (Lentelė 8), o vidutinė vertė buvo lygi $20,3 \text{ Bq/kg}$ ($0,17 \text{ Bq/m}^3$, $N=6$).

Cezis-137. ^{137}Cs aktyvumo vertės Kuršių marių pakibusiose dalelėse buvo žemesnės nei upėje. Jos svyravo nuo $3,4 \pm 1,1 \text{ Bq/kg}$ iki $17,0 \pm 2,2 \text{ Bq/kg}$, o vidutinė vertė siekė $9,3 \text{ Bq/kg}$ ($0,37 \text{ Bq/m}^3$, $N=4$). Rytinėje mėginių ėmimo vietoje (Neris upė) aktyvumas buvo lygus $5,4 \text{ Bq/kg}$ ir $7,4 \text{ Bq/kg}$, o centrinėje vietoje, jau iitekėjus intakams, išmatuotas aktyvumas buvo lygus $5,3 \text{ Bq/kg}$.

Lentelė 8. Radionuklidų aktyvumo lygis dugno nuosėdose bei pakibusiose dalelėse

Vieta	^{137}Cs , Bq/kg		$^{239,240}\text{Pu}$, mBq/kg	
	Dugno nuosėdos	SPM	Dugno nuosėdos	SPM
Neris	$6,4 \pm 0,5$	$4,2(\pm 1,3) - 49(\pm 15)$	90 ± 5	130 ± 7
Nemunas	$7,3 \pm 0,6$	-	80 ± 4	-
Kuršių marios	-	$9,3 \pm 0,7$	$10,0 (\pm 0,5) - 20 (\pm 1)$ $*(1350 (\pm 68))$	30 ± 2

Apibendrinus, nustatytojo aktyvumo įvairovė buvo nedidelė. Ji svyravo nuo $5,3$ iki $8,8 \text{ Bq/kg}$. Šią įvairovę sudarantys rezultatai buvo truputėli žemesni nei išmatuotasis aktyvumas pakibusiose dalelėse, tačiau nustatytojo aktyvumo ribos buvo santykinai artimos.

Plutonis-239,240. $^{239,240}\text{Pu}$ aktyvumo vertės pakibusioje Neris upės medžiagoje, nustatytos alfa spektroskopija, svyravo nuo $0,06$ iki $0,19 \text{ Bq/kg}$ ($0,5$ ir $1,6 \text{ mBq/m}^3$), o vidutinė vertė buvo $0,13 \text{ Bq/kg}$ sausojo svorio (s.s.). Kuršių mariose šios vertės buvo dar žemesnės, ir, įvertinus 4 mėginius, vidutinis kiekis pakibusioje medžiagoje buvo lygus $0,03 \text{ Bq/kg}$ ($1,2 \text{ mBq/m}^3$).

Vidutinis $^{239,240}\text{Pu}$ aktyvumas $< 63 \mu\text{m}$ dugno nuosėdų frakcijoje Nemuno ir Neris upėse buvo $0,08 \text{ Bq/kg}$ ($N=6$), o maksimali vertė siekė $0,15 \text{ Bq/kg}$ stotyje CE. Minimumas buvo užfiksuotas stotyje C, esančioje žemiau Nemuno ir Neris upių santakos. $^{239,240}\text{Pu}$ turinys Kuršių marių dugno

nuosėdose svyravo nuo 10 iki 20 mBq/kg (Lentelė 8). Anomali vertė 1350 mBq/kg buvo nustatyta pietrytinėje šio tyrimo erdvėje priešais Nemuno intaką. Išaugusios aktyvumo vertės CL10 vietoje gali būti priskirtos „karštųjų“ dalelių buvimui arba vietinei radionuklidų kaupimosi zonai.

Dalelių frakcijos. Trijų pakibusių dalelių frakcijų tyrimas (0,2–1 μm, 1–25 μm, > 25 μm) atskleidė, kad tiriamųjų radionuklidų bendrojo aktyvumo didžiausioji dalis buvo nustatyta stambiausioje (C) frakcijoje (> 25 μm). Vidutinės išmatuoto aktyvumo vertės atitinkamai sudarė 65% ir 55% Kuršių marių ir Neries upės verčių. Cezio aktyvumas dominavo stambiausioje frakcijoje (Lentelė 9). Cezio aktyvumo pasiskirstymas (0,26 Bq/m³ ir 0,37 Bq/m³) lyginant vidutinį (M, 1–25 μm) ir stambiausiąją frakciją Neries upėje ir Kuršių mariose atitinkamai buvo 20% ir 80% bei 40% ir 60%. Stambiausioje frakcijoje (> 25 μm) nustatytos radionuklidų vertės buvo apytiksliai tokios pačios, o vidutiniojoje frakcijoje jos daugumoje atvejų skyrėsi dvigubai.

4.2.1.2. Radionuklidų srautas

Remiantis literatūros duomenimis bei matavimų vertėmis, buvo įvertintas metinis cezio ir plutonio pernešimas iš Nemuno upės baseino.

Cezis. Remiantis trejų metų trukmės matavimu, kurį atliko Lujanas et al. (2002), ¹³⁷Cs aktyvumo lygis pakibusioje Neries upės medžiagoje yra panašus į Nemuno upės, į kurią Neris įteka, vertes (68 Bq/kg ir 60 Bq/kg trejų metų vidurkis). Jakimavicius (2012) nustatė, kad, surinkęs iš savo baseino, Nemunas per metus vidutiniškai perneša 21,8 km³ vandens. Darant prielaidą, kad vidutinis ¹³⁷Cs aktyvumas pakibusiose dalelėse lygus 0,17 Bq/m³, vertinama, kad metinis šių dalelių pernešimas į Kuršių marias sudaro 3,6 GBq. Darant prielaidą, kad apie 80% cezio Nemune yra ištirpusio pavidalo (Monte et al., 2002), tuomet galima daryti prielaidą, kad metinis pernešimas lygus 18,2 GBq/metai. Ši vertė artima ankstesniam vertinimui (Lujanas et al., 2002), nustačiusiam vertę 41±34 GBq/metai (irimas koreguotas 2021 metams). Cezio šaltiniai gali būti tiek Černobylio katastrofa, tiek ir pasaulinės kilmės radioaktyviosios dulkės. Taip atsitinka todėl, kad Černobylio dulkės pakibusiose dalelėse pasitaiko įvairiais kiekiais dėl skirtingo jų pasiskirstymo bei depozicijos skirtingose vandenskyros erdvėse. Pietinė Nemuno teritorija turi didesnę dalį iš Černobylio kilusio cezio nei vakarinė teritorija, kurioje šis santykis yra 2–4 kartus žemesnis. Tačiau vidutiniškai 47% viso upės cezio aktyvumo kyla iš Černobylio radioaktyviųjų dulkių (Marčiulionienė et al., 2017). Tad tikėtinas šių šaltinių indėlis į cezio patekimą į Kuršių marias yra maždaug vienodas.

Vandens tekėjimu paremtas požiūris. Metinį plutonio patekimą su pakibusiomis dalelėmis galima vertinti panašiai kaip cezio duomenis. Vidutinis plutonio aktyvumas pakibusioje kietojoje medžiagoje yra $1,0 \pm 0,5$ mBq/m³, taigi, visa plutonio patekimo į Kuršių marias per metus vertė tikėtinai siekia 23 ± 12 MBq/metai.

Nuosėdomis paremtas požiūris. Dar vienas metodas įvertinti plutonio patekimą yra įvertinti plutonio aktyvumą pakibusioje medžiagoje (0,13 Bq/kg) bei įvertinti, koks yra bendras nuosėdų kiekis Kuršių mariose. Mežine et al. (2019) įvertino, kad per metus į Kuršių marias iš Nemuno patenkančių nuosėdų kiekis yra lygus $4,844 \times 10^8 \pm 3,790 \times 10^8$ kg/metai. Remiantis šiais duomenimis, galima vertinti, kad per metus čia patenkančio ^{239,240}Pu kiekis yra 62 ± 49 MBq/metai.

Baseino nuotėkiu paremtas modelis. Kuršių marios gauna pakibusias daleles iš Nemuno upės baseino teritorijos, kuri sudaro 10⁵ km². Norint įvertinti, kiek ^{239,240}Pu susirenka baseino teritorijoje, buvo panaudoti duomenys apie plutonio depoziciją šioje teritorijoje (I), vidutinį plutonio egzistavimo laiką šioje teritorijoje (t) ir plutonio buvimo vietą (S). Šie duomenys buvo panaudoti, siekiant įvertinti plutonio patekimą remiantis Lygtimi 9. Literatūros duomenys teigia, kad ^{239,240}Pu sankaupos baseine sudaro tarp 16 ir 60 Bq/m². Plutonio, išplauto iš dirvožemio baseino teritorijoje kiekis priklauso nuo plutonio išlikimo laiko ($\ln(2)/[\text{išplauta dalis}]$). Remiantis publikuotais duomenimis, 3000 metų egzistavimo laikotarpis turėtų tiksliau atitikti 10⁵ km² baseino teritoriją. Naudojant Lygtį 16, galima numanyti, kad visas su vandeniu patenkančio ^{239,240}Pu kiekis yra 882 ± 510 MBq per metus. Buvo panaudoti įvairūs skaičiavimo metodai, kurie pateikė įvairius rezultatus: 23 ± 11 MBq/metai, 62 ± 49 MBq/metai bei 882 ± 510 MBq. Du pirmieji metodai yra paremti išmatuotojo aktyvumo rezultatais, ir jų patikimumo intervalai persidengia. Gautieji rezultatai artimi Vyslos duomenims 89 MBq/metai (Skwarzec et al., 2011). Kadangi baseinu paremtas požiūris yra plačiai taikomas, jį galima laikyti konservatyviu scenarijumi.

Plutonis Kuršių mariose. Nuosėdų sankaupų rezultatus Mežine et al. (2019) panaudojo, kad nustatytų, jog maždaug 62% nuosėdų, patenkančių į Kuršių marias ir užstringa bei išlieka Kuršių marių teritorijoje. Remiantis kiekiu plutonio, nusėdančio Kuršių mariose, sankaupos sudaro maždaug 39 MBq per metus, o likusieji 24 MBq per metus patenka į Baltijos jūrą. Kitaip tariant, iš upių per metus čia patenka 25 mBq/m². Numanoma, kad toks atitekėjimas tęsis daugiau nei 40 metų, ir taip susikaups 1 Bq/m². Perskaičiuojant vidutinį ^{239,240}Pu aktyvumą dugno plotui, Kuršių marių dugno nuosėdoms gaunama 2,6 Bq/m² vertė (Lujanienė et al., 2022), o toks

vertinimas yra artimesnis realybei. Galima vertinti, kad visa Kuršių marių dugno nuosėdų sankaupa prilygsta 1,56 GBq.

4.2.2. Faktorių, paveikiančių radionuklidų pasiskirstymą Baltijos jūroje, tyrimas

4.2.2.1. Pietrytinės Baltijos jūros dalies pakrančių regionas

4.2.2.1.1. $^{239,240}\text{Pu}$, ^{137}Cs ir ^{241}Am aktyvumo lygis

Kuršių marių stotyje CL10 buvo nustatytos anomalios $^{239,240}\text{Pu}$ ir ^{241}Am aktyvumo vertės, kurios atitinkamai sudarė 15 ir 13,3 Bq/m², 31% iš kurių kilmė buvo Černobylio katastrofos radioaktyvios dulkės. Šis tyrimas neatskleidė akivaizdaus ryšio tarp erdvinio dumblo nuosėdų pasiskirstymo ir ^{137}Cs , $^{239,240}\text{Pu}$ bei ^{241}Am aktyvumo Kuršių marių dugno nuosėdose. Didelis aktyvumas Kuršių marių teritorijoje gali būti kilęs iš „karštųjų“ dalelių bei iš susikaupusių radionuklidų – čia reikalingi tolimesni tyrimai.

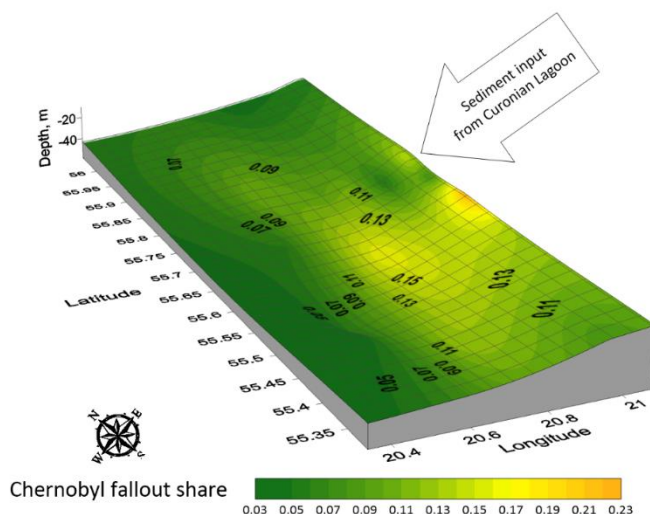
Šio tyrimo kontekste matavimai buvo atlikti 8 stotyse, ir $^{239,240}\text{Pu}$ aktyvumas siekė nuo 0,42 iki 8,94 Bq/m², ^{137}Cs aktyvumas nustatytas nuo 546 iki 2188 Bq/m², o ^{241}Am aktyvumas įvertintas nuo 0,19 iki 3,36 Bq/m². Buvo nustatyta, kad $^{239,240}\text{Pu}$ ir ^{241}Am aktyvumas šio profilio dugno nuosėdose auga sulig mėginio ėmimo gyliu bei mėginio ėmimo stoties nutolimu nuo kranto. $^{239,240}\text{Pu}$ ir ^{241}Am pasiskirstymas dugno nuosėdose palyginus su tyrimo profilio mėginių ėmimo gyliu atskleidžia aktyvumo didėjimo tendenciją dugno nuosėdose, kuomet tolstama į Vakarus nuo Klaipėdos sąsiaurio. Vertinama, kad koreliacija siekia 0,82 $^{239,240}\text{Pu}$ ir 0,64 ^{241}Am . Abiem radionuklidams pastebima ryški linijinė regresija ($R^2 \sim 0,8$) su atstumu nuo kranto. Buvo nustatyta, kad aktyvumas sulig kiekvienu kilometru didėja 0,07 Bq/m² $^{239,240}\text{Pu}$ ir 0,025 Bq/m² ^{241}Am . Šis aktyvumo augimas gali būti kildinamas iš smulkiųjų dalelių poveikio, augančio didėjant gyliui. Šios dalelės yra pagrindinės radionuklidų pernešėjos. Šis reiškinys taip pat yra žinomas kaip „nuosėdų fokusavimo“ efektas.

4.2.2.1.2. Černobylio kilmės radionuklidų dalies nustatymas

Erdvinis $^{239,240}\text{Pu}$ ir ^{241}Am aktyvumo pasiskirstymas ištakų iš Kuršių marių pakrančių teritorijoje (45×82 km) apibūdinamas dviem didelės veiklos teritorijomis, o viršūnė nustatyta stotyje 64B ir N-6. Kuršių mariose užfiksuotas vidutinis $^{239,240}\text{Pu}$ ir ^{241}Am aktyvumas (1,8 Bq/m² ir 0,9 Bq/m², atitinkamai) yra artimas gretimai pakrančių teritorijai (1,6 Bq/m² ir 0,8 Bq/m², atitinkamai). Tai gali būti pasekmė tiek natūralių, tiek ir antropogeninių

faktorių (Klaipėdos sąsiaurio gilinimas), kurie veda prie Kuršių marių nuosėdų pergabenimo į pakrantės teritorijas.

Radionuklidų kilmės tyrimas atskleidžia, kad dominuojanti tarša su $^{239,240}\text{Pu}$ ir ^{241}Am dugno nuosėdose (0–5 cm) pietrytinėje Baltijos jūros dalyje yra susijusi su branduolinėmis dulkėmis, čia patekusiomis iš viso pasaulio. Teritorinis kontūras su išaugusiomis Černobylio branduolinių dulkių žymėmis (nuo 10% iki 20%, Paveikslas 37) buvo interpretuojamas kaip nuosėdų, patenkančių iš Nemuno upės baseino efektas, paveikiantis Kuršių marias ir pasireiškiantis per natūralią ir antropogeninę veiklą (gilinimas). Kuršių marių teritorijoje Černobylio radioaktyviųjų dulkių dalis sudarė nuo 0,3% iki 31%, o vidutinė erdvė siekė 9%, iš ko atsiskleidžia reikšmingas erdvinis $^{239,240}\text{Pu}$ ir ^{241}Am sklaidos nevienodumas.



Paveikslas 37. Erdvinis pasiskirstymas (Kringingo interpoliacijos modelis).

Černobylio radioaktyviųjų dulkių apraiškos pietrytinės Baltijos jūros pakrančių regione (ilguma ir platumą nurodomos laipsniais, o z ašis (gylis, m) yra padidinta ~1000 kartų vardan reprezentatyvumo)

Vertikalaus ^{241}Pu , $^{239,240}\text{Pu}$ ir ^{241}Am pasiskirstymas nuosėdose Baltijos jūros pietrytinėje dalyje atskleidžia, kad iš Černobylio radioaktyviųjų dulkių kilusio plutonio aktyvumas viršutiniam nuosėdų sluoksniui (0–2 cm) sudaro maždaug 20%. Gilesniuose nuosėdų šerdies sluoksniuose aptinkamas plutonis priskirtinas pasaulinės kilmės atmosferos dulkėms, čia patekusiomis dėl atmosferoje vykdomų branduolinių testų. Panaudojant ^{241}Pu - ^{241}Am datavimo modelį, buvo nustatyta, kad šis plutonis yra kilęs iš 1965 metų. Viršutinio nuosėdų šerdies sluoksniu sedimentacijos lygis anot vertinimų sudaro 1,33 mm/metai.

4.2.2.2. Pietinė Baltijos jūros teritorija ir Skagerako įlankos teritorija

4.2.2.2.1. Grūdelių dydžio pasiskirstymas

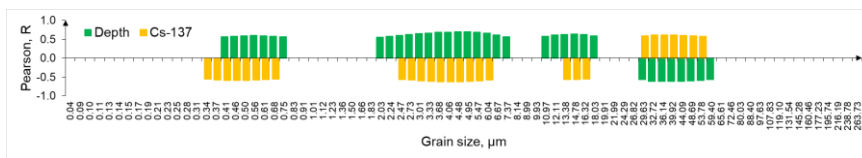
Vidutinis grūdelių dydis atspindi bimodalinį pasiskirstymą, kurio vidutinė vertė siekia 14–45 μm . Pastebima mažėjimo tendencija augant gyliui. Nuosėdos iš Skagerako įlankos yra iš didžiausio mėginių ėmimo gylio (177–220 m) lyginant su kitomis stotimis (43–120 m). Šios nuosėdos yra sudarytos iš didesnės dalies mažesniųjų dalelių ($<6 \mu\text{m}$). Čia aptiktas mažiausias ^{137}Cs aktyvumo lygis (8–11 Bq/kg) bei mažiausias $^{137}\text{Cs}/^{210}\text{Pb}$ santykis (8,6–19). Ši reiškinį galėjo sukelti ribotas poveikis upių, kurių baseino teritorija užteršta ^{137}Cs .

4.2.2.2.2. Radionuklidų aktyvumas

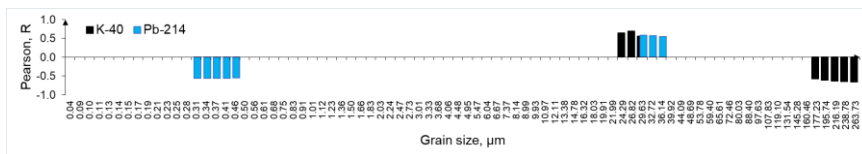
Išmatuota ^{137}Cs aktyvumo įvairovė nuosėdų mėginiuose siekė nuo 8 Bq/kg iki 220 Bq/kg, o vidutinė erdvė buvo lygi 53 Bq/kg. Rytinėje jūros pietinės teritorijos dalyje pastebėtas silpnėsnis ^{214}Pb , ^{40}K ir ^{137}Cs aktyvumas, atitinkamai 49 Bq/kg, 929 Bq/kg ir 116 Bq/kg. Skagerako įlankos kontekste koreliacija tarp ^{210}Pb ir dalelių dydžių nurodo, kad mažesnės nei 20 μm dalelės atlieka reikšmingą vaidmenį ^{210}Pb kaupimosi dugno nuosėdose procese. Tačiau bendrasis duomenų rinkinys (Skagerako įlankos ir pietinės Baltijos jūros dalies stotys) neatskleidė jokios reikšmingesnės koreliacijos tarp ^{210}Pb bei 0–20 μm dydžio dalelių. Tačiau $^{210}\text{Pb}/^{137}\text{Cs}$ santykis atskleidė ryškia tendenciją su 0–20 μm dalelių dydžiu. Iš to taip pat seka, kad $^{210}\text{Pb}/^{137}\text{Cs}$ santykis geriau atskleidžia ^{210}Pb sorbcijos procesą šiomis konkrečiomis jūrinėmis sąlygomis nei kad pradinės ^{210}Pb sorbeto vertės upių aplinkoje.

4.2.2.2.3. Bendrosios tendencijos

Ši analizė atskleidžia, kad radionuklidų sąsajos su įvairaus stambumo grūdeliais yra labai nevienodos (Paveikslas 38). Todėl ^{40}K aktyvumas pozityviai koreliuoja su frakcija nuo 24 iki 30 μm , o ^{214}Pb demonstruoja teigiamą koreliaciją su 30–36 μm frakcija. Vidutinė pozityvi koreliacija taip pat buvo pastebėta tarp ^{137}Cs aktyvumo ir 30–54 μm grūdelio dydžio frakcijos, o tai atitinka cezio pasiskirstymą Neries upės ir Kuršių marių pakibusių dalelių frakcijose. Taigi, susidaro įspūdis, kad 30 μm nuosėdų frakcija yra bendrasis faktorius, paveikiantis šių radionuklidų akumuliaciją Baltijos jūros dugno nuosėdose.



a



b

Paveikslas 38. *Pearsono koreliacijos grūdelių dydžio bei radionuklidų aktyvumo koeficientai ($>0,55$; $\alpha < 0,05$) (^{137}Cs)-a, (^{40}K , ^{214}Pb)-b bei mėginių ėmimo gylis – a*

$^{214}\text{Pb}/^{137}\text{Cs}$ santykis tyrinėtų vietovių dugno nuosėdose (pietinė Baltijos jūra bei Skagerako įlanka) atskleidžia stiprią koreliaciją su 0–20 μm grūdelių dydžiu bei mėginio ėmimo gyliu. Tai buvo priskirta dominuojančiam ^{226}Ra pasišalinimui iš jūros vandens, kuris ypač pasireiškia $<20 \mu\text{m}$ dydžio dalelėms. Pasišalinusio ^{226}Ra kiekis auga su gyliu dėl to, kad dalelės pasiekia didesnę gylį ilgiau prabuvusios vienoje vietoje.

Ryškus ^{214}Pb lygio padidėjimas augant tyrimo gelmei bei ^{40}K aktyvumo išaugimas Skagerako įlankos dugno nuosėdose buvo priskirti faktui, kad dalelės, patekusios į gilius regionus, praleido daugiau laiko jūriniame vandenyje. Ši išaugusi trukmė padidina jų galimybę pašalinti didesnius kiekius ^{226}Ra ir ^{40}K kurie gali būti kilę iš vieno šaltinio. Tikėtina, kad panašus mechanizmas gali paaiškinti ir ^{214}Pb aktyvumo išaugimą dugno nuosėdose didėjant atstumui nuo kranto pietinėje Baltijos jūros dalyje.

Kad suteiktume duomenims dar daugiau konteksto, taip pat įtraukėme ir 2018 metų HELCOM duomenų bazės rezultatus (ICES, 2020), nes tai leidžia padidinti bendrąjį šio tyrimo reprezentatyvumą. Pastebėtoji tendencija ($R=0,83$) skatina manyti, kad cezio šaltinis yra Baltijos jūros teritorijoje, nes aktyvumo lygis mažėja tolstant nuo jūros teritorijos. Šie rezultatai atitinka (Povinec et al., 2004) gautas išvadas.

Cezio transportaciją pakibusioje medžiagoje jūros vandenyje gali paveikti keletas faktorių, tokių kaip fizinės nuosėdų savybės (tokios kaip dydis, tankis ir forma), srovės stiprumas ir kryptis, vandens temperatūra ir druskingumas, dalelių tankis vandens stulpelį ir t.t. (Lujanienė et al., 2014). Nepaisant šių faktorių, tikimybė, kad cezio neturinčios dalelės sumažins cezio tankio lygį bei paskleis cezių iš užterštų dalelių didėja su laiku. Tuo pačiu auga ir atstumas nuo upių arealo. Tai ypač aktualu pačioms smulkiusioms

dalelėms. Bendroji cezio lygio didėjimo tendencija rytine kryptimi (apie 0,27 Bq/km) nuo Skagerako įlankos iki Gotlando baseino gali būti dėl to, kad dalelės mažiau laiko prabuvo upėse. Be to, didėja skaičius upių atneštų dalelių su ceziumi iš jų baseino teritorijų, užterštų po Černobylio katastrofos bei pasaulinės kilmės radioaktyviomis dulkėmis.

4.3 IŠVADOS

Tyrimas pateikia naujus duomenis apie radionuklidų ($^{239,240}\text{Pu}$, ^{241}Pu ir ^{241}Am) transportavimą, pasiskirstymą ir srautus Nemuno vandens, Kuršių marių bei Baltijos jūros vandens aplinkoje Lietuvos ekonominėje zonoje.

Nemuno upės baseinas yra ilgalaikis $^{239,240}\text{Pu}$ šaltinis, kurio vidutinė metinė vertė yra 62 MBq/metai. ^{137}Cs srauto lygis yra vertinamas 3,6 GBq. Ši vertė atitinka ankstesnius duomenis. Didžioji dalis dalelių aktyvumo yra transportuojama į Kuršių marias >1 μm dydžio dalelėmis Nemuno upe.

Pakibusios 25–63 μm dydžio dalelės yra atsakingos už ^{137}Cs bei natūralios kilmės radionuklidų (^7Be , ^{40}K , ^{210}Pb , ^{214}Pb) transportaciją Nemuno upės vandeniui į Kuršių marias. Tačiau ir 30 μm dydžio dalelės atlieka svarbų vaidmenį paskirstant ^{137}Cs , ^{40}K ir ^{214}Pb , o <20 μm pakibusios dalelės paveikia ^{210}Pb transportavimą į Baltijos jūrą.

Gautieji duomenys apie $^{239,240}\text{Pu}$ ir ^{241}Am erdvinį pasiskirstymą Kuršių mariose ir Baltijos jūroje Lietuvos ekonominės zonos teritorijoje atskleidžia dėsningas schemas, kurios, pasiremdamos šių radionuklidų tyrimu, parodo, kaip galima atsekti teršalus ištirtoje teritorijoje.

REFERENCES

- Aarkrog, A., 2003. Input of anthropogenic radionuclides into the World Ocean. *Deep. Res. Part II Top. Stud. Oceanogr.* 50, 2597–2606. [https://doi.org/10.1016/S0967-0645\(03\)00137-1](https://doi.org/10.1016/S0967-0645(03)00137-1).
- Aleksandrov, S., Krek, A., Bubnova, E., Danchenkov, A., 2018. Eutrophication and effects of algal bloom in the south–western part of the Curonian Lagoon alongside the Curonian Spit. *Baltica*. <https://doi.org/10.5200/baltica.2018.31.01>.
- Almroth-Rosell, E., Eilola, K., Hordoir, R., Meier, H.E.M., Hall, P.O.J., 2011. Transport of fresh and resuspended particulate organic material in the Baltic Sea — a model study. *Journal of Marine Systems*. <https://doi.org/10.1016/j.jmarsys.2011.02.005>.
- Andersen, T.J., Rominikan, S., Olsen, I.S., Skinnenbach, K.H., Fruergaard, M., 2021. Flocculation of PVC microplastic and fine-grained cohesive sediment at environmentally realistic concentrations. *Biol. Bull.* 240, 42–51. <https://doi.org/10.1086/712929>.
- Andersson, P.S., Wasserburg, G.J., Chen, J.H., Papanastassiou, D.A., Ingri, J., 1995. ²³⁸U ²³⁴U and ²³²Th ²³⁰Th in the Baltic Sea and in river water. *Earth and Planetary Science Letters*. [https://doi.org/10.1016/0012-821x\(94\)00262-w](https://doi.org/10.1016/0012-821x(94)00262-w).
- Appleby, P.G., Piliposyan, G., Hess, S., 2022. Detection of a hot ¹³⁷Cs particle in marine sediments from Norway: potential implication for ¹³⁷Cs dating. *Geo-Marine Lett.* 42, 2. <https://doi.org/10.1007/s00367-021-00727-2>.
- Asowata, I.T., Akinwumiju, A.S., 2020. Assessment of potentially harmful elements in floodplain soils and stream sediments in Ile-Ife area, South-western Nigeria. *SN Appl. Sci.* 2, 1506. <https://doi.org/10.1007/s42452-020-03286-w>.
- Avşar, U., Hubert-Ferrari, A., De Batist, M., Schmidt, S., Fagel, N., 2015. Sedimentary records of past earthquakes in Boraboy Lake during the last ca 600years (North Anatolian Fault, Turkey). *Palaeogeogr. Palaeoclimatol. Palaeoecol.* 433, 1–9. <https://doi.org/10.1016/j.palaeo.2015.04.031>.
- Bam, W., Maiti, K., 2021. ²¹⁰Po–²¹⁰Pb distribution and carbon export in the northern Gulf of Mexico continental slope. *Deep. Res. Part I Oceanogr. Res. Pap.* 172, 103535. <https://doi.org/10.1016/j.dsr.2021.103535>.
- Baskaran, M., Ravichandran, M., Bianchi, T.S., 1997. Cycling of ⁷Be and ²¹⁰Pb in a high DOC, shallow, turbid estuary of south-east Texas. *Estuar. Coast. Shelf Sci.* 45, 165–176. <https://doi.org/10.1006/ecss.1996.0181>.

Baskaran, M., 2011. Po-210 and Pb-210 as atmospheric tracers and global atmospheric Pb-210 fallout: a Review. *Journal of Environmental Radioactivity*. <https://doi.org/10.1016/j.jenvrad.2010.10.007>.

Baskaran, M., Mudbidre, R., Schweitzer, L., 2020. Quantification of Po-210 and Pb-210 as tracer of sediment resuspension rate in a shallow riverine system: Case study from southeast Michigan, USA. *J. Environ. Radioact.* 222, 106339. <https://doi.org/10.1016/j.jenvrad.2020.106339>.

Baskaran, M., Krupp, K., 2021. Novel Application of ²¹⁰Po-²¹⁰Pb Disequilibria to Date Snow, Melt Pond, Ice Core, and Ice-Rafted Sediments in the Arctic Ocean. *Front. Mar. Sci.* 8. <https://doi.org/10.3389/fmars.2021.692631>.

Beasley, T.M., Carpenter, R., Jennings, C.D., 1982. Plutonium, ²⁴¹Am and ¹³⁷Cs ratios, inventories and vertical profiles in Washington and Oregon continental shelf sediments. *Geochim. Cosmochim. Acta* 46, 1931–1946. [https://doi.org/10.1016/0016-7037\(82\)90131-4](https://doi.org/10.1016/0016-7037(82)90131-4).

Beasley, T.M., Jennings, C. David., 1984. The inventories of plutonium-239, -240, americium-241, cesium-137, and cobalt-60 in Columbia River sediments from Hanford to the Columbia River Estuary. *Environ. Sci. Technol.* <https://doi.org/10.1021/es00121a014>.

Belivermiş, M., Kılıç, Ö., Sezer, N., Sıkdokur, E., Güngör, N.D., Altuğ, G., 2021. Microplastic inventory in sediment profile: A case study of Golden Horn Estuary, Sea of Marmara. *Mar. Pollut. Bull.* 173, 113117. <https://doi.org/10.1016/j.marpolbul.2021.113117>.

Benoit, G., Hirschbeck, M., Bisson, B., 2020. Beryllium-7 Elucidate Sediment Dynamics of the Branford River Estuary, Connecticut, USA. *Estuaries and Coasts* 43, 831–842. <https://doi.org/10.1007/s12237-020-00712-5>.

Black, E.E., Buesseler, K.O., Pike, S.M., Lam, P.J., 2018. ²³⁴Th as a tracer of particulate export and remineralization in the southeastern tropical Pacific. *Mar. Chem.* 201, 35–50. <https://doi.org/10.1016/j.marchem.2017.06.009>.

Boelens, R., Kershaw, P., Angelidis, M., Baker, A., Bakker, D.C., Bowmer, T., Hedgecock, I. and Tyack, P., 2016. Pollution in the open oceans: 2009-2013.

Bollmann, U.E., Simon, M., Vollertsen, J., Bester, K., 2019. Assessment of input of organic micropollutants and microplastics into the Baltic Sea by urban waters. *Marine Pollution Bulletin*. <https://doi.org/10.1016/j.marpolbul.2019.07.014>.

Bolstad, W.M., Curran, J.M., 2016. Introduction to Bayesian Statistics, Third Edition. Introd. to Bayesian Stat. Third Ed. <https://doi.org/10.1002/9781118593165>.

Bonniwell, E.C., Matisoff, G., Whiting, P.J., 1999. Determining the times and distances of particle transit in a mountain stream using fallout radionuclides. *Geomorphology* 27, 75–92. [https://doi.org/10.1016/S0169-555X\(98\)00091-9](https://doi.org/10.1016/S0169-555X(98)00091-9).

Boudreault, M., Koiter, A.J., Lobb, D.A., Liu, K., Benoy, G., Owens, P.N., Danielescu, S., Li, S., 2018. Using colour, shape and radionuclide fingerprints to identify sources of sediment in an agricultural watershed in Atlantic Canada. *Can. Water Resour. J. / Rev. Can. des ressources hydriques* 43, 347–365. <https://doi.org/10.1080/07011784.2018.1451781>.

Brewer, P.G., Spencer, D.W., Robertson, D.E., 1972. Trace element profiles from the Geosecs-II test station in the Sargasso Sea. *Earth and Planetary Science Letters*. [https://doi.org/10.1016/0012-821x\(72\)90243-9](https://doi.org/10.1016/0012-821x(72)90243-9).

Buesseler, K.O., Benitez-Nelson, C.R., Moran, S.B., Burd, A., Charette, M., Cochran, J.K., Coppola, L., Fisher, N.S., Fowler, S.W., Gardner, W.D., Guo, L.D., Gustafsson, Ö., Lamborg, C., Masque, P., Miquel, J.C., Passow, U., Santschi, P.H., Savoye, N., Stewart, G., Trull, T., 2006. An assessment of particulate organic carbon to thorium-234 ratios in the ocean and their impact on the application of ^{234}Th as a POC flux proxy. *Mar. Chem.* 100, 213–233. <https://doi.org/10.1016/j.marchem.2005.10.013>.

Cao, Z., Wang, D., Zhang, Z., Zhou, K., Liu, X., Wang, L., Huang, B., Cai, P., Dai, M., 2020. Seasonal dynamics and export of biogenic silica in the upper water column of a large marginal sea, the northern South China Sea. *Prog. Oceanogr.* 188, 102421. <https://doi.org/10.1016/j.pocean.2020.102421>.

Charlesworth, M.E., Service, M., Gibson, C.E., 2006. The distribution and transport of Sellafield derived ^{137}Cs and ^{241}Am to western Irish Sea sediments. *Science of The Total Environment*. <https://doi.org/10.1016/j.scitotenv.2004.12.062>.

Chen, H., Liu, G., Zhang, X., Shi, H., Li, H., 2021. Quantifying sediment source contributions in an agricultural catchment with ephemeral and classic gullies using ^{137}Cs technique. *Geoderma* 398, 115112. <https://doi.org/10.1016/j.geoderma.2021.115112>.

Choppin, G.R., Morgenstern, A., 2001. Distribution and movement of environmental plutonium. *Radioactivity in the Environment*. [https://doi.org/10.1016/s1569-4867u0\(01\)80009-7](https://doi.org/10.1016/s1569-4867u0(01)80009-7).

Ciszewski, D., Łokas, E., 2019. Application of $^{239,240}\text{Pu}$, ^{137}Cs and heavy metals for dating of river sediments. *Geochronometria* 46, 138–147. <https://doi.org/10.1515/geochr-2015-0111>

Cochran, J.K., Masqué, P., 2003. Short-lived U/Th series radionuclides in the ocean: Tracers for scavenging rates, export fluxes and particle dynamics. *Rev. Mineral. Geochemistry* 52, 461–492. <https://doi.org/10.2113/0520461>.

Collins, A.L., Walling, D.E., Webb, L., King, P., 2010. Apportioning catchment scale sediment sources using a modified composite fingerprinting technique incorporating property weightings and prior information. *Geoderma*. <https://doi.org/10.1016/j.geoderma.2009.12.008>.

Collins, A.L., Pulley, S., Foster, I.D.L., Gellis, A., Porto, P., Horowitz, A.J., 2017. Sediment source fingerprinting as an aid to catchment management: A review of the current state of knowledge and a methodological decision-tree for end-users. *Journal of Environmental Management*. <https://doi.org/10.1016/j.jenvman.2016.09.075>.

Cook, G.T., MacKenzie, A.B., McDonald, P., Jones, S.R., 1997. Remobilization of Sellafield-derived radionuclides and transport from the north-east Irish Sea. *Journal of Environmental Radioactivity*. [https://doi.org/10.1016/s0265-931x\(96\)00070-7](https://doi.org/10.1016/s0265-931x(96)00070-7).

Corcho-Alvarado, J.A., Díaz-Asencio, M., Röllin, S., Herguera, J.C., 2022. Distribution and source of plutonium in sediments from the southern Gulf of Mexico. *Environ. Sci. Pollut. Res.* <https://doi.org/10.1007/s11356-022-18770-6>.

Cressie, N., 2015. *Statistics for spatial data*. John Wiley & Sons.

Davis, C.M., Fox, J.F., 2009. Sediment Fingerprinting: Review of the Method and Future Improvements for Allocating Nonpoint Source Pollution. *J. Environ. Eng.* 135, 490–504. [https://doi.org/10.1061/\(asce\)0733-9372\(2009\)135:7\(490\)](https://doi.org/10.1061/(asce)0733-9372(2009)135:7(490)).

Davulienė, L., Tarasiuk, N., Spirkauskaitė, N., Trinkunas, G., Valkunas, L., 2006. Assessment of ¹³⁷Cs outspread in the Lithuanian part of the Baltic Sea. *Radionuclides in the Environment - Int. Conf. On Isotopes in Env. Studies*. [https://doi.org/10.1016/s1569-4860\(05\)08038-1](https://doi.org/10.1016/s1569-4860(05)08038-1).

De La Rocha, C.L., Passow, U., 2007. Factors influencing the sinking of POC and the efficiency of the biological carbon pump. *Deep. Res. Part II Top. Stud. Oceanogr.* 54, 639–658. <https://doi.org/10.1016/j.dsr2.2007.01.004>.

Díaz-Asencio, M., Alonso-Hernández, C.M., Bolanos-Álvarez, Y., Gómez-Batista, M., Pinto, V., Morabito, R., Hernández-Albernas, J.I., Eriksson, M., Sanchez-Cabeza, J.A., 2009. One century sedimentary record of Hg and Pb pollution in the Sagua estuary (Cuba) derived from ²¹⁰Pb and ¹³⁷Cs chronology. *Mar. Pollut. Bull.* 59, 108–115. <https://doi.org/10.1016/j.marpolbul.2009.02.010>.

Du, J., Wu, Y., Huang, D., Zhang, J., 2010. Use of ⁷Be, ²¹⁰Pb and ¹³⁷Cs tracers to the transport of surface sediments of the Changjiang Estuary, China. *J. Mar. Syst.* 82, 286–294. <https://doi.org/10.1016/j.jmarsys.2010.06.003>.

Du, P., Huang, D., Ning, D., Chen, Y., Liu, B., Wang, J., Xu, J., 2019. Application of Bayesian model and discriminant function analysis to the estimation of sediment source contributions. *Int. J. Sediment Res.* 34, 577–590. <https://doi.org/10.1016/j.ijsrc.2019.05.005>.

Du, Jinqiu, Wang, Z., Du, Jinzhou, Lin, W., Lu, B., Qi, Y., Gao, H., Wang, Y., Yao, Z., 2021. Radionuclides in sediment as tracers for evolution of modern sedimentary processes in the Bohai Sea. *Reg. Stud. Mar. Sci.* 48, 102061. <https://doi.org/10.1016/j.rsma.2021.102061>.

European Environment Agency. Baltic Sea Physiography Map. 12 November 2009. <http://www.eea.europa.eu/data-and-maps/figures/baltic-sea-physiography-depth-distribution-and-main-currents>.

Evrard, O., Chaboche, P.-A., Ramon, R., Foucher, A., Lacey, J.P., 2020. A global review of sediment source fingerprinting research incorporating fallout radiocesium (¹³⁷Cs). *Geomorphology*. <https://doi.org/10.1016/j.geomorph.2020.107103>.

Feng, H., Cochran, J.K., Hirschberg, D.J., 1999. ²³⁴Th and ⁷Be as tracers for the transport and dynamics of suspended particles in a partially mixed estuary. *Geochimica et Cosmochimica Acta*. [https://doi.org/10.1016/s0016-7037\(99\)00060-5](https://doi.org/10.1016/s0016-7037(99)00060-5).

Feng, N., Yang, W., Zhao, X., Chen, M., Qiu, Y., Zheng, M., 2021. Seasonal export of ²³⁴Th and POC in Daya Bay, northern South China Sea. *Cont. Shelf Res.* 216, 104359. <https://doi.org/10.1016/j.csr.2021.104359>.

Feng, N., Yang, W., Zhao, X., Chen, M., Qiu, Y., Zheng, M., 2021. Semi-enclosed bays serve as hotspots for black carbon burial: A case study in Jiaozhou Bay, western Yellow Sea. *Sci. Total Environ.* 797, 149100. <https://doi.org/10.1016/j.scitotenv.2021.149100>.

Foster, G.R., Hakonson, T.E., 1984. Predicted Erosion and Sediment Delivery of Fallout Plutonium. *J. environ. qual.* <https://doi.org/10.2134/jeq1984.00472425001300040017x>.

Foucher, A., Chaboche, P.A., Sabatier, P., Evrard, O., 2021. A worldwide meta-analysis (1977-2020) of sediment core dating using fallout radionuclides including ¹³⁷Cs and ²¹⁰Pbxs. *Earth Syst. Sci. Data* 13, 4951–4966. <https://doi.org/10.5194/essd-13-4951-2021>.

Fritsch company manual for the ANALYSETTE 22MicroTec plus device.

Fukai, R., Yokoyama, Y., 1982. Natural Radionuclides in the Environment. The Natural Environment and the Biogeochemical Cycles. https://doi.org/10.1007/978-3-540-38597-4_2

García-Comendador, J., Martínez-Carreras, N., Fortesa, J., Borràs, A., Calsamiglia, A., Estrany, J., 2020. Analysis of post-fire suspended sediment sources by using colour parameters. *Geoderma* 379, 114638. <https://doi.org/10.1016/j.geoderma.2020.114638>.

García-Comendador, J., Martínez-Carreras, N., Fortesa, J., Company, J., Borràs, A., Estrany, J., 2021. Combining sediment fingerprinting and hydro-sedimentary monitoring to assess suspended sediment provenance in a mid-mountainous Mediterranean catchment. *J. Environ. Manage.* 299, 113593. <https://doi.org/10.1016/j.jenvman.2021.113593>.

Gardes, T., Portet-Kotalo, F., Debret, M., Copard, Y., 2021. Historical and post-ban releases of organochlorine pesticides recorded in sediment deposits in an agricultural watershed, France. *Environ. Pollut.* 288. <https://doi.org/10.1016/j.envpol.2021.117769>.

Geckeis, H., Zavarin, M., Salbu, B., Lind, O., Skipperud, L. 2019 Plutonium handbook 2nd edition, *Nucl. Sci. Eng.* 34, 198–199.

Gellis, A.C., Fuller, C.C., Van Metre, P., Filstrup, C.T., Tomer, M.D., Cole, K.J., Sabitov, T.Y., 2019. Combining sediment fingerprinting with age-dating sediment using fallout radionuclides for an agricultural stream, Walnut Creek, Iowa, USA. *J. Soils Sediments* 19, 3374–3396. <https://doi.org/10.1007/s11368-018-2168-z>.

Gellis, A.C., Noe, G.B., 2013. Sediment source analysis in the Linganore Creek watershed, Maryland, USA, using the sediment fingerprinting approach: 2008 to 2010. *J. Soils Sediments* 13, 1735–1753. <https://doi.org/10.1007/s11368-013-0771-6>.

Giannakopoulou, F., Haidouti, C., Chronopoulou, A., Gasparatos, D., 2007. Sorption behavior of cesium on various soils under different pH levels. *Journal of Hazardous Materials.* <https://doi.org/10.1016/j.jhazmat.2007.06.109>.

Gleason, Robert A., Euliss, Ned H., Hubbard, Daniel E., & Duffy, Walter G. 2003. Effects of sediment load on emergence of aquatic invertebrates and plants from wetland soil egg and seed banks. *Wetlands*, volume 23, pages 26–34.

Graham, L.P., Bergstrom, S., 2001. Water balance modelling in the Baltic Sea drainage basin - analysis of meteorological and hydrological approaches. *Meteorology and Atmospheric Physics.* <https://doi.org/10.1007/s007030170016>.

Gray, J., Jones, S.R., Smith, A.D., 1995. Discharges to the environment from the Sellafield site, 1951-1992. *J. Radiol. Prot.* <https://doi.org/10.1088/0952-4746/15/2/001>.

Griffitts, W.R., Allaway, W.H., Groth, D.H. and Mertz, W., 1977. Beryllium. *Geochemistry and the Environment*, 2.

Guegueniat, P., Kershaw, P., Hermann, J., du Bois, P.B., 1997. New estimation of La Hague contribution to the artificial radioactivity of Norwegian waters (1992–1995) and Barents Sea (1992–1997). *Science of The Total Environment*. [https://doi.org/10.1016/s0048-9697\(97\)00120-4](https://doi.org/10.1016/s0048-9697(97)00120-4).

Guo, J., Costa, O.S., Wang, Y., Lin, W., Wang, S., Zhang, B., Cui, Y., Fu, H., Zhang, L., 2020. Accumulation rates and chronologies from depth profiles of ²¹⁰Pb and ¹³⁷Cs in sediments of northern Beibu Gulf, South China sea. *J. Environ. Radioact.* 213, 106136. <https://doi.org/10.1016/j.jenvrad.2019.106136>.

Guo, H., Xu, Y., Pan, S., Liu, Z., 2021. Distinctive distribution and migration of global fallout plutonium isotopes in an alpine lake and its implications for sediment dating. *Chemosphere* 279, 130535. <https://doi.org/10.1016/j.chemosphere.2021.130535>.

Habibi, S., Gholami, H., Fathabadi, A., Jansen, J.D., 2019. Fingerprinting sources of reservoir sediment via two modelling approaches. *Sci. Total Environ.* 663, 78–96. <https://doi.org/10.1016/j.scitotenv.2019.01.327>.

Haddadchi, A., Ryder, D.S., Evrard, O., Olley, J., 2013. Sediment fingerprinting in fluvial systems: Review of tracers, sediment sources and mixing models. *Int. J. Sediment Res.* 28, 560–578. [https://doi.org/10.1016/S1001-6279\(14\)60013-5](https://doi.org/10.1016/S1001-6279(14)60013-5).

Håkanson, L., 2006. Suspended particulate matter in lakes, rivers, and marine systems (p. 331). Caldwell, New Jersey:: Blackburn Press.

Hao, Y., Xu, Y., Pan, S., Song, X., Zhang, K., Guo, H., Gu, Z., 2018. Sources of plutonium isotopes and ¹³⁷Cs in coastal seawaters of Liaodong Bay and Bohai Strait, China and its environmental implications. *Mar. Pollut. Bull.* 130, 240–248. <https://doi.org/10.1016/j.marpolbul.2018.03.037>.

Hardy, E.P., Krey, P.W., Volchok, H.L., 1973. Global Inventory and Distribution of Fallout Plutonium. *Nature*. <https://doi.org/10.1038/241444a0>.

Hassen, N.E.H., Reguigui, N., Helali, M.A., Mejjad, N., Laissaoui, A., Benkdad, A., Benmansour, M., 2019. Evaluating the historical sedimentation patterns in two different Mediterranean deep environments (Sardinia and Sicily channels). *Mediterr. Mar. Sci.* 20, 542–548. <https://doi.org/10.12681/mms.19558>.

Hayes, C.T., Black, E.E., Anderson, R.F., Baskaran, M., Buesseler, K.O., Charette, M.A., Cheng, H., Cochran, J.K., Edwards, R.L., Fitzgerald, P., Lam, P.J., Lu, Y., Morris, S.O., Ohnemus, D.C., Pavia, F.J., Stewart, G., Tang, Y., 2018. Flux of Particulate Elements in the North Atlantic Ocean Constrained by Multiple Radionuclides. *Global Biogeochemical Cycles*. <https://doi.org/10.1029/2018gb005994>.

HELCOM (Helsinki), 1996. Third Periodic Assessment of the State of the Marine Environment of the Baltic Sea, 1989-1993: Executive Summary: Background Document. Helsinki commission, Baltic marine environment protection commission.

HELCOM, 2003. Radioactivity in the Baltic Sea 1992–1998. In: *Baltic Sea Environment Proceedings*, vol. 85, pp. 5–15.

Hernández, E., Obrist-Farner, J., Brenner, M., Kenney, W.F., Curtis, J.H., Duarte, E., 2020. Natural and anthropogenic sources of lead, zinc, and nickel in sediments of Lake Izabal, Guatemala. *J. Environ. Sci. (China)* 96, 117–126. <https://doi.org/10.1016/j.jes.2020.04.020>.

Holleman, A.F., Wiberg, E. and Wiberg, N., 2001. *Inorganic chemistry*. Academic press.

Holm, E., Aarkrog, A., Ballestra, S., Dahlgard, H., 1986. Origin and isotopic ratios of plutonium in the Barents and Greenland Seas. *Earth and Planetary Science Letters*. [https://doi.org/10.1016/0012-821x\(86\)90037-3](https://doi.org/10.1016/0012-821x(86)90037-3).

Holm, E., 1995. Plutonium in the Baltic Sea. *Applied Radiation and Isotopes*. [https://doi.org/10.1016/0969-8043\(95\)00164-9](https://doi.org/10.1016/0969-8043(95)00164-9).

Hong, G.-H., Hamilton, T.F., Baskaran, M., Kenna, T.C., 2011. Applications of Anthropogenic Radionuclides as Tracers to Investigate Marine Environmental Processes. *Advances in Isotope Geochemistry*. https://doi.org/10.1007/978-3-642-10637-8_19.

Hong, Q., Peng, S., Zhao, D., Cai, P., 2021. Cross-shelf export of particulate organic carbon in the northern South China Sea: Insights from a ^{234}Th mass balance. *Prog. Oceanogr.* 193, 102532. <https://doi.org/10.1016/j.pocean.2021.102532>.

Huang, D., Du, J., Wu, Y., Li, D., Zhang, J., 2010. Sinking of particulates ^{234}Th s, ^7Be and ^{210}Pb s in the Changjiang estuary, China. *Chinese J. Oceanol. Limnol.* 28, 1152–1159. <https://doi.org/10.1007/s00343-010-9036-z>.

Huang, D., Du, J., Moore, W.S., Zhang, J., 2013. Particle dynamics of the Changjiang Estuary and adjacent coastal region determined by natural particle-reactive radionuclides (^7Be , ^{210}Pb , and ^{234}Th). *J. Geophys. Res. Ocean.* 118, 1736–1748. <https://doi.org/10.1002/jgrc.20148>.

Huang, D., Pei, M., Zhou, L., Fan, H., Jia, Y., 2020. Identification of sediment sources and exploration of scale effects in the black soil region of Northeast China. *Catena* 195, 104848. <https://doi.org/10.1016/j.catena.2020.104848>.

Hughes, A.O., Olley, J.M., Croke, J.C., McKergow, L.A., 2009. Sediment source changes over the last 250 years in a dry-tropical catchment, central Queensland, Australia. *Geomorphology* 104, 262–275. <https://doi.org/10.1016/j.geomorph.2008.09.003>.

Hung, T.T., Huyen, D.T., Tu, T.A., Vinh, B.T., 2021. Dating core sediment by applying the ^{210}Pb method and verifying by residual of dioxin (during the Vietnam war) in Can Gio biosphere reserve. *Environ. Earth Sci.* 80, 544. <https://doi.org/10.1007/s12665-021-09827-9>.

ICES Dataset on Ocean Hydrography, 2020. ICES, Copenhagen.

Ikäheimonen, T.K., Outola, I., Varti, V.-P., Kotilainen, P., 2009. Radioactivity in the Baltic Sea: inventories and temporal trends of ^{137}Cs and ^{90}Sr in water and sediments. *J Radioanal Nucl Chem.* <https://doi.org/10.1007/s10967-009-0144-1>.

Imanaka, T., Hayashi, G., Endo, S., 2015. Comparison of the accident process, radioactivity release and ground contamination between Chernobyl and Fukushima-1. *J Radiat Res.* <https://doi.org/10.1093/jrr/rrv074>.

International Atomic Energy Agency (IAEA), 2004. Sediment distribution coefficients and concentration factors for biota in the marine environment. Technical Reports Series No. 422.

Ivanoff, M.D., Toldo, E.E., Figueira, R.C.L., de Lima Ferreira, P.A., 2020. Use of ^{210}Pb and ^{137}Cs in the assessment of recent sedimentation in Patos Lagoon, southern Brazil. *Geo-Marine Lett.* 40, 1057–1067. <https://doi.org/10.1007/s00367-019-00633-8>.

Izrael, Y.A., Vakulovsky, S.M., Vetrov, V.A., Petrov, V.N., Rovinsky, F.Y. and Stukin, E.D., 1990. Chernobyl: radioactive contamination of the environment. Leningrad: Gidrometeoizdat.

Jakimavičius, D. and Kovalenkoviėnė, M., 2010. Long-term water balance of the Curonian Lagoon in the context of anthropogenic factors and climate change. *Baltica*, 23(1), pp.33-46.

Jakimavicius, D., 2012. Changes of water balance elements of the Curonian Lagoon and their forecast due to anthropogenic and natural factors. Doctor thesis, Kaunas.

Jalowska, A.M., McKee, B.A., Laceby, J.P., Rodriguez, A.B., 2017. Tracing the sources, fate, and recycling of fine sediments across a river-delta interface. *Catena* 154, 95–106. <https://doi.org/10.1016/j.catena.2017.02.016>.

Ji, M., Chang, M., Liao, H., Wang, X., Bai, Y., 2021. Vertical distribution of ¹³⁷Cs and plutonium in Lake Taihu and Dianchi sediment cores: loss of radionuclides in shallow, eutrophic lakes. *J Radioanal Nucl Chem.* <https://doi.org/10.1007/s10967-021-07594-2>.

Jinlong, W., Jinzhou, D., Jian, Z., 2020. Plutonium Isotopes Research in the Marine Environment: A synthesis. *J. Nucl. Radiochem. Sci.* 20, 1–11. <https://doi.org/10.14494/jnrs.20.1>.

Jokšas, K., Galkus, A., Stakėnienė, R., 2016. Heavy metal contamination of the Curonian Lagoon bottom sediments (Lithuanian waters area). *Baltica.* <https://doi.org/10.5200/baltica.2016.29.10>.

Juez, C., Hassan, M.A., Franca, M.J., 2018. The Origin of Fine Sediment Determines the Observations of Suspended Sediment Fluxes Under Unsteady Flow Conditions. *Water Resour. Res.* 54, 5654–5669. <https://doi.org/10.1029/2018WR022982>.

Kashparov, V.A., Lundin, S.M., Zvarich, S.I., Ioshchenko, V.I., Levchuk, S.E., Khomutinin, Y.V., Maloshtan, I.M., Protsak, V.P. and Pazukhin, E.M., 2003. Soil contamination with fuel component of Chernobyl radioactive fallout. *Radiochemistry*, 45, pp.189-200. <https://doi.org/10.1023/a:1023897612740>.

Ketterer, M.E., Hafer, K.M., Mietelski, J.W., 2004. Resolving Chernobyl vs. global fallout contributions in soils from Poland using Plutonium atom ratios measured by inductively coupled plasma mass spectrometry. *Journal of Environmental Radioactivity.* <https://doi.org/10.1016/j.jenvrad.2003.09.001>.

Kinoshita, N., Nagaoka, M., Nakanishi, T., 2021. Distribution and settling behavior of americium-241 in the tropical East Pacific. *Science of The Total Environment.* <https://doi.org/10.1016/j.scitotenv.2020.142087>.

Kitheka, J.U., Okoyo, S., Mboya, N., 2021. Hydrology and Climate Impacts on Streamflow and Sediment Yield in the Nyando River Basin, Kenya, in: *Climate Change and Water Resources in Africa.* Springer International Publishing, Cham, pp. 219–238. <https://doi.org/10.1007/978-3-030-61225-2>.

Knuutila, S., Svendsen, L.M., Staaf, H., Kotilainen, P., Boutrup, S., Pyhala, M. and Durkin, M., 2011. Fifth Baltic Sea pollution load compilation (PLC-5).

Korobova, E.M., Chizhikova, N.P., Linnik, V.G., 2007. Distribution of ¹³⁷Cs in the particle-size fractions and in the profiles of alluvial soils on floodplains of the Iput and its tributary Buldynka Rivers (Bryansk oblast). *Eurasian Soil Sc.* <https://doi.org/10.1134/s1064229307040023>.

Krause, A.K., Franks, S.W., Kalma, J.D., Loughran, R.J., Rowan, J.S., 2003. Multi-parameter fingerprinting of sediment deposition in a small gullied catchment in SE Australia. *Catena* 53, 327–348. [https://doi.org/10.1016/S0341-8162\(03\)00085-7](https://doi.org/10.1016/S0341-8162(03)00085-7).

Krey, P.W., 1976. Remote plutonium contamination and total inventories from Rocky Flats. *Health Physics*, 30(2), pp.209-214.

Kullenberg, G., Jacobsen, T.S., 1981. The Baltic Sea: an outline of its physical oceanography. *Marine Pollution Bulletin*. [https://doi.org/10.1016/0025-326x\(81\)90168-5](https://doi.org/10.1016/0025-326x(81)90168-5).

Kuwabara, J., Yamamoto, M., Oikawa, S., Komura, K., Assinder, D.J., 1999. Measurements of ⁹⁹Tc, ¹³⁷Cs, ²³⁷Np, Pu isotopes and ²⁴¹Am in sediment cores from intertidal coastal and estuarine regions in the Irish Sea. *J Radioanal Nucl Chem*. <https://doi.org/10.1007/bf02349419>.

Lacey, J.P., Olley, J., 2015. An examination of geochemical modelling approaches to tracing sediment sources incorporating distribution mixing and elemental correlations. *Hydrol. Process.* 29, 1669–1685. <https://doi.org/10.1002/hyp.10287>.

Lacey, J.P., Olley, J., Pietsch, T.J., Sheldon, F., Bunn, S.E., 2015. Identifying subsoil sediment sources with carbon and nitrogen stable isotope ratios. *Hydrol. Process.* 29, 1956–1971. <https://doi.org/10.1002/hyp.10311>.

Lacey, J.P., Evrard, O., Smith, H.G., Blake, W.H., Olley, J.M., Minella, J.P.G., Owens, P.N., 2017. The challenges and opportunities of addressing particle size effects in sediment source fingerprinting: A review. *Earth-Science Reviews* 169, 85–103. <https://doi.org/10.1016/j.earscirev.2017.04.009>.

Lamba, J., Karthikeyan, K.G., Thompson, A.M., Malhotra, K., Huisman, N.L.H., Panuska, J., Peaslee, G., 2019. Using atmospheric fallout radionuclides ¹³⁷Cs and ²¹⁰Pb to identify sources of suspended sediment in an agricultural watershed. *Trans. ASABE* 62, 529–538. <https://doi.org/10.13031/trans.12976>.

Latorre, B., Lizaga, I., Gaspar, L., Navas, A., 2021. A novel method for analysing consistency and unravelling multiple solutions in sediment fingerprinting. *Sci. Total Environ.* 789, 147804. <https://doi.org/10.1016/j.scitotenv.2021.147804>.

Le Gall, M., Evrard, O., Foucher, A., Lacey, J.P., Salvador-Blanes, S., Manière, L., Lefèvre, I., Cerdan, O., Ayrault, S., 2017. Investigating the temporal dynamics of suspended sediment during flood events with ⁷Be and ²¹⁰Pb measurements in a drained lowland catchment. *Sci. Rep.* 7, 42099. <https://doi.org/10.1038/srep42099>.

Le Gall, M., Ayrault, S., Evrard, O., Lacey, J.P., Gateuille, D., Lefèvre, I., Mouchel, J.M., Meybeck, M., 2018. Investigating the metal contamination of sediment transported by the 2016 Seine River flood (Paris, France). *Environ. Pollut.* 240, 125–139. <https://doi.org/10.1016/j.envpol.2018.04.082>.

Le Roy, E., Sanial, V., Charette, M.A., van Beek, P., Lacan, F., Jacquet, S.H.M., Henderson, P.B., Souhaut, M., García-Ibáñez, M.I., Jeandel, C., Pérez, F.F., Sarthou, G., 2018. The 226Ra–Ba relationship in the North Atlantic during GEOTRACES-GA01. *Biogeosciences*. <https://doi.org/10.5194/bg-15-3027-2018>

Li, Y., Zhou, S., Liu, K., Wang, G., Wang, J., 2020. Application of APCA-MLR receptor model for source apportionment of char and soot in sediments. *Sci. Total Environ.* 746, 141165. <https://doi.org/10.1016/j.scitotenv.2020.141165>.

Li, W., Li, X., Mei, X., Zhang, F., Xu, J., Liu, C., Wei, C., Liu, Q., 2021. A review of current and emerging approaches for Quaternary marine sediment dating. *Sci. Total Environ.* 780, 146522. <https://doi.org/10.1016/j.scitotenv.2021.146522>.

Lim, Y.S., Kim, J.W., Kim, J.K., 2019. Suspended sediment source tracing at the Juksan Weir in the Yeongsan River using composite fingerprints. *Quat. Int.* 519, 245–254. <https://doi.org/10.1016/j.quaint.2019.01.004>.

Lin, P., Xu, C., Kaplan, D.I., Chen, H., Yeager, C.M., Xing, W., Sun, L., Schwehr, K.A., Yamazaki, H., Saito-Kokubu, Y., Hatcher, P.G., Santschi, P.H., 2019. Nagasaki sediments reveal that long-term fate of plutonium is controlled by select organic matter moieties. *Science of The Total Environment*. <https://doi.org/10.1016/j.scitotenv.2019.04.375>.

Lin, W., Feng, Y., Yu, K., Lan, W., Wang, Y., Mo, Z., Ning, Q., Feng, L., He, X., Huang, Y., 2020. Long-lived radionuclides in marine sediments from the Beibu Gulf, South China Sea: Spatial distribution, controlling factors, and proxy for transport pathway. *Mar. Geol.* 424, 106157. <https://doi.org/10.1016/j.margeo.2020.106157>.

Lindahl, P., Lee, S.H., Worsfold, P., Keith-Roach, M., 2010. Plutonium isotopes as tracers for ocean processes: A review. *Mar. Environ. Res.* 69, 73–84. <https://doi.org/10.1016/j.marenvres.2009.08.002>.

Lindahl, P., Asami, R., Iryu, Y., Worsfold, P., Keith-Roach, M., Choi, M.S., 2011. Sources of plutonium to the tropical Northwest Pacific Ocean (1943-1999) identified using a natural coral archive. *Geochim. Cosmochim. Acta* 75, 1346–1356. <https://doi.org/10.1016/j.gca.2010.12.012>.

Liu, Z., Hu, J., Yamada, M., Yang, G., 2020. Uranium and plutonium isotopes and their environmental implications in surface sediments from the

Yangtze River catchment and estuary. *Catena* 193, 104605. <https://doi.org/10.1016/j.catena.2020.104605>.

Liu, M., Chen, M., Duan, M., Lin, Y., Liu, X., Liang, J., Ke, H., Li, H., Chen, M., Cai, M., 2021. Particulate Export of PAHs Firstly Traced by ²¹⁰Po/²¹⁰Pb Disequilibrium: Implication on the “Shelf Sink Effect” in the Arctic Ocean. *J. Geophys. Res. Ocean.* 126. <https://doi.org/10.1029/2021JC017384>.

Livens, F.R., Loveland, P.J., 1988. The influence of soil properties on the environmental mobility of caesium in Cumbria. *Soil Use & Management*. <https://doi.org/10.1111/j.1475-2743.1988.tb00739.x>.

Livingston, H.D. and Povinec, P.P., 2002. A millennium perspective on the contribution of global fallout radionuclides to ocean science. *Health Physics*, 82(5), pp.656-668.

Lizaga, I., Gaspar, L., Latorre, B., Navas, A., 2020. Variations in transport of suspended sediment and associated elements induced by rainfall and agricultural cycle in a Mediterranean agroforestry catchment. *J. Environ. Manage.* 272. <https://doi.org/10.1016/j.jenvman.2020.111020>.

Loba, A., Waroszewski, J., Sykuła, M., Kabala, C., Egli, M., 2022. Meteoric ¹⁰Be, ¹³⁷Cs and ²³⁹⁺²⁴⁰Pu as Tracers of Long- and Medium-Term Soil Erosion—A Review. *Minerals*. <https://doi.org/10.3390/min12030359>.

Lujanás, V., Tarasyuk, N. and Spirkauskaitė, N., 2002. The peculiarities of radiocesium migration in the Nemunas-Neris water system (Lithuania). *Radionuclide transport dynamics in freshwater resources*, p.77.

Lujanienė, G., Šilobritienė, B., Jokšas, K. and Morkūnienė, R., 2004. Behaviour of radiocesium in marine environment. *Environmental research, engineering and management*, 2(28), pp.23-32.

Lujanienė, G., Aninkevičius, V., Lujanás, V., 2009. Artificial radionuclides in the atmosphere over Lithuania. *Journal of Environmental Radioactivity*. <https://doi.org/10.1016/j.jenvrad.2007.07.015>.

Lujanienė, G., Beneš, P., Štamberg, K., Jokšas, K., Vopalka, D., Radžiūtė, E., Šilobritienė, B., Šapolaitė, J., 2010. Experimental study and modelling of ¹³⁷Cs sorption behaviour in the Baltic Sea and the Curonian Lagoon. *J Radioanal Nucl Chem*. <https://doi.org/10.1007/s10967-010-0727-x>.

Lujanienė, G., Garnaga, G., Remeikaitė-Nikienė, N., Jokšas, K., Garbaras, A., Skipitytė, R., Barisevičiūtė, R., Šilobritienė, B., Stankevičius, A., Kulakauskaitė, I., Ščiglo, T., 2012. Cs, Am and Pu isotopes as tracers of sedimentation processes in the Curonian Lagoon–Baltic Sea system. *J Radioanal Nucl Chem*. <https://doi.org/10.1007/s10967-012-2029-y>.

Lujanienė, G., Beneš, P., Štamberg, K., Jokšas, K., Kulakauskaitė, I., 2012. Pu and Am sorption to the Baltic Sea bottom sediments. *J Radioanal Nucl Chem.* <https://doi.org/10.1007/s10967-012-2281-1>.

Lujanienė, G., Povinec, P.P., Li, H.C., Barisevičiūtė, R., Remeikaitė-Nikienė, N., Malejevas, V., Garnaga-Budrė, G., Terrassi, F., Pánik, J., Kaizer, J., Šemčuk, S., Jokšas, K., Tracevičienė, D., Stankevičius, A., 2013. Cs, Am and Pu isotopes as tracers of sedimentation processes in the Curonian Lagoon–Baltic Sea system. *J. Radioanal. Nucl. Chem.* 296, 787–792. <https://doi.org/10.1007/s10967-012-2029-y>.

Lujanienė, G., 2013. Determination of Pu, Am and Cm in environmental samples. In *Isotopes in Hydrology, Marine Ecosystems and Climate Change Studies, Vol. 2. Proceedings of the International Symposium.*

Lujanienė, G., Remeikaitė-Nikienė, N., Garnaga, G., Jokšas, K., Šilobritienė, B., Stankevičius, A., Šemčuk, S., Kulakauskaitė, I., 2014. Transport of ¹³⁷Cs, ²⁴¹Am and Pu isotopes in the Curonian Lagoon and the Baltic Sea. *Journal of Environmental Radioactivity.* <https://doi.org/10.1016/j.jenvrad.2013.09.013>.

Lujanienė, G., Povinec, P.P., Li, H.-C., Barisevičiūtė, R., Remeikaitė-Nikienė, N., Malejevas, V., Garnaga-Budrė, G., Terrassi, F., Pánik, J., Kaizer, J., Šemčuk, S., Jokšas, K., Tracevičienė, D., Stankevičius, A., 2017. Carbon and Pu isotopes in Baltic Sea sediments. *Applied Radiation and Isotopes.* <https://doi.org/10.1016/j.apradiso.2017.02.026>.

Lujanienė, G., Šilobritienė, B., Tracevičienė, D., Šemčuk, S., Romanenko, V., Garnaga-Budrė, G., Kaizer, J., Povinec, P.P., 2022. Distribution of ²⁴¹Am and Pu isotopes in the Curonian Lagoon and the south-eastern Baltic Sea seawater, suspended particles, sediments and biota. *Journal of Environmental Radioactivity.* <https://doi.org/10.1016/j.jenvrad.2022.106892>.

Lukšienė, B., Puzas, A., Remeikis, V., Druteikienė, R., Gudelis, A., Gvozdaitė, R., Buivydas, Š., Davidonis, R., Kandrotas, G., 2015. Spatial patterns and ratios of ¹³⁷Cs, ⁹⁰Sr, and Pu isotopes in the top layer of undisturbed meadow soils as indicators for contamination origin. *Environ Monit Assess.* <https://doi.org/10.1007/s10661-015-4491-9>.

Ma, Q., Qiu, Y., Zhang, R., Lv, E., Huang, Y., Chen, M., 2021. ²¹⁰Po/²¹⁰Pb Disequilibria in the Eastern Tropical North Pacific. *Front. Mar. Sci.* 8. <https://doi.org/10.3389/fmars.2021.716688>.

Mabit, L., Benmansour, M., Walling, D.E., 2008. Comparative advantages and limitations of the fallout radionuclides ¹³⁷Cs, ²¹⁰Pbex and ⁷Be for assessing soil erosion and sedimentation. *J. Environ. Radioact.* 99, 1799–1807. <https://doi.org/10.1016/j.jenvrad.2008.08.009>.

Maina, C.W., Sang, J.K., Raude, J.M., Mutua, B.M., 2019. Geochronological and spatial distribution of heavy metal contamination in sediment from Lake Naivasha, Kenya. *J. Radiat. Res. Appl. Sci.* 12, 37–54. <https://doi.org/10.1080/16878507.2019.1593718>.

Manton, M., Makrickas, E., Banaszuk, P., Kołos, A., Kamocki, A., Grygoruk, M., Stachowicz, M., Jarašius, L., Zableckis, N., Sendžikaitė, J., Peters, J., Napreenko, M., Wichtmann, W., Angelstam, P., 2021. Assessment and Spatial Planning for Peatland Conservation and Restoration: Europe's Trans-Border Neman River Basin as a Case Study. *Land*. <https://doi.org/10.3390/land10020174>.

Marčiulionienė, D., Lukšienė, B., Montvydienė, D., Jefanova, O., Mažeika, J., Taraškevičius, R., Stakėnienė, R., Petrošius, R., Maceika, E., Tarasiuk, N., Žukauskaitė, Z., Kazakevičiūtė, L., Volkova, M., 2017. ¹³⁷Cs and plutonium isotopes accumulation/retention in bottom sediments and soil in Lithuania: A case study of the activity concentration of anthropogenic radionuclides and their provenance before the start of operation of the Belarusian Nuclear Power Plant (NPP). *Journal of Environmental Radioactivity*. <https://doi.org/10.1016/j.jenvrad.2017.07.024>.

Martin, J.M., Whitfield, M., 1983. Significance of the River Input of Chemical Elements To the Ocean., in: *NATO Conference Series, (Series) 4: Marine Sciences*. Springer US, Boston, MA, pp. 265–296. https://doi.org/10.1007/978-1-4757-6864-0_16.

Matisoff, G., Wilson, C.G., Whiting, P.J., 2005. The ⁷Be/²¹⁰PbXS ratio as an indicator of suspended sediment age or fraction new sediment in suspension. *Earth Surf. Process. Landforms* 30, 1191–1201. <https://doi.org/10.1002/esp.1270>.

Matthäus, W. and Schinke, H., 1999. The influence of river runoff on deep water conditions of the Baltic Sea. In *Biological, Physical and Geochemical Features of Enclosed and Semi-enclosed Marine Systems: Proceedings of the Joint BMB 15 and ECSA 27 Symposium, 9–13 June 1997, Åland Islands, Finland* (pp. 1-10). Springer Netherlands.

Mattila, J., Kankaanpää, H. and Ilus, E., 2006. Estimation of recent sediment accumulation rates in the Baltic Sea using artificial radionuclides ¹³⁷Cs and ^{239,240}Pu as time markers. *Boreal Environment Research*, 11(2), p.95.

Mežine, J., Ferrarin, C., Vaičiute, D., Idzelyte, R., Zemlys, P., Umgiesser, G., 2019. Sediment transport mechanisms in a lagoon with high river discharge and sediment loading. *Water (Switzerland)* 11, 1970. <https://doi.org/10.3390/w11101970>.

Mietelski, J.W., 2001. Plutonium in the environment of Poland (a review). *Radioactivity in the Environment*. [https://doi.org/10.1016/s1569-4860\(01\)80026-7](https://doi.org/10.1016/s1569-4860(01)80026-7).

Michel, H., Barci-Funel, G., Barci, V., Ardisson, G., 2002. Input contribution and vertical migration of plutonium, americium and cesium in lake sediments (Belham Tarn, Cumbria, UK). *Radiochimica Acta*. https://doi.org/10.1524/ract.2002.90.9-11_2002.747.

Monte, L., Klyashtorin, A.I., Strebl, F., Bossew, P. and Aggarwal, P., 2002. Radionuclide transport in freshwater systems: A synthesis of the results of the CRP. *Radionuclide transport dynamics in freshwater resources*, p.5.

Moore, J.W., Semmens, B.X., 2008. Incorporating uncertainty and prior information into sTable isotope mixing models. *Ecol Letters*. <https://doi.org/10.1111/j.1461-0248.2008.01163.x>.

Moros, M., Andersen, T.J., Schulz-Bull, D., Häusler, K., Bunke, D., Snowball, I., Kotilainen, A., Zillén, L., Jensen, J.B., Kabel, K., Hand, I., Leipe, T., Loughheed, B.C., Wagner, B., Arz, H.W., 2017. Towards an event stratigraphy for Baltic Sea sediments deposited since AD 1900: approaches and challenges. *Boreas* 46, 129–142. <https://doi.org/10.1111/bor.12193>.

Morris, K., Raiswell, R., 2002. Chapter 4 Biogeochemical cycles and remobilisation of the actinide elements. *Radioactivity in the Environment*. [https://doi.org/10.1016/s1569-4860\(02\)80033-x](https://doi.org/10.1016/s1569-4860(02)80033-x).

Motha, J.A., Wallbrink, P.J., Hairsine, P.B., Grayson, R.B., 2003. Determining the sources of suspended sediment in a forested catchment in southeastern Australia. *Water Resour. Res.* 39. <https://doi.org/10.1029/2001WR000794>.

Mulsow, S., Piovano, E., Cordoba, F., 2009. Recent aquatic ecosystem response to environmental events revealed from 210Pb sediment profiles. *Mar. Pollut. Bull.* 59, 175–181. <https://doi.org/10.1016/j.marpolbul.2009.05.018>.

Muñoz-Arcos, E., Castillo, A., Cuevas-Aedo, A., Ovando-Fuentealba, L., Taylor, A., Bustamante-Ortega, R., Blake, W.H., Bravo-Linares, C., 2021. Sediment source apportionment following wildfire in an upland commercial forest catchment. *J. Soils Sediments* 21, 2432–2449. <https://doi.org/10.1007/s11368-021-02943-w>.

National Nuclear Data Center NNDC. Available at: <https://www.nndc.bnl.gov/nudat3/> (Accessed: March 9, 2023).

Navas, A., Lizaga, I., Gaspar, L., Latorre, B., Dercon, G., 2020. Unveiling the provenance of sediments in the moraine complex of Aldegonda Glacier (Svalbard) after glacial retreat using radionuclides and elemental

fingerprints. *Geomorphology* 367, 107304.
<https://doi.org/10.1016/j.geomorph.2020.107304>.

Nielsen, S.P., Bengtson, P., Bojanowsky, R., Hagel, P., Herrmann, J., Ilus, E., Jakobson, E., Motiejunas, S., Panteleev, Y., Skujina, A., Suplinska, M., 1999. The radiological exposure of man from radioactivity in the Baltic Sea. *Science of The Total Environment*. [https://doi.org/10.1016/s0048-9697\(99\)00130-8](https://doi.org/10.1016/s0048-9697(99)00130-8).

Nosrati, K., Collins, A.L., Madankan, M., 2018. Fingerprinting sub-basin spatial sediment sources using different multivariate statistical techniques and the Modified MixSIR model. *Catena* 164, 32–43. <https://doi.org/10.1016/j.catena.2018.01.003>.

Nosrati, K., Akbari-Mahdiabad, M., Ayoubi, S., Collins, A.L., 2021. An exploratory study on the use of different composite magnetic and colour fingerprints in aeolian sediment provenance fingerprinting. *CATENA* 200, 105182. <https://doi.org/10.1016/j.catena.2021.105182>.

Oldfield, F., Rummery, T.A., Thompson, R., Walling, D.E., 1979. Identification of suspended sediment sources by means of magnetic measurements: Some preliminary results. *Water Resour. Res.* 15, 211–218. <https://doi.org/10.1029/WR015i002p00211>.

Olley, J., Burton, J., Smolders, K., Pantus, F., Pietsch, T., 2013. The application of fallout radionuclides to determine the dominant erosion process in water supply catchments of subtropical South-east Queensland, Australia. *Hydrol. Process.* 27, 885–895. <https://doi.org/10.1002/hyp.9422>.

Olsen, C.R., Larsen, I.L., Lowry, P.D., Cutshall, N.H., Nichols, M.M., 1986. Geochemistry and deposition of ⁷Be in river-estuarine and coastal waters. *J. Geophys. Res.* 91, 896–908. <https://doi.org/10.1029/jc091ic01p0089>.

Olsen, C.R., Larsen, I.L., Lowry, P.D., McLean, R.I., Domotor, S.L., 1989. Radionuclide distributions and sorption behavior in the Susquehanna--Chesapeake Bay System. Office of Scientific and Technical Information (OSTI). <https://doi.org/10.2172/6352159>.

Owens, S.A., Pike, S., Buesseler, K.O., 2015. Thorium-234 as a tracer of particle dynamics and upper ocean export in the Atlantic Ocean. *Deep. Res. Part II Top. Stud. Oceanogr.* 116, 42–59. <https://doi.org/10.1016/j.dsr2.2014.11.010>.

Owens, P.N., Blake, W.H., Gaspar, L., Gateuille, D., Koiter, A.J., Lobb, D.A., Peticrew, E.L., Reiffarth, D.G., Smith, H.G., Woodward, J.C., 2016. Fingerprinting and tracing the sources of soils and sediments: Earth and ocean science, geoarchaeological, forensic, and human health applications. *Earth-Science Rev.* 162, 1–23. <https://doi.org/10.1016/j.earscirev.2016.08.012>.

Paatero, J., Jaakkol, T., Reponen, A., 1994. Determination of the ^{241}Pu Deposition in Finland after the Chernobyl Accident. *Radiochimica Acta*. <https://doi.org/10.1524/ract.1994.64.2.139>

Peart, M.R. and Walling, D.E., 1986. Fingerprinting sediment source: the example of a drainage basin in Devon, UK. In *Drainage basin sediment delivery: proceedings of a symposium held in Albuquerque, NM., 4-8 August 1986*.

Percich, A., Husic, A., Ketterer, M.E., 2022. Plutonium Isotopes: An Effective Tool for Fluvial Sediment Sourcing in Urbanized Catchments. *Geophysical Research Letters*. <https://doi.org/10.1029/2021gl094497>.

Paychev, V. and Stancheva, M., 2009. Changes of sediment balance at the Bulgarian Black Sea coastal zone influenced by anthropogenic impacts. *Compt. Rend. Acad. Bulg. Sci*, 62(2), pp.277-285.

Pham, M.K., Chamizo, E., Mas Balbuena, J.L., Miquel, J.C., Martín, J., Osvath, I., Povinec, P.P., 2017. Impact of Saharan dust events on radionuclide levels in Monaco air and in the water column of the northwest Mediterranean Sea. *J. Environ. Radioact.* 166, 2–9. <https://doi.org/10.1016/j.jenvrad.2016.04.014>.

Pittauer, D., Tims, S.G., Froehlich, M.B., Fifield, L.K., Wallner, A., McNeil, S.D., Fischer, H.W., 2017. Continuous transport of Pacific-derived anthropogenic radionuclides towards the Indian Ocean. *Sci. Rep.* 7, 44679. <https://doi.org/10.1038/srep44679>.

Plummer, M., Best, N., Cowles, K. and Vines, K., 2006. CODA: convergence diagnosis and output analysis for MCMC. *R news*, 6(1), pp.7-11.

Portes, R., Dahms, D., Brandová, D., Raab, G., Christl, M., Kühn, P., Ketterer, M., Egli, M., 2018. Evolution of soil erosion rates in alpine soils of the Central Rocky Mountains using fallout Pu and $\delta^{13}\text{C}$. *Earth Planet. Sci. Lett.* 496, 257–269. <https://doi.org/10.1016/j.epsl.2018.06.002>.

Povinec, P.P., Bailly du Bois, P., Kershaw, P.J., Nies, H., Scotto, P., 2003. Temporal and spatial trends in the distribution of ^{137}Cs in surface waters of Northern European Seas—a record of 40 years of investigations. *Deep Sea Research Part II: Topical Studies in Oceanography*. [https://doi.org/10.1016/s0967-0645\(03\)00148-6](https://doi.org/10.1016/s0967-0645(03)00148-6).

Povinec, P.P., Aarkrog, A. and Buesseler, O., 2004. Worldwide marine radioactivity studies (WOMARS) (No. IAEA-CN--118).

Proshad, R., Kormoker, T., Abdullah Al, M., Islam, M.S., Khadka, S., Idris, A.M., 2022. Receptor model-based source apportionment and ecological risk of metals in sediments of an urban river in Bangladesh. *J. Hazard. Mater.* 423, 127030. <https://doi.org/10.1016/j.jhazmat.2021.127030>.

Pulley, S., Collins, A.L., 2021. The potential for colour to provide a robust alternative to high-cost sediment source fingerprinting: Assessment using eight catchments in England. *Sci. Total Environ.* 792, 148416. <https://doi.org/10.1016/j.scitotenv.2021.148416>.

Qiao, S., Shi, X., Wang, G., Zhou, L., Hu, B., Hu, L., Yang, G., Liu, Y., Yao, Z., Liu, S., 2017. Sediment accumulation and budget in the Bohai Sea, Yellow Sea and East China Sea. *Mar. Geol.* 390, 270–281. <https://doi.org/10.1016/j.margeo.2017.06.004>.

Ravichandran, M., Baskaran, M., Santschi, P.H., Bianchi, T.S., 1995. Geochronology of sediments in the Sabine-Neches estuary, Texas, U.S.A. *Chemical Geology.* [https://doi.org/10.1016/0009-2541\(95\)00082-w](https://doi.org/10.1016/0009-2541(95)00082-w).

Rode, M., op de Hipt, F., Collins, A.L., Zhang, Y., Theuring, P., Schkade, U.K., Diekkrüger, B., 2018. Subsurface sources contribute substantially to fine-grained suspended sediment transported in a tropical West African watershed in Burkina Faso. *L. Degrad. Dev.* 29, 4092–4105. <https://doi.org/10.1002/ldr.3165>.

Romanenko, V., Lujanienė, G., 2023. Short review of plutonium applications for the sediment transport studies. *Journal of Environmental Radioactivity.* <https://doi.org/10.1016/j.jenvrad.2022.107066>.

Rose, L.A., Karwan, D.L., Aufdenkampe, A.K., 2018. Sediment Fingerprinting Suggests Differential Suspended Particulate Matter Formation and Transport Processes Across Hydrologic Regimes. *J. Geophys. Res. Biogeosciences* 123, 1213–1229. <https://doi.org/10.1002/2017JG004210>.

Rutgers Van Der Loeff, M.M., Boudreau, B.P., 1997. The effect of resuspension on chemical exchanges at the sediment-water interface in the deep sea - A modelling and natural radiotracer approach. *J. Mar. Syst.* 11, 305–342. [https://doi.org/10.1016/S0924-7963\(96\)00128-5](https://doi.org/10.1016/S0924-7963(96)00128-5).

Salminen, S., Paatero, J., Jaakkola, T., Lehto, J., 2005. Americium and curium deposition in Finland from the Chernobyl accident. *Radiochimica Acta.* <https://doi.org/10.1524/ract.2005.93.12.771>.

Salminen-Paatero, S., Nygren, U., Paatero, J., 2012. $^{240}\text{Pu}/^{239}\text{Pu}$ mass ratio in environmental samples in Finland. *J. Environ. Radioact.* 113, 163–170. <https://doi.org/10.1016/j.jenvrad.2012.06.005>.

SALO, A., TUOMAINEN, K., VOIPIO, A., 1986. Inventories of some long-lived radionuclides in the Baltic Sea. *Science of The Total Environment.* [https://doi.org/10.1016/0048-9697\(86\)90270-6](https://doi.org/10.1016/0048-9697(86)90270-6).

Savoye, N., Benitez-Nelson, C., Burd, A.B., Cochran, J.K., Charette, M., Buesseler, K.O., Jackson, G.A., Roy-Barman, M., Schmidt, S., Elskens, M., 2006. ^{234}Th sorption and export models in the water column: A review. *Mar. Chem.* 100, 234–249. <https://doi.org/10.1016/j.marchem.2005.10.014>.

Sawe, S.F., Shilla, D.A., Machiwa, J.F., 2021. Lead (Pb) contamination trends in Msimbazi estuary reconstructed from ^{210}Pb -dated sediment cores (Msimbazi River, Tanzania). *Environ. Forensics* 22, 99–107. <https://doi.org/10.1080/15275922.2020.1805823>.

Schmidt, N.M., 2021. Cold front sediment resuspension, age, and residence times of suspended sediment using $^{7}\text{Be}/^{210}\text{Pb}$ ratio in Galveston Bay (doctoral dissertation).

Sellier, V., Navratil, O., Laceby, J.P., Allenbach, M., Lefèvre, I., Evrard, O., 2020. Investigating the use of fallout and geogenic radionuclides as potential tracing properties to quantify the sources of suspended sediment in a mining catchment in New Caledonia, South Pacific. *J. Soils Sediments* 20, 1112–1128. <https://doi.org/10.1007/s11368-019-02447-8>.

Semmens, B.X., Moore, J.W., Ward, E.J., 2009. Improving Bayesian isotope mixing models: a response to Jackson et al. (2009). *Ecology Letters*. <https://doi.org/10.1111/j.1461-0248.2009.01283.x>.

Seo, H., Joung, D., Kim, G., 2021. Contrasting Behaviors of ^{210}Pb and ^{210}Po in the Productive Shelf Water Versus the Oligotrophic Water. *Front. Mar. Sci.* 8. <https://doi.org/10.3389/fmars.2021.701441>.

Seo, H., Kim, G., Kim, Y.-I., Kim, I., 2021. Tracing the Atmospheric Input of Seawater-Dissolvable Pb Based on the Budget of ^{210}Pb in the East Sea (Japan Sea). *Front. Mar. Sci.* 8. <https://doi.org/10.3389/fmars.2021.756076>.

Singh, K.K., Vasudevan, S., 2021. Reconstruction of sedimentation rates based on the chronological framework of Lake Pykara, Tamil Nadu, India. *Environ. Monit. Assess.* 193, 428. <https://doi.org/10.1007/s10661-021-09200-0>.

Skwarzec, B., Bojanowski, R., 1992. Distribution of Plutonium in selected components of the Baltic ecosystem within the Polish economic zone. *Journal of Environmental Radioactivity*. [https://doi.org/10.1016/0265-931x\(92\)90061-w](https://doi.org/10.1016/0265-931x(92)90061-w).

Skwarzec, B., Strumińska, D.I., Prucnal, M., 2003. Estimates of $^{239+240}\text{Pu}$ inventories in Gdańsk bay and Gdańsk basin. *Journal of Environmental Radioactivity*. [https://doi.org/10.1016/s0265-931x\(03\)00107-3](https://doi.org/10.1016/s0265-931x(03)00107-3).

Skwarzec, B., Jahnz-Bielawska, A., Strumińska-Parulska, D.I., 2011. The inflow of ^{238}Pu and $^{239+240}\text{Pu}$ from the Vistula River catchment area to the Baltic Sea. *Journal of Environmental Radioactivity*. <https://doi.org/10.1016/j.jenvrad.2011.03.017>.

Smith, J.N., Ellis, K.M. and Nelson, D.M., 1987. Time-dependent modeling of fallout radionuclide transport in a drainage basin: Significance of

“slow” erosional and “fast” hydrological components. *Chemical geology*, 63(1-2), pp.157-180.

Smith, J.T., Comans, R.N.J., 1996. Modelling the diffusive transport and remobilisation of ^{137}Cs in sediments: The effects of sorption kinetics and reversibility. *Geochimica et Cosmochimica Acta*. [https://doi.org/10.1016/0016-7037\(96\)00030-0](https://doi.org/10.1016/0016-7037(96)00030-0).

Stakėnienė, R., Jokšas, K., Zinkutė, R., Raudonytė-Svirbutavičienė, E., 2019. Oil pollution and geochemical hydrocarbon origin markers in sediments of the Curonian Lagoon and the Nemunas River Delta. *Baltica*. <https://doi.org/10.5200/baltica.2019.1.3>.

Stan Development Team. 2015. Stan modelling language: User's guide and reference manual. Version 2.9.0.

Sternecker, K., Wild, R., Geist, J., 2013. Effects of substratum restoration on salmonid habitat quality in a subalpine stream. *Environ. Biol. Fishes* 96, 1341–1351. <https://doi.org/10.1007/s10641-013-0111-0>.

Stock, B. C., and Semmens, B. X., 2013. MixSIAR GUI User Manual. Version 3.1, March, 1–42. <https://doi.org/10.5281/zenodo.47719.1>.

Stock, B.C., Semmens, B.X., 2016. Unifying error structures in commonly used biotracer mixing models. *Ecology*. <https://doi.org/10.1002/ecy.1517>.

Strumińska, D.I., Strumińska, D.I., Strumińska, D.I., Skwarzec, B., Skwarzec, B., Skwarzec, B., 2006. ^{241}Pu concentration in southern Baltic Sea ecosystem. *J Radioanal Nucl Chem*. <https://doi.org/10.1007/s10967-006-0124-7>.

Stukel, M.R., Kelly, T.B., Landry, M.R., Selph, K.E., Swalethorp, R., 2021. Sinking carbon, nitrogen, and pigment flux within and beneath the euphotic zone in the oligotrophic, open-ocean Gulf of Mexico. *J. Plankton Res*. <https://doi.org/10.1093/plankt/fbab001>.

Subha Anand, S., Rengarajan, R., Shenoy, D., Gauns, M., Naqvi, S.W.A., 2017. POC export fluxes in the Arabian Sea and the Bay of Bengal: A simultaneous $^{234}\text{Th}/^{238}\text{U}$ and $^{210}\text{Po}/^{210}\text{Pb}$ study. *Mar. Chem*. <https://doi.org/10.1016/j.marchem.2017.11.005>.

Syvitski, J., Ángel, J.R., Saito, Y., Overeem, I., Vörösmarty, C.J., Wang, H., Olago, D., 2022. Earth's sediment cycle during the Anthropocene. *Nat. Rev. Earth Environ*. 3, 179–196. <https://doi.org/10.1038/s43017-021-00253-w>.

Szymczycha, B., Zaborska, A., Bełdowski, J., Kuliński, K., Beszczyńska-Möller, A., Kędra, M., Pempkowiak, J., 2019. The Baltic Sea. *World Seas: an Environmental Evaluation*. <https://doi.org/10.1016/b978-0-12-805068-2.00005-x>.

Takahashi, Y., Minai, Y., Kimura, T., Meguro, Y., Tominaga, T., 1994. Formation of Actinide(III)-Humate and its Influence on Adsorption on Kaolinite. *MRS Proc.* <https://doi.org/10.1557/proc-353-189>.

Tang, Q., Fu, B., Wen, A., Zhang, X., He, X., Collins, A.L., 2019. Fingerprinting the sources of water-mobilized sediment threatening agricultural and water resource sustainability: Progress, challenges and prospects in China. *Sci. China Earth Sci.* 62, 2017–2030. <https://doi.org/10.1007/s11430-018-9349-0>.

Tang, Y., Lemaitre, N., Castrillejo, M., Roca-Martí, M., Masqué, P., Stewart, G., 2019. The export flux of particulate organic carbon derived from ²¹⁰Po/²¹⁰Pb disequilibria along the North Atlantic GEOTRACES GA01 transect: GEOVIDE cruise. *Biogeosciences* 16, 309–327. <https://doi.org/10.5194/bg-16-309-2019>.

Taylor, A., Blake, W.H., Smith, H.G., Mabit, L., Keith-Roach, M.J., 2013. Assumptions and challenges in the use of fallout beryllium-7 as a soil and sediment tracer in river basins. *Earth-Science Rev.* 126, 85. <https://doi.org/10.1016/j.earscirev.2013.08.002>.

Thakur, P., Ward, A.L., 2018. ²⁴¹Pu in the environment: insight into the understudied isotope of plutonium. *J Radioanal Nucl Chem.* <https://doi.org/10.1007/s10967-018-5946-6>.

Tomczak, W., Boyer, P., Eyrolle, F., Radakovitch, O., Krimissa, M., Lepage, H., Amielh, M., Anselmet, F., 2021. Modelling of solid / liquid fractionation of trace metals for suspended sediments according to the hydro-sedimentary conditions of rivers - Application to ¹³⁷Cs in the Rhône River (France). *Environmental Modelling & Software.* <https://doi.org/10.1016/j.envsoft.2021.105211>.

Turner, A., Millward, G.E., 2002. Suspended particles: Their role in Estuarine biogeochemical cycles. *Estuar. Coast. Shelf Sci.* 55, 857–883. <https://doi.org/10.1006/ecss.2002.1033>.

Turner, S., Horton, A.A., Rose, N.L., Hall, C., 2019. A temporal sediment record of microplastics in an urban lake, London, UK. *J. Paleolimnol.* 61, 449–462. <https://doi.org/10.1007/s10933-019-00071-7>.

United Nations Scientific Committee on the Effects of Atomic Radiation, 1982. Ionizing Radiation, Sources and Biological Effects, United Nations Scientific Committee on the Effects of Atomic Radiation (UNSCEAR) 1982 Report: Report to the General Assembly, with Scientific Annexes.

United Nations Scientific Committee on the Effects of Atomic Radiation (UNSCEAR), New York, NY (United States), Sources and Effects

of Ionizing Radiation UNSCEAR 2000 Report to the General Assembly, with Scientific Annexes Volume I: Sources (United Nations (UN)), (2000).

USSR State Committee on the Utilization of Atomic Energy, 1986, August. The accident at the Chernobyl nuclear power plant and its consequences. In Information compiled for the International Atomic Energy Agency Experts Meeting, August 25–29, 1986, Vienna. Moscow: USSR State Committee on the Utilization of Atomic Energy.

Vaičiūtė, D., Bučas, M., Bresciani, M., Dabulevičienė, T., Gintauskas, J., Mėžinė, J., Tiškus, E., Umgiesser, G., Morkūnas, J., De Santi, F., Bartoli, M., 2021. Hot moments and hotspots of cyanobacteria hyperblooms in the Curonian Lagoon (SE Baltic Sea) revealed via remote sensing-based retrospective analysis. *Science of The Total Environment*. <https://doi.org/10.1016/j.scitotenv.2021.145053>.

Vaikutienė, G., Skipitytė, R., Mažeika, J., Martma, T., Garbaras, A., Barisevičiūtė, R., Remeikis, V., 2017. Environmental changes induced by human activities in the Northern Curonian Lagoon (Eastern Baltic): diatoms and stable isotope data. *Estonian J. Earth Sci.* <https://doi.org/10.3176/earth.2017.07>.

Valente, M.L., Reichert, J.M., Legout, C., Tiecher, T., Cavalcante, R.B.L., Evrard, O., 2020. Quantification of sediment source contributions in two paired catchments of the Brazilian Pampa using conventional and alternative fingerprinting approaches. *Hydrol. Process.* 34, 2965–2986. <https://doi.org/10.1002/hyp.13768>.

Vercruyse, K., Grabowski, R.C., 2018. Using source-specific models to test the impact of sediment source classification on sediment fingerprinting. *Hydrol. Process.* 32, 3402–3415. <https://doi.org/10.1002/hyp.13269>.

Verdeny, E., Masqué, P., Garcia-Orellana, J., Hanfland, C., Kirk Cochran, J., Stewart, G.M., 2009. POC export from ocean surface waters by means of $^{234}\text{Th}/^{238}\text{U}$ and $^{210}\text{Po}/^{210}\text{Pb}$ disequilibria: A review of the use of two radiotracer pairs. *Deep. Res. Part II Top. Stud. Oceanogr.* 56, 1502–1518. <https://doi.org/10.1016/j.dsr2.2008.12.018>.

Vintró, L.L., Smith, K.J., Lucey, J.A. and Mitchell, P.I., 2000, December. The environmental impact of the Sellafield discharges. In SCOPE-RADSITE Workshop Proceedings, Brussels (pp. 4-6).

Walling, D.E. and Woodward, J.C., 1992. Use of radiometric fingerprints to derive information on suspended sediment sources. In Erosion and sediment monitoring programmes in river basins. Proc. international symposium, Oslo, 1992| (pp. 153-164). International Association of Hydrological Sciences.

Walling, D.E., 2013. The evolution of sediment source fingerprinting investigations in fluvial systems. *J. Soils Sediments* 13, 1658–1675. <https://doi.org/10.1007/s11368-013-0767-2>.

Wang, J., Du, J., Baskaran, M., Zhang, J., 2016. Mobile mud dynamics in the East China Sea elucidated using ²¹⁰Pb, ¹³⁷Cs, ⁷Be, and ²³⁴Th as tracers. *J. Geophys. Res. Ocean.* 121, 224–239. <https://doi.org/10.1002/2015JC011300>.

Wang, J., Du, J., Zheng, J., Bi, Q., Ke, Y., Qu, J., 2020. Plutonium in Southern Yellow Sea sediments and its implications for the quantification of oceanic-derived mercury and zinc. *Environ. Pollut.* 266, 115262. <https://doi.org/10.1016/j.envpol.2020.115262>.

Wang, J., Du, J., Qu, J. and Bi, Q., 2021a. Distribution of Pu isotopes and ²¹⁰Pb in the Bohai Sea and Yellow Sea: Implications for provenance and transportation. *Chemosphere*, 263, p.127896. <https://doi.org/10.1016/j.chemosphere.2020.127896>.

Wang, J., Huang, D., Xie, W., He, Q., Du, J., 2021b. Particle Dynamics in a Managed Navigation Channel Under Different Tidal Conditions as Determined Using Multiple Radionuclide Tracers. *J. Geophys. Res. Ocean.* 126. <https://doi.org/10.1029/2020JC016683>.

Wang, J., Wu, J., Zhan, S., Zhou, J., 2021c. Records of hydrological change and environmental disasters in sediments from deep Lake Issyk-Kul. *Hydrol. Process.* 35. <https://doi.org/10.1002/hyp.14136>.

Waples, J.T., 2022. Bismuth-210, its parent, and daughter and their use as particle tracers in aquatic systems. *Mar. Chem.* 239, 104072. <https://doi.org/10.1016/j.marchem.2021.104072>.

Wilkinson, S.N., Hancock, G.J., Bartley, R., Hawdon, A.A., Keen, R.J., 2013. Using sediment tracing to assess processes and spatial patterns of erosion in grazed rangelands, Burdekin River basin, Australia. *Agric. Ecosyst. Environ.* 180, 90–102. <https://doi.org/10.1016/j.agee.2012.02.002>.

Wilson, C.G., Kuhnte, R.A., Bosch, D.D., Steiner, J.L., Starks, P.J., Tomer, M.D., Wilson, G. V., 2008. Quantifying relative contributions from sediment sources in Conservation Effects Assessment Project watersheds. *J. Soil Water Conserv.* 63, 523–532. <https://doi.org/10.2489/jswc.63.6.523>.

Winkler, P. and Roider, G., 1997. HELCOM-EMEP-PARCOM-AMAP. Field intercomparison of heavy metals in precipitation 1995.

Worrall, F., Burt, T.P., Howden, N.J.K., 2014. The fluvial flux of particulate organic matter from the UK: Quantifying in-stream losses and carbon sinks. *J. Hydrol.* 519, 611–625. <https://doi.org/10.1016/j.jhydrol.2014.07.051>.

Wu, J., 2018. Sources and scavenging of plutonium in the East China Sea. *Marine Pollution Bulletin*. <https://doi.org/10.1016/j.marpolbul.2018.08.014>.

Wu, J., Rabouille, C., Charmasson, S., Reyss, J.L., Cagnat, X., 2018. Constraining the origin of recently deposited particles using natural radionuclides ^7Be and ^{234}Th in deltaic sediments. *Cont. Shelf Res.* 165, 106–119. <https://doi.org/10.1016/j.csr.2018.06.010>.

Xie, R.C., Le Moigne, F.A.C., Rapp, I., Lüdke, J., Gasser, B., Dengler, M., Liebetrau, V., Achterberg, E.P., 2020. Effects of ^{238}U variability and physical transport on water column ^{234}Th downward fluxes in the coastal upwelling system off Peru. *Biogeosciences* 17, 4919–4936. <https://doi.org/10.5194/bg-17-4919-2020>.

Xu, Y., Pan, S., Wu, M., Zhang, K., Hao, Y., 2017. Association of Plutonium isotopes with natural soil particles of different size and comparison with ^{137}Cs . *Sci. Total Environ.* 581–582, 541–549. <https://doi.org/10.1016/j.scitotenv.2016.12.162>.

Yamada, M., Zheng, J., 2020. $^{240}\text{Pu}/^{239}\text{Pu}$ atom ratios in water columns from the North Pacific Ocean and Bering Sea: Transport of Pacific Proving Grounds-derived Pu by ocean currents. *Sci. Total Environ.* 718, 137362. <https://doi.org/10.1016/j.scitotenv.2020.137362>.

Yamada, M., Oikawa, S., 2022. ^{239}Pu , ^{240}Pu , ^{241}Pu , ^{241}Am , ^{137}Cs , and ^{210}Pb in seafloor sediments in the western North Pacific Ocean and the Sea of Japan: distributions, sources and budgets. *J. Radioanal. Nucl. Chem.* <https://doi.org/10.1007/s10967-022-08332-y>.

Yang, W., Zhang, X., Chen, M., Fang, Z., Qiu, Y., 2021. Utilizing $^{234}\text{Th}/^{238}\text{U}$ disequilibrium to constrain particle dynamics in hydrothermal plumes in the Southwest Indian Ocean. *Acta Oceanol. Sin.* 40, 16–25. <https://doi.org/10.1007/s13131-021-1786-2>.

Yang, W., Zhao, X., Guo, L., Huang, B., Chen, M., Fang, Z., Zhang, X., Qiu, Y., 2021. Utilization of Soot and ^{210}Po - ^{210}Pb Disequilibria to Constrain Particulate Organic Carbon Fluxes in the Northeastern South China Sea. *Front. Mar. Sci.* 8. <https://doi.org/10.3389/fmars.2021.694428>.

Yeager, K.M., Schwehr, K.A., Schindler, K.J., Santschi, P.H., 2018. Sediment accumulation and mixing in the Penobscot River and estuary, Maine. *Sci. Total Environ.* 635, 228–239. <https://doi.org/10.1016/j.scitotenv.2018.04.026>.

Zeng, S., Deng, B., Wang, J., Du, Juan, Du, Jinzhou, 2022. Distribution of gamma-ray radionuclides in surface sediments of the Kongsfjorden, Arctic: Implications for sediment provenance. *Acta Oceanol. Sin.* 41, 21–29. <https://doi.org/10.1007/s13131-021-1916-x>.

Zhang, K., Pan, S., Liu, Z., Li, G., Xu, Y., Hao, Y., 2018. Vertical distributions and source identification of the radionuclides ^{239}Pu and ^{240}Pu in the sediments of the Liao River estuary, China. *J. Environ. Radioact.* 181, 78–84. <https://doi.org/10.1016/j.jenvrad.2017.10.016>.

Zhang, F., Wang, J., Liu, D., Bi, Q., Du, J., 2019. Distribution of ^{137}Cs in the Bohai Sea, Yellow Sea and East China Sea: Sources, budgets and environmental implications. *Sci. Total Environ.* 672, 1004–1016. <https://doi.org/10.1016/j.scitotenv.2019.04.001>.

Zhang, S., Yang, G., Zheng, J., Pan, S., Cao, L., Aono, T., Yamazaki, S., Zhang, W., Shen, J., Wang, Y., 2022. Vertical Distribution Characteristics of Pu Isotopes, ^{137}Cs and ^{237}Np in Sediments of Lake Xingkai and the Response to Catchment Environmental Changes. *SSRN Electron. J.* <https://doi.org/10.2139/ssrn.3983961>.

Zhuang, Q., Li, G., Wang, F., Tian, L., Jiang, X., Zhang, K., Liu, G., Pan, S., Liu, Z., 2019. ^{137}Cs and $^{239,240}\text{Pu}$ in the Bohai Sea of China: Comparison in distribution and source identification between the inner bay and the tidal flat. *Mar. Pollut. Bull.* 138, 604–617. <https://doi.org/10.1016/j.marpolbul.2018.12.005>.

CURRICULUM VITAE

Vitaliy Romanenko
1986-07-05, Semey, Republic of Kazakhstan

Education:

Shakarim State University of Semey, faculty of Engineering and Technology | 2004–2008
Bachelor of technical physics

Shakarim State University of Semey, faculty of Engineering and Technology | 2013–2015
Master of technical physics

Center for Physical Sciences and Technology | 2019–2023
PhD studies

Training courses:

Actions in emergencies: “Preparedness for radiological accidents”. As part of the agreement "Training in the field of peaceful uses of atomic energy" between the Kazakh National University, Al-Farabi, the National Nuclear Center and the Japanese Atomic Energy Agency. Kazakhstan, Kurchatov, September 9-13, 2013. | 2013

IAEA courses: “Regional training course on technology 2: remediation design and long-term performance assessment”. Austria, Vienna, April 13-17, 2015. | 2015

IAEA courses: “Regional training course on occupational radiation protection programs and safety culture”. Lithuania, Vilnius, May 30 - June 3, 2016. | 2016

Professional career:

Institute of Atomic Energy of National Nuclear Center, Kurchatov, Kazakhstan | 2008–2010
Engineer

Institute of Radiation Safety and Ecology of National Nuclear Center, Kurchatov, Kazakhstan | 2010–2019
Team leader

ACKNOWLEDGEMENTS

This research would not have been possible without the invaluable help of many friends and colleagues to whom I am sincerely grateful. I thank my supervisor for her unfailing support and guidance. The Department of Environmental Research has provided me with valuable support and suggestions. My special thanks to the PhD studies administrator who helped me with formalities and clarifying insurance issues. My thanks to the staff of the Nature Research Centre for their prompt and high-quality laboratory work. The insightful comments and recommendations of the reviewers greatly improved my dissertation. The love and support of my parents was my constant motivation. I am grateful to all who contributed to my doctoral studies.

Part of the data obtained has not yet been fully published due to unforeseen circumstances. These results will be published in scientific journals in the near future, listing all researchers who contributed to the sampling and experiments.

FOR NOTES

FOR NOTES

FOR NOTES

Vilnius University Press
9 Saulėtekio Ave., Building III, LT-10222 Vilnius
Email: info@leidykla.vu.lt, www.leidykla.vu.lt
bookshop.vu.lt, journals.vu.lt
Print run copies 23